

https://dspace.org/

A comparison between two calcite-rich deposits in palaeoproterozoic dolomitic units of the Transvaal supergroup: beestekraal, North West province and lime acres, Northern Cape

Ntibane, Thabile Malecia

2018

https://hdl.handle.net/10539/26733

Ntibane, Thabile Malecia, (2018) A comparison between two calcite-rich deposits in palaeoproterozoic dolomitic units of the Transvaal Supergroup: Beestekraal, North West Province and Lime Acres, Northern Cape, University of the Witwatersrand, Johannesburg, https://hdl.handle.net/10539/26733.

Downloaded from a DSpace repository. https://dspace.org/

A COMPARISON BETWEEN TWO CALCITE-RICH DEPOSITS IN PALAEOPROTEROZOIC DOLOMITIC UNITS OF THE TRANSVAAL SUPERGROUP: BEESTEKRAAL; NORTH WEST PROVINCE AND LIME ACRES; NORTHERN CAPE.

Thabile Malecia Ntibane

747796

A THESIS/DISSERTATION SUBMITTED IN PARTIAL FULFILMENT OF THE

REQUIREMENTS FOR THE DEGREE

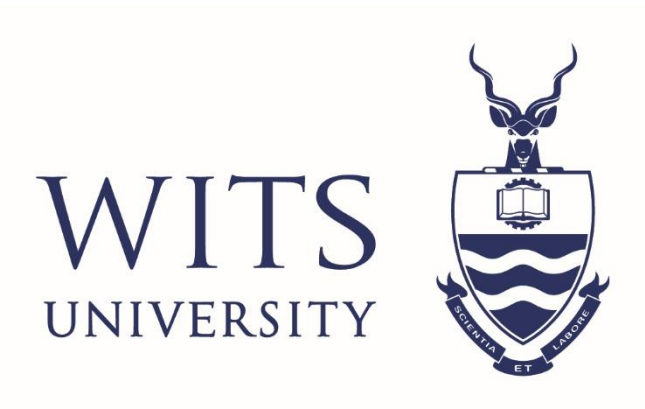
MASTER OF SCIENCE IN ECONOMIC GEOLOGY

THE UNIVERSITY OF THE WITWATERSRAND

FACULTY OF SCIENCE

SCHOOL OF GEOSCIENCES

2018



Supervisor: Dr. Zubair Jinnah

Declaration

I declare that this dissertation is my own, unaided work. It is being submitted for the Degree of Masters of Science in Economic Geology at the University of the Witwatersrand, Johannesburg. It has not been submitted before for any degree or examination in any other University



_____

(Thabile Malecia Ntibane) On the 12th day of September 2018

Abstract

The Malmani and Campbellrand Subgroups have small zones of calcite that did not undergo dolomitisation when it took place within the Transvaal Supergroup. To get the calcite rich zonations of limestone the Malmani and Campbellrand Subgroups may have avoided dolomitisation and dedolomitisation during the geological events of the Transvaal Supergroup.

This project integrated geological mapping, petrology, microprobe analysis, mineral identification, bulk geochemistry and point geochemistry in an attempt to understand and compare the calcite rich limestone zonations that occur in the Malmani and Campbellrand Subgroups. The calcite rich limestone either pre-existed the deformation of the Transvaal Supergroup or resulted from dedolomitisation of the deformed Transvaal Supergroup.

The Campbellrand Subgroup of the Griqualand West Basin is composed of shallow shelf carbonates that were deposited under shallow subtidal conditions, whereas the Malmani Subgroup has the Oaktree Formation which is generally dolomitic, except in the Crocodile River fragment. The sedimentary structures on the Lime Acres Member are interbedded by fine grained limestone, chert and dolomitic matrix. The Lime Acres Member has two NS fault which have high grade limestone between them and on the far western side of the faults, dolomite ore deposit lies on the eastern side. The limestone structures and textures which are found on the western side of the fault 2 (F2) and eastern side of the fault 1 (F1) in Lime Acres were well preserved. The dip is at about 3^{o} -7^{o} to the west. The Oaktree Formation in the Malmani Subgroup hosts the carbonate deposit at Beestekraal which comprises dolomitic limestone with chert-rich and chert-poor zones within the limestone. The deposit dips to the west at an angle of about 33^{o} and strikes NS. There are four faults that cut across the deposit and these are striking WE. The faults form normal faults that are fairly steep. Folding is noted in the hanging wall where the WE faults that cut across the deposit.

The Campbellrand Subgroup deposit is interbedded with limestone and dolomites. The dolomite is coarse grained and can be classified as replacement rock that formed by diagenetic replacement of the older limestones, while the limestone is fine-crystalline and can be classified as primary limestone i.e. not dedolomitised. The dolomite crystals show twinning and cross-cuttings of cleavage planes under a microscope and has proven to have Mg/Ca value of 0.8 -0.9 with a shallow dip.

The characteristics that affect each site are different as Lime Acres has preserved sedimentary structures such as stylolite and stromatolites, whereas such structures are lacking at Beestekraal, where there is a dominance of calcite rich veinlets. The calcite veinlets have upgraded the dolomites at Beestekraal, while the chert downgrades the deposit. Faults, calcite veinlets and quartz inclusions were post depositional of the limestone and dolomite deposit. No evidence was found that the faults could have eroded, downgrade or upgraded the limestone zones. The faults fissures are filled with reddish-clay at Lime Acres and deformed chert at Beestekraal. Re-entrance angles, twinning, fenestrae and cross-cutting cleavage planes were noted in both electron microprobe analysis and petrology analysis. These features are consistent with dolomite structures.

There is evidence of three geological events that have occurred on both site where;

- Deposition of the magnesium-calcite occurred;

- Some silica and calcite veinlets were introduced by fluids, the fluid introduction put pressure on the deposit which resulted in compaction. Re-entrance angles formed during compaction and left the prominent calcite veinlets. The calcite veins only appear in Beestekraal;

- Faulting occurred post the formation earlier compaction evensts. The faulting caused compression of the existing structures and resulted in wavy stylolites at Lime Acres, deformation along the faults and mud fissures being introduced to the joints.

There was uniformity between the X-Ray Fluorescence, X-Ray Diffraction, and electron microprobe analysis results. Both sites have similar mineral composition which are rich in calcium with little deformation. The study has found that the mining areas have somehow not been altered during the dolomitasation phase that affected the Transvaal Supergroup rocks. The pockets of high calcium deposits can be classified as primary limestone, which was somehow preserved during the dolomitisation phase. Post depositional alterations had two different effects on the sites. At Lime Acres the chert, which filled the contacts between the different bedding, was compressed due to high pressure from the overlying material and faulting. The traces of chert have been noted as stylolite and small traceable carbon partings/bands within the limestone and dolomites. At Beestekraal there is infill of iron rich and chert material, which occurs within the cleavage planes and contacts.

Both sites have significantly increased calcium content with low magnesium content in production zones, having little impurities from the chert and dolomites that overlie the limestone. The Mg/Ca ratios showed that for all zones used for cement and lime production the Mg/Ca ratios are below 0.6 and 0.1 respectively. Mg/Ca ratios closer to 1 and above are not economically viable for lime and cement production. The low Mg/Ca ratios indicate that the dolomites are more of magnesium calcite content and of primary depositional environment than secondary.

Acknowledgements

I am appreciative of those who have assisted me during the time devoted on this thesis.

To Zubair Jinnah who took the opportunity to work on this exciting project and also provided a great deal of thorough feedback and ideas. Thank you for being a patient and firm supervisor, your constant excitement over the project has rubbed off on me. The time spent with you on field work, XRF analysis and petrology has been invaluable.

Judith Kinnaird and Paul Nex for the opportunity to be part of the MSc programme. The two of you invest so much time and dedication towards your work. The lessons learnt during these past two years go far beyond the science of economic geology. Thank you for the time invested and the always very honest and constructive criticism and guidance during this whole programme.

Caiphas Majola and Samuel Tshabalala are acknowledged for thin section preparation. Peter Horvath who has been generous with both his time and knowledge while assisting me with microprobe analysing. The PPC GLO team for their assistance with the relevant XRF analysis especially Thandeka Mamabolo who has encouraged supported me beyond her chemistry duties.

At PPC I was granted the opportunity and budget by Piet Booysen and Niru Govender who administered financial support and permitted me to pursue my studies. My colleagues who allowed me to tap into their knowledge, experience and visit their quarries, I am grateful. The support and contributions from Oscar Bowers, Busisiwe Xolo, Dakalo Mudau, Lazarus Meko, Kovilan Govender and Emraan Khan was invaluable.

Finally, this thesis would not have been possible without the love and support of my family Kenneth, Tamasha and Luyanda. Thank you for sacrificing our family time and allowing me the support to pursue my studies.

Table of Contents

INTORDUCTION **1**

1.1 Background 1

1.2 Dolomitisation and De-Dolomisation 1

1.3 Geological Setting 4

1.3.1 Regional Geology 4

1.3.2 Malmani Subgroup: Beestekraal, North West Province 6

1.3.3 Campbellrand Subgroup: Lime Acres, Northern Cape Province 7

1.4 Hypothesis Setting 10

1.5 Aims Setting 10

1.6 Project Methodology Setting 10

1.6.1 Field Mapping 10

1.6.2 Petrology 11

1.6.3 Geochemical Analysis 11

1.6.4 Mineral Identification 11

Literature Review **12**

2.1 Regional Geology 12

2.1.1 Campbellrand Subgroup in the Griqualand Basin ,“Lime Acres” 13

2.1.1.1 Stratigraphy and Sedimentology 13

2.1.1.2 Structural geology 16

2.1.2 Malmani Subgroup in the Crocodile River Dome, “Beestekraal” 16

2.1.2.1 Stratigraphy and Sedimentology 16

2.1.2.2 Structural geology 17

2.2 Analytical techniques on the study of Carbonates 19

2.3 EMPA 19

2.4 Major and Minor trace elements 20

2.5 Mineral Identification (XRD) 21

Methods **22**

3.1 Field Data 22

3.2 Thin Section Petrology and EMPA 24

3.3 Major and Minor Trace elements 24

3.4 Mineral Identification 25

Results 27
4.1 Beestekraal 27
4.1.1 Lithostraphy 27
4.1.2 Structural Geology 29
4.1.3 Thin Section Petrology 30
4.1.4 Major and Minor Trace elements 33
4.1.5 Electron Microprobe 34
4.1.6 XRD Analysis 36
4.1 Lime Acres 38
4.2.1 Lithostraphy 38
4.2.2 Structural Geology 41
4.2.3 Thin Section Petrology 42
4.2.4 Major and Minor Trace elements 46
4.2.5 Electron Microprobe 48
4.2.6 XRD Analysis 51

Discussion 55
5.1 Discussion 55
5.1.1 Structural controls that host calcite rich deposits 55
5.1.2 Mineralogical variations between two deposits 56
5.1.3 Geochemical Data 58
5.1.4 Conclusion 58
References 60

List of Appendices

Appendix 1: Map of Lime Acres
Appendix 2: Map of Beestekraal
Appendix 3: Petrology Data of Lime Acres and Beestekraal
Appendix 4: Geochemical Data of Lime Acres
Appendix 5: Geochemical Data of Beestekraal
Appendix 6: EMPA Data of Lime Acres and Beestekraal
Appendix 7: XRD Data of Lime Acres and Beestekraal

List of Figures

Figure 1.1 Dolomite Models (Boggs, 2006).

Figure 1.2 Generalized stratigraphy and correlation of the Transvaal Supergroup in the Griqualand West and Transvaal (Frauenstein et al., 2009).

Figure 1.3 Geology of the Transvaal and Griqualand west sequence (Truswell, 1990).

Figure 1.4 Map of the Transvaal Supergroup stratigraphic units, showing the distribution of the Campbellrand–Malmani carbonate platform (Knoll and Beukes, 2009).

Figure 1.5 Geology at the Beestekraal Mine. (Modified after Eriksson *et al.,* 2006).

Figure 1.6 Geology of the Lime Acres mine (Modified after Eriksson *et al.,* 2006).

Figure 2.1 The regional geological map of exposures of the Transvaal Supergroup with indications on the Campbellrand Subgroup and Malmani Subgroup (Moore *et al.,* 2012).

Figure 2.2 Correlation chart for the Transvaal Supergroup in the Griqualand West and Transvaal structural basins, South Africa (modified from Bekker *et al.,* 2004).

Figure 2.3 Map showing the location of Lime Acres (Note: the Griguatown Fault which cuts across the Campbellrand Subgroup), Northern Cape Province, and South Africa in the Campbellrand Subgroup (Altermann *et al.,* 1995).

Figure 2.4 Simplified stratigraphic columns for a portion of the Griqualand West Basin. (Modified from Fairey *et al.,* 2013).

Figure 2.5 Simplified stratigraphic columns for a portion of the Malmani Subgroup with empasis to the Oaktree Formation. (Modified from Truswell, 1990; Eroglu *et al.,* 2015).

Figure 2.6 Simplified geological structure of the crocodile dome (Hartzer, 2000).

Figure 2.7 steps in preparation of a sample for XRF analysis. The particle size and mass are given as examples (Modified from Willis *et al.,* 2014).

Figure 3.1: Cross sectional indication of Beestekraal's mining face.

Figure 3.2: Cross sectional indication of Lime Acres' mining face.

Figure 4.1.1 Lithostratigraphic log of Beestekraal's mining face.

Figure 4.1.2 West-East cross sectional view of the Beestekraal quarry with indications dip and strike.

Figure 4.1.3 An indication of the crystal structure with re-entrance angles and twinning patterns.

Figure 4.1.4 Calcite veinlets which cuts between the coarse grained crystals with twining and silt sized quartz in cementation.

Figure 4.1.5 Fenestrae filled with chert nodules in high magnesium calcites.

Figure 4.1.6 bedding plane showing the quartz crystals on the contacts.

Figure 4.1.7 Deformed crystals of dolomite with some quartz inclussions.

Figure 4.1.8 Calcite Magnesium representation at Beestekraal and Mg/Ca ratios with corresponding depths and brief field descriptions of the samples.

Fig 4.1.9 Microprobe image of the stylolite on Beestekraal sample SAM 21.

Figure 4.1.10 Whole rock XRD data showing dolomite (green) magnesium calcite (red) and quartz (blue) of SAM 1 collected at Beestekraal.

Figure 4.1.11 Whole rock XRD data showing magnesium calcite (red) and quartz (blue) of SAM 33 collected at Beestekraal.

Figure 4.1.12 Whole rock XRD data showing dolomite (green) magnesium calcite (red) and quartz (blue) of SAM 26 collected at Beestekraal.

Figure 4.2.1 Cross sectional indication of the lithostratigraphic mapping at Lime Acres' mining face.

Figure 4.2.2 Fault 1 and Fault 2 as noted in Lime Acres. Fault 1 (F1) lies west of the existing quarry while Fault 2 (F2) lies on the Eastern edge of the quarry.

Figure 4.2.3 West-East cross sectional view Fault 1 with depth indications of how each limestone zone is shifted.

Figure 4.2.4: wavy stylolite on the fine grained dolomite with some quartz crystals.

Figure 4.2.5 coarse to medium grained dolomite with fenestrae and re-entrance angles.

Figure 4.2.5 coarse to medium grained dolomite with fenestrae and re-entrance angles.

Figure 4.2.6 dolomite sample with re-entrance angles and no twinning.

Figure 4.2.7 Coarse grained crystals with re-entrance angles.

Figure 4.2.8 fenestrae in varying grain sizes filled with well-defined twinning structures.

Figure 4.2.9 Irregular shaped silicate crystals are surrounded by fine grained crystals.

Figure 4.2.10 Whole rock XRF data showing Mg/Ca (orange) ratios and Calcite (blue), Magnesium (red) representation at the Lime Acres dolomite quarry with corresponding depths.

Figure 4.2.11 Whole rock XRF data showing Calcite (blue) Magnesium (red) representation at the Lime Acres limestone quarry and Mg/Ca (yellow) ratios with corresponding depths.

Fig 4.2.12 Point analysis analysed on the stylolite of Lime Acres sample TMN 24.

Fig 4.2.13 Microprobe image of Lime Acres sample TMN 6.

Figure 4.2.14 Whole rock XRD data showing dolomite (green) of TMN 28 collected at Lime Acres.

Figure 4.2.15 Whole rock XRD data showing magnesium calcite (red) and quartz (blue) of TMN 12 collected at Lime Acres.

Figure 4.2.16 Whole rock XRD data showing dolomite (green) and quartz (blue) of TMN 1 collected at Lime Acres.

Figure 4.1.17 Whole rock XRD data showing dolomite (green) of TMN 4 collected at Lime Acres.

Figure 4.2.18 Whole rock XRD data showing magnesium calcite (red) and quartz (blue) of TMN 21 collected at Lime Acres.

List of Tables

Table 4.1 Samples analysed through microprobe showing sample ID, depth at which sampling occurred and related description.

Table 4.2 Samples analysed through microprobe showing sample ID, depth at which sampling occurred and related description.

Chapter 1
Introduction

1.1. Background

Limestones are one of the most important of all sedimentary rocks as it is the first raw material for cement making industry (Bouazza *et al.,* 2015). Limestones are composed mostly of the mineral calcite ($CaCO_3$). They may also contain some other carbonate minerals and several non-carbonate impurities (Bouazza *et al.,* 2015). There is a debatable relationship between limestone and dolomite due to the uncertainty in how dolomite form (Bouazza *et al.,* 2015). Some limestones are economically viable for lime and cement production within dolomitised formations in South Africa. The two study areas are limestone quarries located in the Campbellrand Subgroup and Malmani Subgroup of the lower Transvaal Supergroup in South Africa, where the limestone is mined for lime and cement production respectively. It is however not clear if the limestone is primary, or if it was de-dolomitised. This project aims to address this issue.

Evaluation of limestone deposits for cement manufacture involves the study of the geological setting and determination of the physical, mechanical mineralogical and chemical properties of the rock. The chemical content of limestone is fundamental in cement making, therefore geological assessment should begin with an initial field investigation involving field mapping, section measuring and sampling (Bouazza *et al.,* 2015).

1.2. Dolomitisation and De-Dolomisation

Dolomites are calcium-magnesium carbonate rocks composed of more than 50 percent of the mineral dolomite [$CaMg(CO_3)_2$] (Boggs, 2006). They are widely distributed in the geologic records, ranging in age from Precambrian to Holocene, although the greatest volumes of dolomites are Palaeozoic and older (Zenger *et al.,* 1994). Dolomites occur in close association with limestones and in many stratigraphic units as interbeds in the limestones. The origin of dolomites has been thoroughly researched, yet remain poorly understood (Zenger et al., 1994). The coarsely crystalline dolomites are classified as secondary rocks due to the presence of limestone textures and structures (Zenger et al., 1994). These dolomites have formed by diagenetic replacement of the older limestones, however, the fine-crystalline dolomites cannot be linked to the process of diagenetic alteration of limestone (Zenger *et al.,* 1994). It is these fine-crystalline dolomites that have created the "dolomite problem" (Warren, 2000). The "dolomite problem" and its associated models was investigated by Hardie (1987). This said problem is due to the fact that laboratory experiments have so far not been successful in precipitating perfectly ordered dolomite (stoichiometric dolomite) at the normal temperature (~250^oC) and pressure (~1 atm) (Shinn, 1986). Laboratory experiments done so far have shown that temperatures of at least 600^oC are required to produce stoichiometric dolomite in the laboratory, as only a dolomite-like material called protodolomite forms at the normal temperatures that are found in natural environments, the protodolomite contains excess $CaCO_3$ (Shinn, 1986). Nonetheless, geologic evidence suggests that dolomite form naturally at, or near, near-surface temperatures. Natural protodolomite can be found as a very minor cement component in some modern carbonates (Shinn, 1986). Warren (2000) asked three questions in an attempt to define the "dolomite problem"; these were; 1. Why there is so little modern dolomite? 2. Why there is so much ancient dolomite? 3. How has the chemistry of ancient dolomite forming settings evolved over time? These questions showed that the dolomite problem arises because the relative importance of kinetics

versus equivalence in dolomite precipitation and variation in volume of dolomite precipitation through time is not understood. Studies have not yet answered whether dolomite precipitation is controlled by seawater chemistry or whether it controls seawater chemistry, and what the effect of bacterial mediation is (Warren, 2000).

According to Boggs (2006) early-formed dolomites include those formed at or near the surface in an unconsolidated state as opposed to diagenetic dolomites that formed during burial and uplift by replacement of older, consolidated limestones.

Modern carbonate sediments generally comprise three minerals: aragonite, low-Mg calcite and high-Mg calcite, with up to 20-30 mol% magnesium. Mesozoic and older limestones generally comprise low-Mg calcite and ordered, near-ideal dolomite (Bridge and Demico 2008). The theory that dolomite is a replacement of pre-existing calcite is supported by several lines of evidence (Bridge and Demico, 2008), and the chemical reactions with respect to formation of dolomite are:

- Direct precipitation of dolomite from aqueous solution
  Ca^{2+} (aq) +Mg^{2+} (aq) +$2CO_3^{2-}$ (aq) =$CaMg(CO_3)_2$ (solid),
- Replacement of calcite or aragonite by dolomite
  $2CaCO_3$ (solid) +Mg^{2+} (aq) = $CaMg(CO3)_2$ (solid) +Ca^{2+} (aq).

Theoretical considerations suggest that dolomite formation is favoured kinetically by high Mg/Ca ratios, low Ca/CO_3 ratios, and low salinity (Machel and Mountjoy, 1986). Finding the diagenetic conditions under which dolomitisation takes place is the crux of the so-called “dolomite problem” (Bridge and Demico, 2008). Hardie (1987) investigated the dolomite problem in a series of successive models and examined the different conditions under which dolomites in modern environments are forming. The three models that have been proposed (figure 1.1) by Hardie (1987) Badiozamani (1973) Carballo *et al. (*1987) and Land (1991); can described as follows;

- Hypersaline model

  This occurs in the sabkhas of the Persian Gulf and the supratidal zones of arid climates. Under strong evaporative conditions, where rates of evaporation exceeds rates of precipitation, sea water beneath the sediments surface become concentrated in increased Mg/Ca hypersaline brines by evaporation (Boggs, 2006). The formation of dolomite is considered to be the result of the conversion of aragonite into dolomite by saline water that precipitated gypsum in the upper sabkha sediments and were thus enriched in $Mg^{2+.}$ (Hardie, 1987). Upward flow of water from the saturated groundwater zone replaces the water lost by capillary evaporation, a process called evaporative pumping (Boggs, 2006). The brines may also be concentrated in surface ponds or bays by surface evaporation of water (Land, 1991). These concentrated brines have higher density than that of normal seawater, causing them to sink downward (Bridge and Demico, 2008). Flushing of large volumes of Mg-rich brine downward through calcium carbonate sediment can putatively bring about dolomitization, a process referred to as seepage reflux (Boggs, 2006). Figure 1.1a shows a graphical illustration of the model associated with this Hypersaline model.

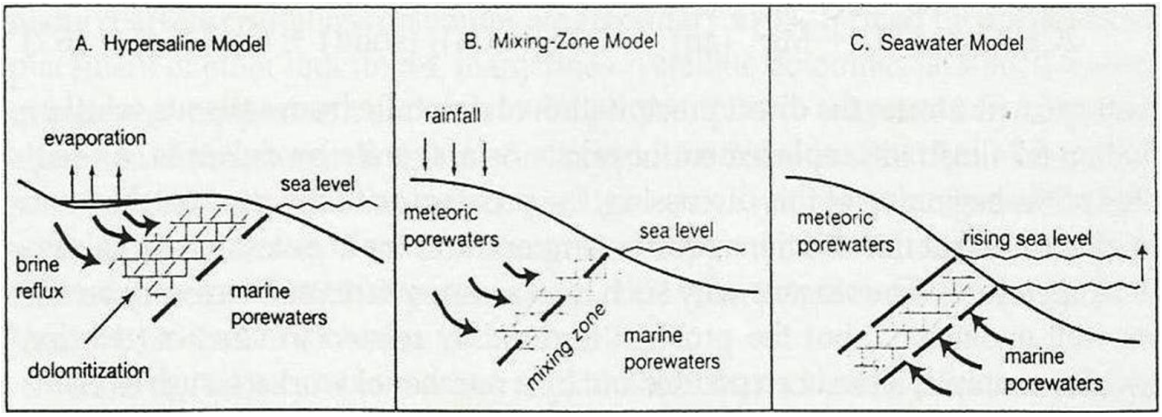


Figure 1.1 Dolomite models (Boggs, 2006).

- Mixed-water (mixing-zone) model

Brackish ground waters produced by mixing of seawater with meteoric water could be saturated with respect to dolomite at Mg^{2+} /Ca^{2+} ratios much lower than those required under hypersaline conditions (Boggs, 2006). Mixing of fresh water and saline water in environments such as the subsurface zones of coastal areas where meteoric waters come in contact with seawater (Fig 1.1B) is suggested to lower salinities sufficiently so that dolomites can form at Mg^{2+} /Ca^{2+} ratios ranging from normal seawater values of about 5:1 to as low as 1:1 (Boggs, 2006). Presumably, dolomite can form at lower Mg^{2+} /Ca^{2+} ratios in these mixed waters compared to seawater because of less competition by other ions in the less saline water (Boggs, 2006).

Eriksson and Warren (1983) tested the mixing-zone model in the Malmani dolomite and concluded that near-surface diagenetic features existed in the shallow subtidal, intertidal and lower supratidal facies and produced coarse-grained dolomite and chert nodules. A sandy aquifer was not present in the deeper subtidal stromatolite mound sequence (Eriksson, 1977) therefore the aquifer did not undergo extensive near-surface diagenesis. The upper portion of the supratidal unit did not undergo mixing-zone diagenesis, this then evidently shows that the Malmani Dolomite are best preserved in the subtidal and the upper supratidal sediments. (Eriksson and Warren., 1983) the mixing-zone model therefore becomes inapplicable to this study.

- Seawater (shallow-subtidal) Model

Seawater modified by evaporation processes is required for dolomitisation. According to the concept embodied in this model, dolomitisation can occur in normal seawater if a sufficient volume of seawater is forced through the sediment so that each pore volume of water in the sediment is constantly being renewed with new seawater) (Boggs, 2006). Thus, new Mg^{2+} is constantly being supplied while replaced Ca^{2+} ions and other ions that might "poison" the dolomite crystal structure are removed. Seawater is forced upward and downward through Holocene carbonate mud during rise and fall of seawater accompanying spring tides, a process they call tidal pumping. (Boggs, 2006).

The concentration of Mg^{2+} ions in the ocean was higher during precipitation periods of “aragonite seas” when rates of seafloor spreading and sea levels were low, than during periods of “calcite seas” when substantial amounts of Mg^{2+} were being absorbed onto the seafloor basalts (Boggs, 2006). Much dolomite in the geologic record has relict textures that indicate the dolomite was

formed by replacement (dolomitisation) of precursor limestone. Dolomitisation can apparently take place readily in any buried limestone that has sufficient porosity and permeability to allow circulation of large volumes of Mg-bearing water. (Boggs, 2006).

1.3. Geological Setting

1.3.1. Regional geology of the Transvaal Supergroup

Moore *et al.* (2001) described the Transvaal Supergroup as an end-Archaean/earliest Proterozoic platform succession on the Kaapvaal Craton which spans the approximate period of 2.65–2.05 Ga. The Transvaal and the Griqualand West Basin are two structural basins that were established by Molengraaf (1901). At the broadest level virtually all of the lower part of each sequence (the Chuniespoort and Ghaap groups respectively in Gauteng and the Northern Cape) is composed of chemical sedimentary rocks: carbonates, and some banded iron formations (BIF) (Molengraaf, 1901). Figure 1.2 the stratigraphic columns of the Transvaal and the Griqualand West Basin.For these rocks research since the 70s has confirmed the existence of a single basin extending over at least 500 000 km^2 and has now begun to develop an understanding of the manner in which the overall basin fill accumulated and of how this ultracratonic basin may have developed. (Truswell, 1990 and Frauenstein *et al.,* 2009).

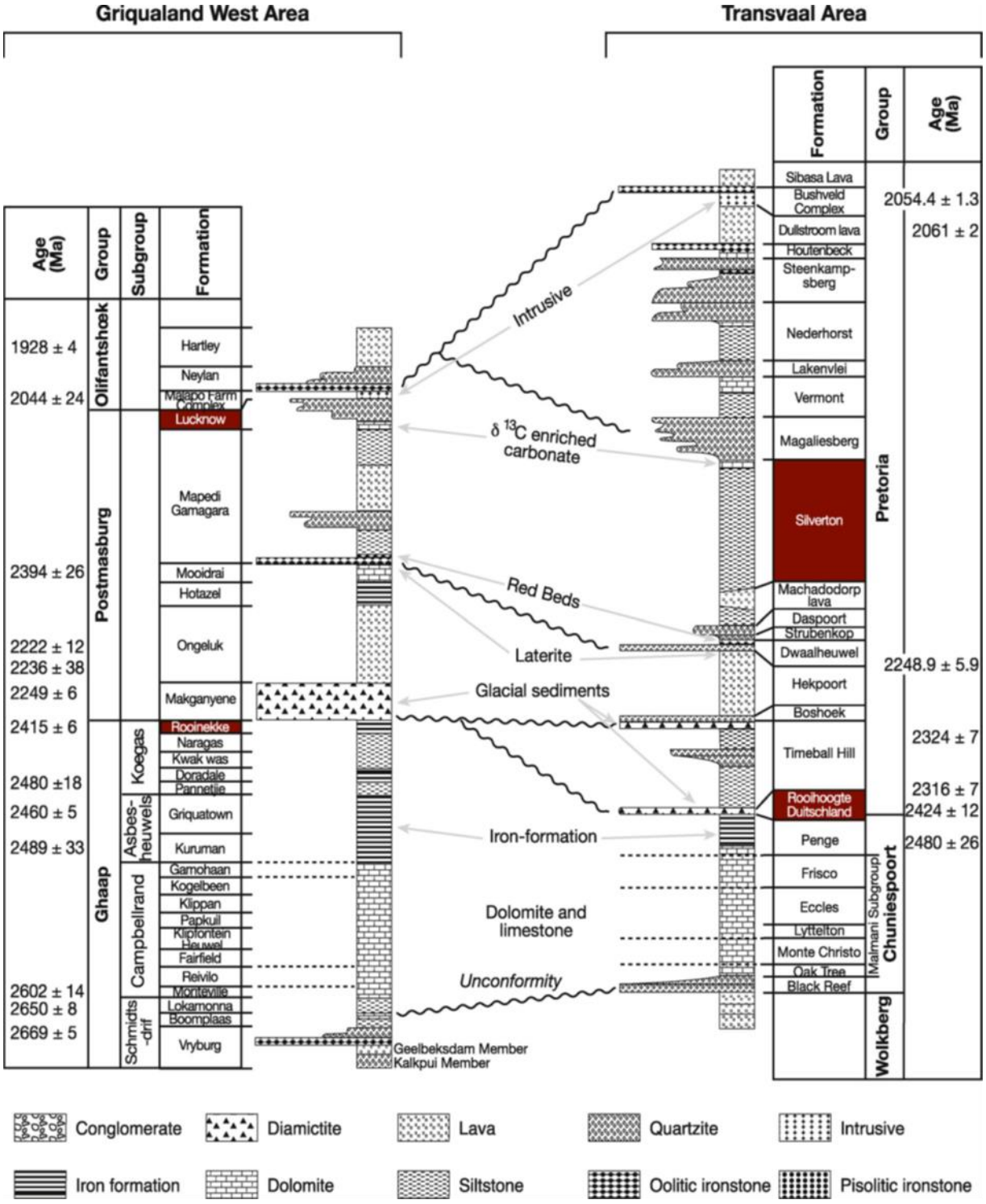


Figure 1.2: Generalized stratigraphy and correlation of the Transvaal Supergroup in the Griqualand West and Transvaal (Frauenstein et al., 2009).

In Gauteng, the Chuniespoort Group is truncated by major uniformity, the significance of which should not be underestimated (Truswell, 1990). Above this lies the thick Pretoria Group. Traditionally this Pretoria Group is correlated with the significantly thinner Postmasburg Group in the Northern Cape (Figure 1.3). This correlation can only be related to coeval volcanic (Hekpoort, Ongeluk) underlain by diamictites. The overlying chemical sedimentary rocks in the Postmasburg Group are distal facies of silicates in the Transvaal Supergroup (Truswell, 1990).

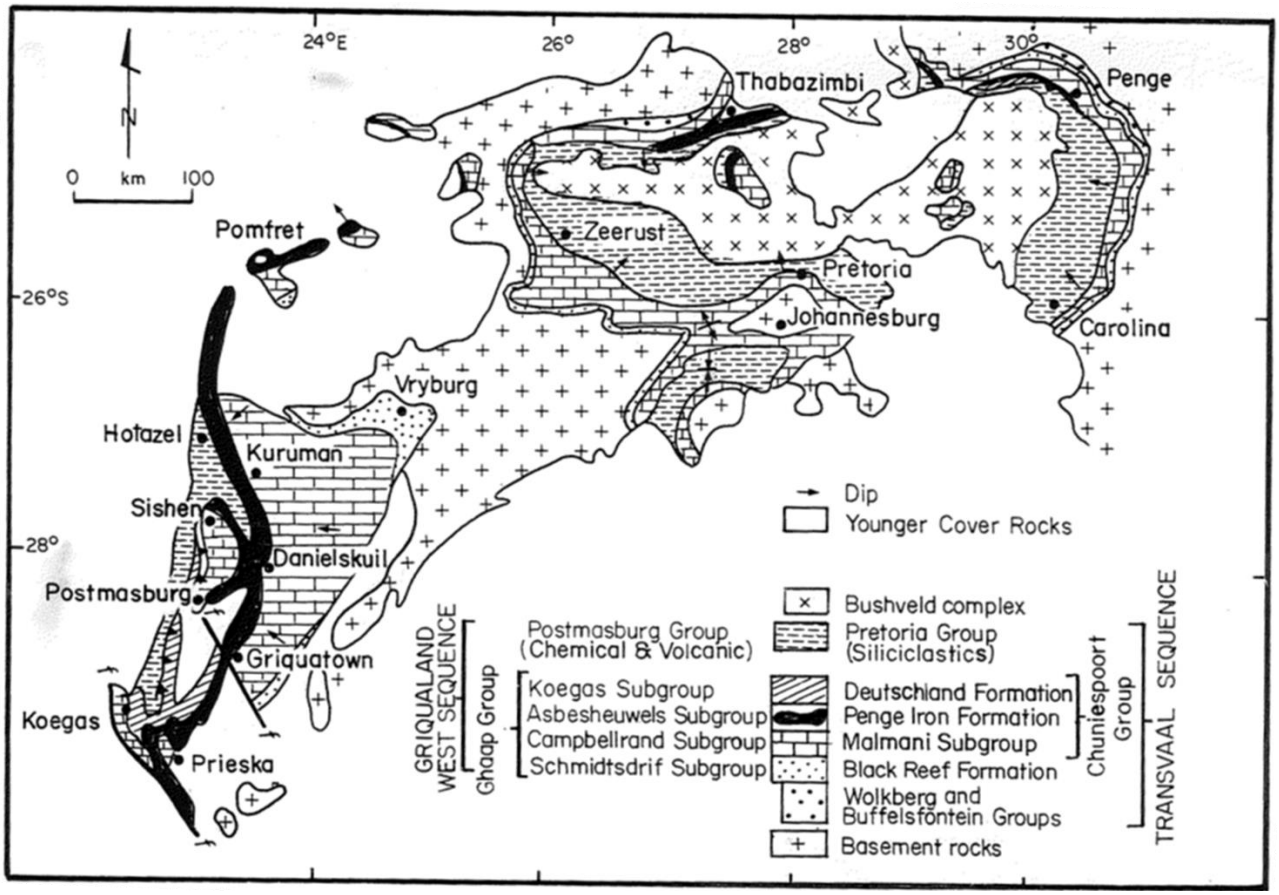


Figure 1.3 Geology of the Transvaal and Griqualand west sequences (Truswell, 1990).

According to Truswell (1990) the lower Transvaal Supergroup consists of a mixed siliciclastic-carbonate ramp that grades upward into an extensive carbonate platform, overlain by banded iron formation (BIF). It was deposited on the Kaapvaal Craton. Lower Transvaal Supergroup strata are extremely well preserved and structural disruption is limited to gentle warping over most of the craton with locally steeper dips around the ~2.06 Ga Bushveld Complex and Doornberg Fault Zone, which coincides with the western boundary of the Kaapvaal Craton (Figure 1.4) (Beukes and Smit 1987). Truswell (1990) further mentions that post depositional erosion limits the distribution of preserved strata, which does not reflect the extent and shape of the original depositional basin. The eastern half of the platform is traditionally called the Transvaal Basin (TB), whereas the western half is called the Griqualand West Basin (GB). Early, fabric-retentive dolomite replaced most of the Malmani Subgroup carbonates, particularly the peritidal facies (Sumner *et al.,* 2006). The peritidal facies are also associated with chert replacement. Significant amounts of the Campbellrand Subgroup however still consists of limestone (Sumner *et al.,* 2006).

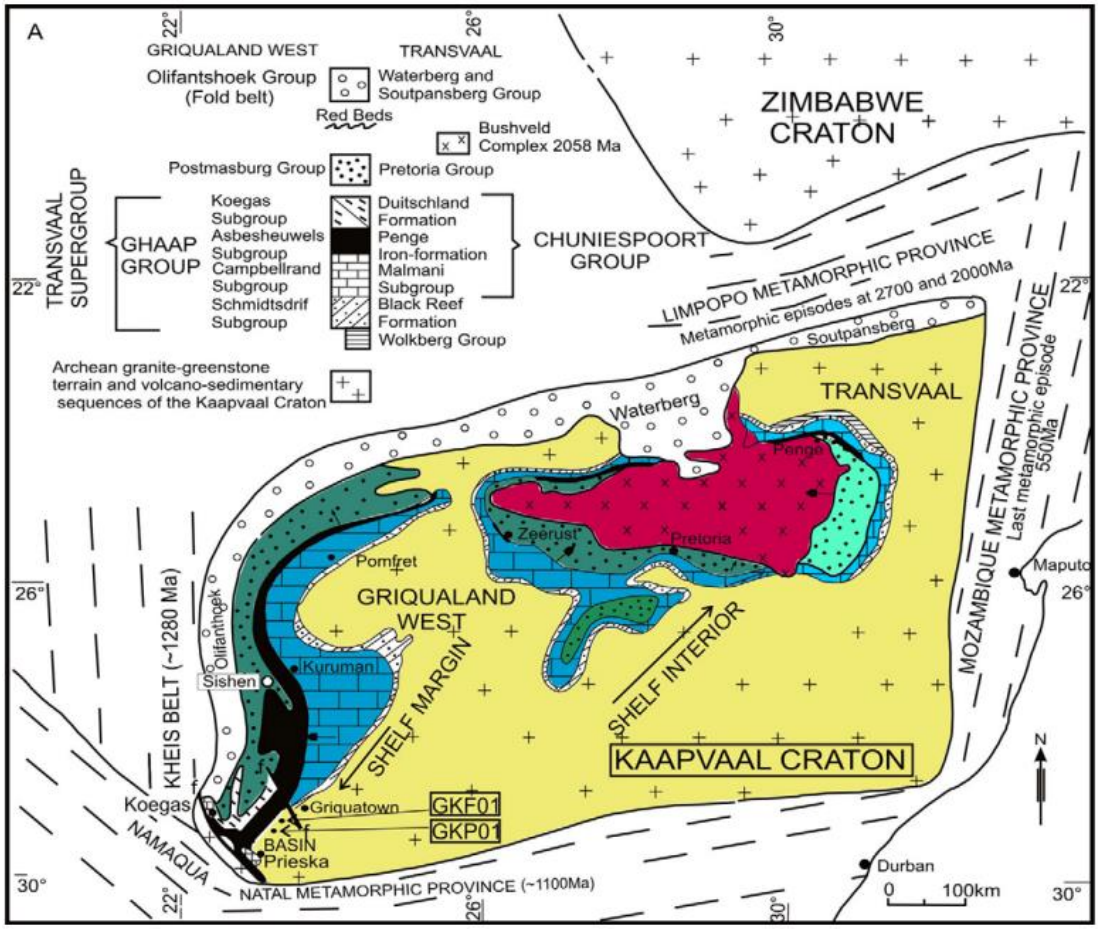


Figure 1.4 Map of the Transvaal Supergroup stratigraphic units, showing the distribution of the Campbellrand–Malmani carbonate platform (Knoll and Beukes, 2009).

1.3.2. Malmani Subgroup: Beestekraal, North West Province

In the Transvaal Supergroup basin the Oaktree Formation is generally dolomitic, except in the Crocodile River fragment, which lies 80 km northwest of Pretoria On the farms Border 84 JQ and Rooinek 83 JQ, the basal part of the sequence consists of high-grade, though relatively magnesian rich, limestone (90% carbonate and 5-6% magnesia). It is quarried for cement and added to low grade, low magnesia calcrete. On Rooikraal 156 IR, a 10 m thick bed of carbonaceous dolomite, probably part of the Monte Christo Formation, is quarried on a large scale for agricultural lime (Martini and Wilson, 1998).

The PPC Beestekraal mining operation is located within the Crocodile fragment of sedimentary rocks forming the Transvaal Super group (Figure 1.5). This Crocodile River fragment is surrounded by igneous rocks of the Bushveld Complex.

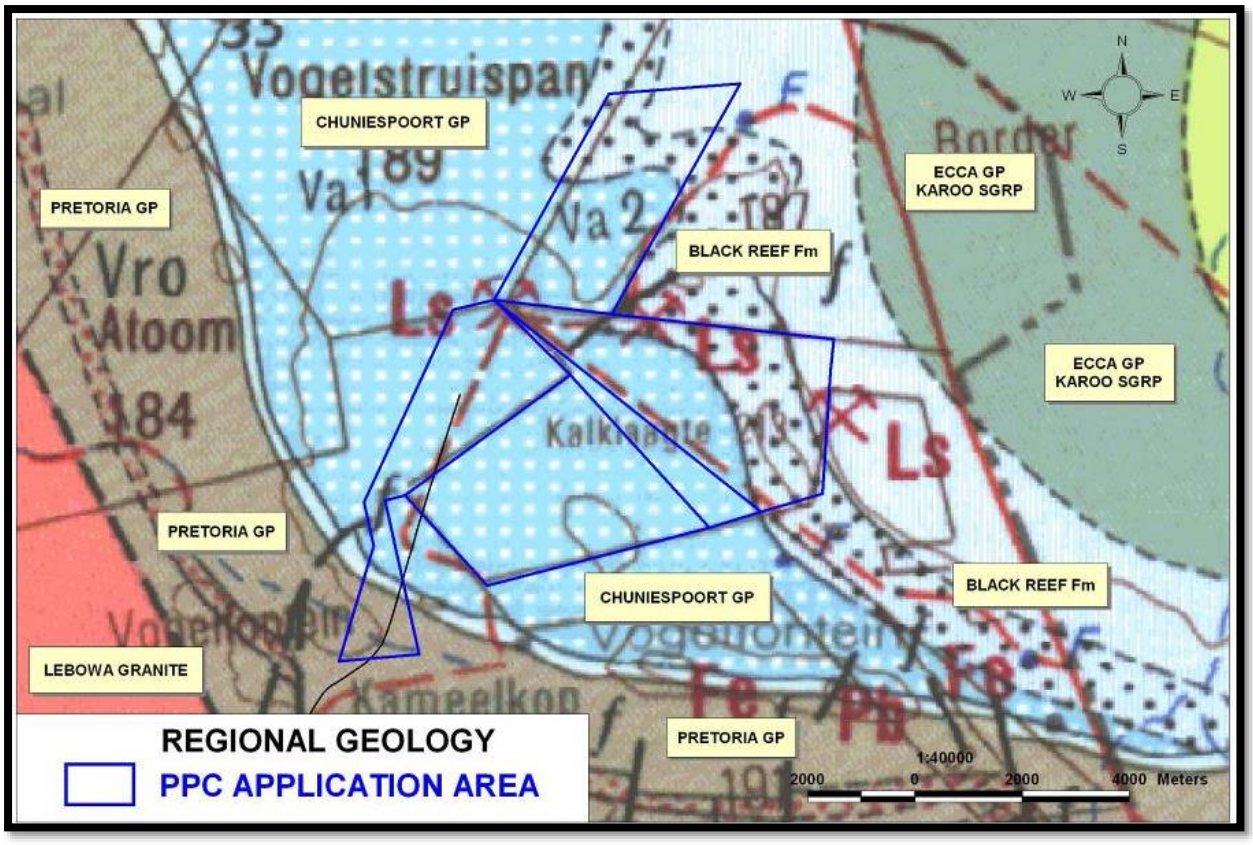


Figure 1.5 Geology at the Beestekraal Mine. (Modified after Eriksson *et al.,* 2006).

Within the Crocodile River Fragment rocks of the Chuniespoort Group carbonates occur. The Chuniespoort carbonates comprise dolomitic limestone with chert-rich and chert-poor zones, which are mined, occurs within the Oaktree Formation of the Malmani Subgroup. This limestone deposit occurs immediately above the Black Reef Formation. Various dolomites and cherts of the Malmani Subgroup form the hanging wall of the deposit. The limestone dips in a westerly direction, between 25° and 45° strikes in a NS direction. The final mining depth will be approximately 123 m below surface. The length of the quarry on strike is 1000 m and the width of the quarry on dip is 350 m. Although the limestone zone within the Oaktree Formation can be traced for many kilometres, the thickness and quality is extremely variable. The mineable deposit is restricted to a strike length of some 1200 m (PPC Cement Ltd, 2015).

1.3.3. Campbellrand Subgroup: Lime Acres, Northern Cape Province

The largest limestone resources in South Africa are contained in the upper part of the Campbellrand Subgroup, which crops out in the Northern Cape. The limestone occurs in a 150 km-long belt a few kilometres wide, that extends from Griquatown in the south to Kuruman in the north. Within this belt the strata dips gentle to the west and the limestone is present in large lenses up to 10 km long and 200 km thick. The limestone is dark grey to blue and fine-grained, with calcium carbonate contents above 90% and magnesium carbonates seldom exceeding 5%. Manganese, accommodated in the calcite lattice, reaches concentrations of between 0.5 and 1%, while insoluble material generally makes up between 0.5 and 2% (Martini and Wilson, 1998).

The main Campbellrand-Malmani carbonate platform contains 12 sequences, whose boundaries can be correlated across most of the preserved platform. Sequences generally thin to the northeast and several

pinch out entirely towards the platform interior (Beukes, 1984 and Sumner *et al.,* 2000). They reflect the flooding of the Kaapvaal Craton and initiation of widespread carbonate deposition, development of a platform with a steepened margin, re-flooding of the platform, development of a rimmed platform with lagoonal to supratidal deposition dominating platform aggradation, and final drowning of the carbonate platform and initiation of regional iron-formation deposition (Sumner *et al.,* 2000).

The limestone deposit is situated in the Lime Acres Member of the Ghaapplato Formation, Campbellrand Subgroup, Griqualand West sequence (Figure 1.6). It consists of high-grade strata bound limestone beds on the eastern flank of a large north/south striking syncline. The beds have a dip of about 3° to the west. The limestone is inter-bedded with low grade limestone, high magnesium limestone and chert being the main contaminants. The rock is well jointed, parallel and normal to the strike, and several vertical N-S faults occur. It is overlain by stromatolitic dolomite grading upwards through the passage beds to the BIF. The limestone is subject to secondary dolomitisation caused by the percolation of magnesian rich solutions through the unconsolidated limestone beds, and the replacement of calcite by dolomite. This has rendered some rock unsuitable for lime production (PPC Lime Ltd., 2015).

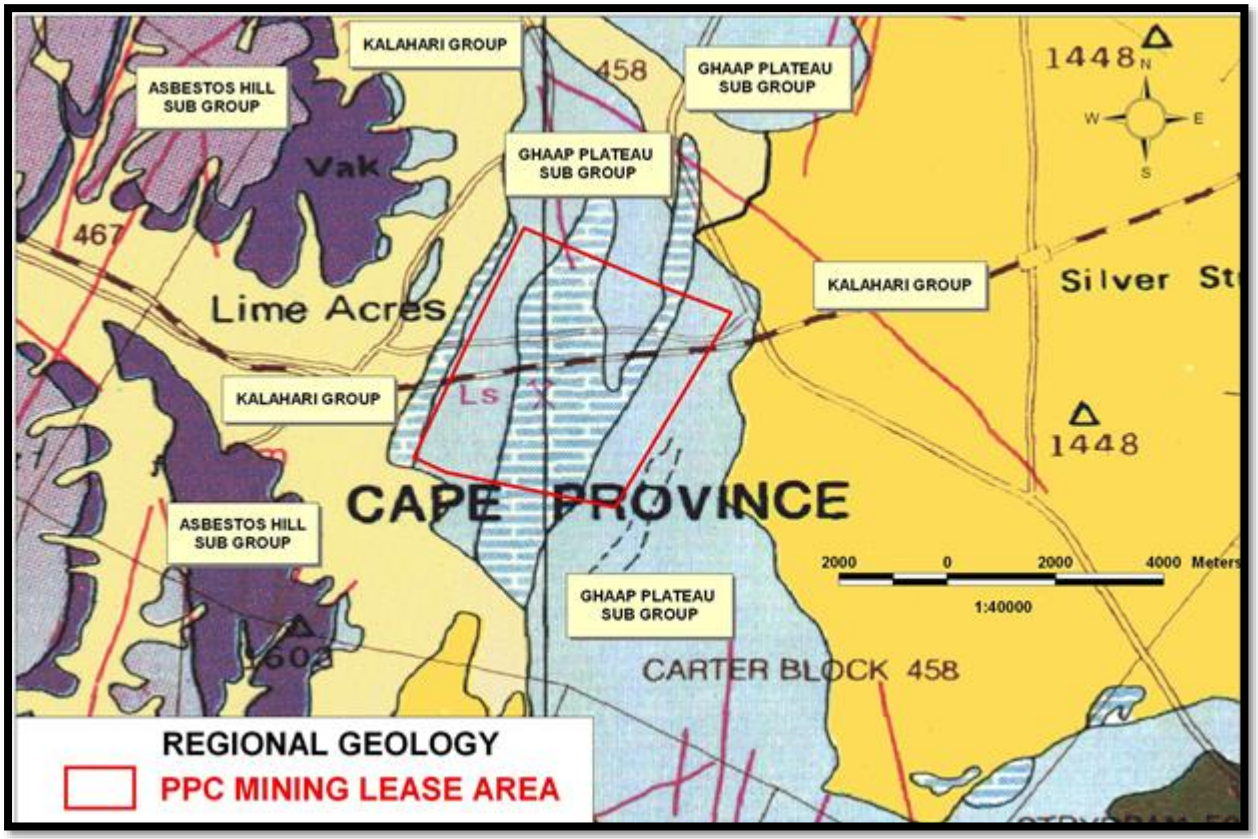


Figure 1.6 Geology of the Lime Acres mine (Modified after Eriksson *et al.,* 2006).

Owing to the dip of the deposit, the overburden increases from the east to the west. The present practical mining limit is about 20 m of waste above the upper limestone zone. There is a very thin soil cover underlain by banded ironstone and chert rubble over the primary limestone. Beige and white secondary limestone has been derived from the limestone and contains much windblown Kalahari sand, re-cemented chert and banded ironstone fragments. Extensive erosion channels occur in the top of the limestone and these manifest themselves as clay and rubble filled fissures and horizons, which may contaminate the

limestone. Dykes of dolerite occur as major linear structures that intersect the sedimentary formations perpendicularly (PPC Lime Ltd., 2015).

1.4. Hypothesis

The Malmani and Campbellrand Subgroups have small zones of calcite that did not undergo dolomitisation when it took place within the Transvaal Supergroup. To get the calcite rich zonations of limestone the Malmani and Campbellrand Subgroups may have avoided a dolomitisation and dedolomitisation during the geological events of the Transvaal Supergroup.

1.5. Aims

The primary aim of this project is to integrate the geological mapping, petrology, microprobe analysis, mineral identification, bulk geochemistry and point geochemistry in an attempt to understand and compare the calcite rich limestone zonations which lie in both the Malmani and Campbellrand Subgroups. The calcite rich limestone either pre-existed the deformation of the Transvaal Supergroup or it is a result of dedolomitisation of the deformed material. Some of the specific objectives that will be addressed include:

- To understand differences between the structural controls within the calcite rich deposits and those that are within deposits that are less economically viable;
- To determine the mineralogical variations between the two deposits. Samples of different mineralogical composition and texture will be analysed to show which the mineralogical structures within different crystal forms show economic values;
- To analyse the geochemical data to distinguish the key elements that have deemed the two ore deposits as economically viable for their intended purpose.

1.6. Project Methodology

1.6.1. Field Mapping

Geological mapping of the exposed (in-pit) ore deposit and surrounding surface was carried out at two localities of study. The strike and angle of dip for the bedding planes, fractures, joints and fault planes were measured separately to understand the structural controls of the limestone and dolomite deposits. Mineralogical variations in the field were also noted and sampled accordingly. The mapped zones will be sampled to help understand and differentiate the structures that are related to the limestone of economic value and that of lower calcium content.

1.6.2. Petrology

Samples collected at different levels of both the Beestekraal mine and Lime Acres mine were looked at under a microscope. The mineralogical composition and texture of the limestone samples was analysed and correlated with data collected from the Electron Microprobe Analysis, mineral identification and the geochemical analysis. These analysis was done to give a scientific indication of

the different trace elements on each site and to compare these with the other site to possibly show any relationship between economic viability and crystal form of the limestone and dolomite samples.

1.6.3. Geochemical Analysis

Limestone samples were collected at different mining levels during field work. These were taken to the laboratory where they will be prepared for analysis. The geochemical analysis was done using the X-Ray Fluorescence (XRF) and Electron Microprobe Analysis (EMPA). The analysis of the geochemical data showed the calcium-magnesium (Ca/Mg ratio) ratio, Silica (Sio2), Iron (Fe) and Oxygen (O) content of both bulk and point samples. The cut-off grade for limestone at PPC is 85% $CaCO_3$ and 95% $CaCO_3$ for cement and lime production respectively.

1.6.4. Mineral Identification

Part of the samples that will be analysed through electron microprobe and geochemical analysis will be analysed through the X-Ray Diffraction (XRD). This analysis will be conducted at the University of the Witwatersrand to identify the minerals associated with the geochemical analysis conducted using the XRF. An indication of the mineral composition per bulk sample will be analysed and compared with the composition of the elements as indicated on both XRD and EMP analysis.

Chapter 2

Literature review

2.1 Regional Geology

The study is based on limestone deposits that are currently being mined for the production of lime and cement, these are located in the Campbellrand Subgroup and Malmani Subgroup of the lower Transvaal Supergroup in South Africa (Fig 2.1). The Transvaal Supergroup is a Neoarchean to Palaeoproterozoic sedimentary succession that developed on the Kaapvaal Craton (Eroglu *et al.,* 2015; Fairey *et al.,* 2013; Moore *et al.,* 2001). It consists of chemical and siliciclastic sedimentary rocks with subordinate volcanic units followed by a rimmed margin that separated lagoonal environments from the open ocean (Eroglu *et al.,* 2015; Sumner and Beukes 1995). The base of the Transvaal Supergroup is defined by the the 2642 ± 3 Ma unconformity that is rested on older supracrustal volcano-sedimentary granite-greenstone terrains of the Kaapvaal Craton in southern Africa (Eroglu *et al.,* 2015 and Kock *et al.,* 2009).

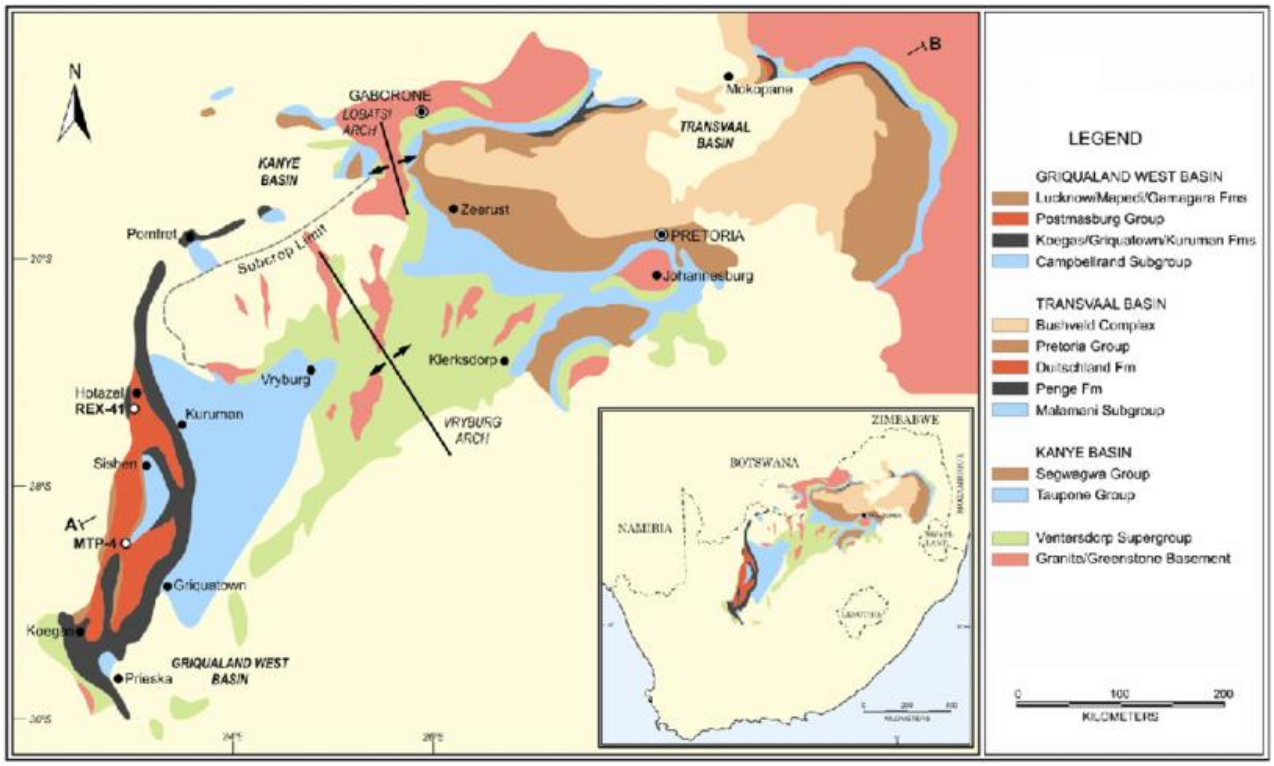


Figure 2.1 The regional geological map of exposures of the Transvaal Supergroup with indications on the Campbellrand Subgroup and Malmani Subgroup (Moore *et al.,* 2012).

The lower Transvaal Supergroup carbonate succession is erosionally preserved in three area that are divided; into several Formations; these areas are; the Transvaal Basin in the eastern part where it circumscribes the Bushveld Complex and the Griqualand West Basin in the western Kaapvaal Craton that extends into southern Botswana, as well beneath Kalahari cover as the Kanye Basin in the north-central part of the platform (Eroglu et al., 2015; Falrey *et al.,* 2013, Moore *et al.,* 2001). According to Moore *et al*., (2001), there is a thick succession of the carbonate platform which can easily be correlated across the middle sequence which is represented in both the Transvaal and Griqualand West Basin (fig 2.2).The carbonate succession extends over an area of ~190,000 km^2 and is representative of one of the first largest and well-preserved stromatolitic

carbonate platform systems on earth known as the Campbellrand/Malmani carbonate, this platform is composed of alternating stromatolitic carbonates and mudstones (Eroglu *et al.,* 2015).

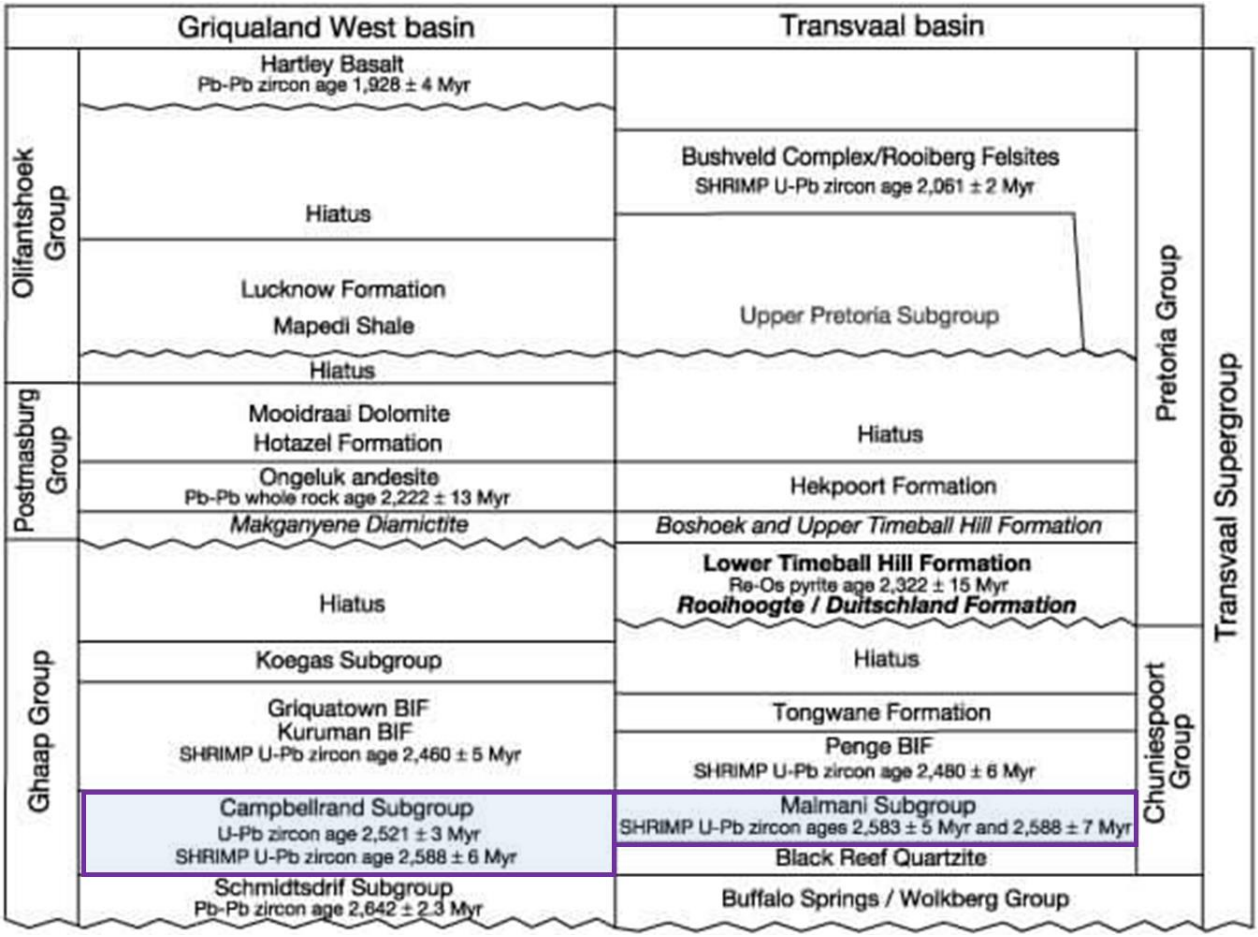


Figure 2.2 Correlation chart for the Transvaal Supergroup in the Griqualand West and Transvaal structural basins, South Africa (Bekker *et al.,* 2004).

The Campbellrand/Malmani carbonate succession was deposited between ~2.58 and 2.50 Ga due to extensive flooding of the Kaapvaal Craton which resulted from thermal subsidence that followed the crustal heating and thinning events related to prior 2.74–2.69 Ga Ventersdorp Supergroup magmatism (Eroglu *et al.,* 2015 and Kock *et al.,* 2009). The deposition of the Campbellrand-Malmani Sequences was detailed by Sumner and Beukes (1995), who was concluded that the geometry and stacking of these sequences are consistent with younger patterns of carbonate accumulation, demonstrating that Neoarchean carbonate accumulation responded to subsidence, sea level change, and carbonate production similarly to Proterozoic and Phanerozoic platforms.

2.1.1. Campbellrand Subgroup in Griqualand Basin ("Lime Acres")

2.1.1.1 Stratigraphy and Sedimentology

Schröder *et al*., (2006), there are three distinct lithological units in the Griqualand West Basin these are Schmidtsdrif, the Campbellrand and the Asbestos Hills Subgroups, which are from base to top (see figure 2.3 for the location of the Campbellrand). The Campbellrand Subgroup is ~2.67 to ~2.5 Ga (Schröder *et al.,* 2006

and De Kick *et al.,* 2008). Eroglu *et al.,* (2015), described the Campbellrand Subgroup of the Griqualand West Basin in the western Kaapvaal Craton as the contemporaneous shallow shelf carbonates which were deposited under shallow subtidal conditions with the far southwestern slope and basinal succession of the being sub-classified as the Prieska facies. Altermann (1995) mentioned that Beukes (1978) developed a complex facies distribution model for the entire Griqualand West Basin and a new stratigraphic subdivision to distinguish between the Schmidtsdrift and Campbellrand Subgroups of the Ghaap Group.

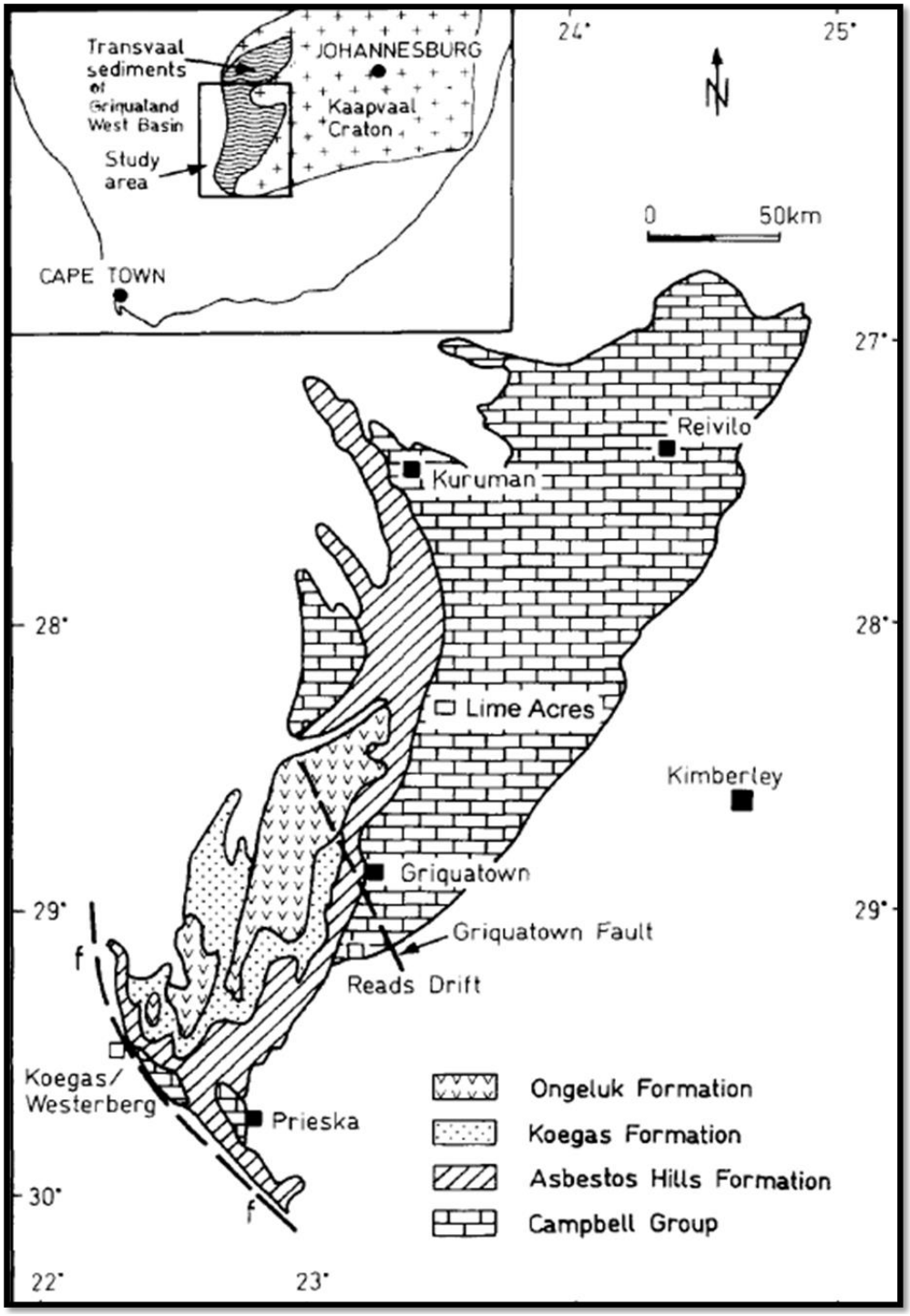


Figure 2.3 Map showing the location of Lime Acres (Note: the Griguatown Fault which cuts across the Campbellrand Subgroup), Northern Cape Province, and South Africa in the Campbellrand Subgroup (Altermann *et al.,* 1995).

The Campbellrand Subgroup is conformably overlain by the Kuruman Member of the Asbestos Hills (see figure 2.4). The Campbellrand Subgroup has older to younger Members which are respectively; the Ulco, Fairfield, and Lime Acres members (Schröder *et al.,* 2006). Altermann *et al*. (1995) describe the Lime Acres member of the Ghaap Plateau Dolomite as composed chiefly of stromatolitic limestones and dolostones with its top consisting of platy dolostones and shales. The stratigraphy is said to be; from older to younger the: Monteville; Reivilo; Fairfield; Kliepfontain heuwel; Papkuil; Kippan; Kogelbeen and Gamohaan formations (Schröder *et al.,* 2006).

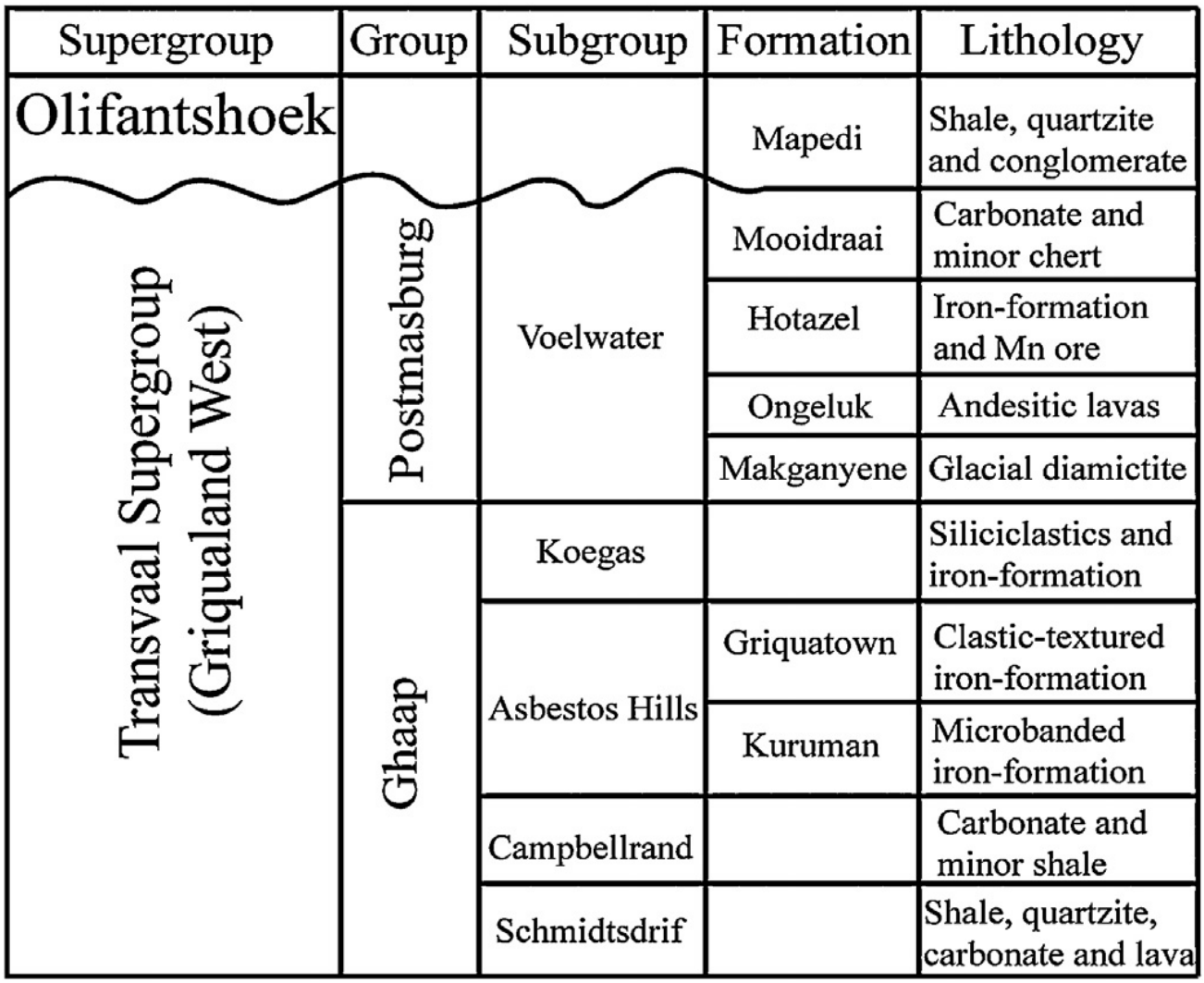


Figure 2.4 Simplified stratigraphic columns for a portion of the Griqualand West Basin (Fairey *et al.,* 2013).

2.1.1.2 Structural Geology

The entire Campbellrand and Transvaal carbonate platforms are Proterozoic in age, and are thus among the oldest relatively well-preserved stromatolitic carbonate platforms known (Altermann *et al.,* 1995). According to Truswell (1990), De Kock *et al.* (2008) and Schröder *et al.* (2008) the Campbellrand Subgroup conformably underlies the chert and BIF of the Asbestos Hills Subgroup, this representing drowning of the platform at about 2.5 Ga.

The Ghaap Group over the Archean- Paleoproterozoic boundary records a complicated magnetic history reflecting at least 500 million years of tectono-thermal evolution (De Kock *et al.,* 2008). This has led to the unique preservation of the Postmasburg Group in the western Griqualand West portion of the Transvaal Supergroup which was not affected by the strongly erosive forces in pre- and early Pretoria Group times (Moore *et al.,* 2012). A distinct platform margin, which possibly corresponded to a sedimentary growth fault with northwest-southeast strike, separated the platform from the basinal area in the southwest (Schröder *et al.,* 2008). Sumner and Beukes (1995) concluded that the stratigraphic patterns during deposition of the Campbellrand-Malmani Subgroups are most consistent with variable thinning of the Kaapvaal Craton during extrusion of the ~2.7 Ga Ventersdorp lavas.

The dip in of the Griqualand west strata in the Northern Cape is usually very low, to the west. With the western part lying on a thrust and fold belt which postdates the formations and the south being truncated by lateral dextral shearing zones (Truswell, 1990).

2.1.2. Malmani Subgroup in the Crocodile River Dome ("Beestekraal")

2.1.2.1 Stratigraphy and Sedimentology

The Malmani Subgroup is divided into different formations based on the presence or absence of early diagenetic chert bands (Buttrick *et al*., 1993; Eroglu *et al*., 2015). These Subgroups (see figure 2.5) are the Monte Christo, Eccles, Oaktree and Lyttleton formations.

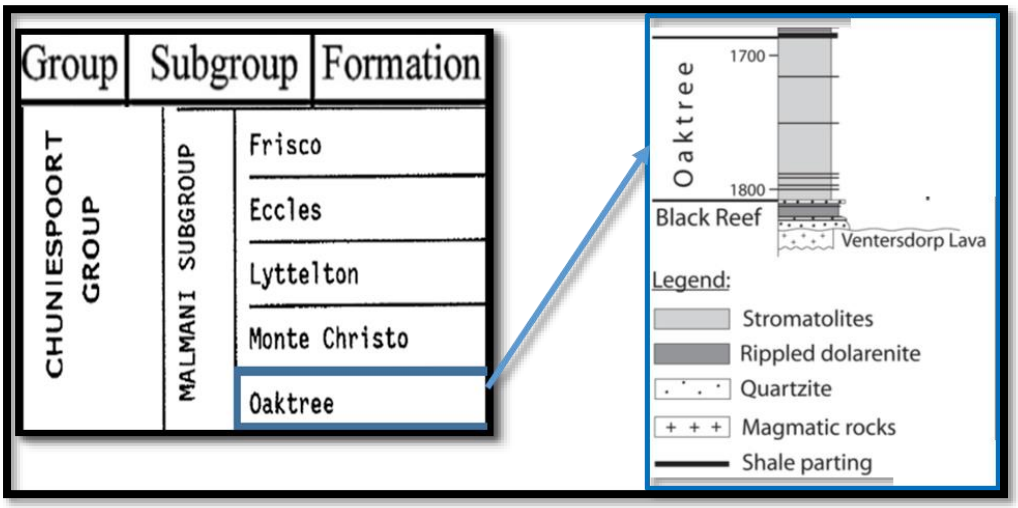


Figure 2.5 Simplified stratigraphic columns for a portion of the Malmani Subgroup with empasis to the Oaktree Formation. (Modified from Truswell, 1990 and Eroglu *et al.,* 2015).

The Oaktree and Lyttleton Formations are chert-free and the Monte Christo and Eccles Formations chert-bearing (Buttrick *et al*., 1993; Eroglu *et al*., 2015). The chert-free Oaktree and Lyttleton Formations are dominantly composed of very dark gray fine micritic dolomite, whereas the chert-bearing Monte Christo and Eccles Formations are dominantly medium to light gray in colour with abundant sparry fenestral and sugary dolarenite interbeds (Eroglu *et al*., 2015). In outcrop the micritic dolomite of the Oaktree and Lyttleton Formations weather to a chocolate brown, while those of the Monte Christo and Eccles Formations weather to mainly gray colors (Eroglu *et al*., 2015). This difference is ascribed to the relatively higher concentration of manganese in the structure of dolomites of the Oaktree and Lyttleton fomations (Buttrick *et al.,* 1993).

The Beestekraal mine is located in the Crocodile River Fragment of the Oaktree Formation of the Malmani Subgroup where the formation is approximately two hundred metres thick (Buttrick *et al.,* 1993). The formation consists of dark coloured, chert-poor dolomite with some carbonaceous shale towards the base (Buttrick *et al.,* 1993). Hartzer (2000) described the Crocodile River Fragment as a large domal structure with the beds of the Pretoria Group dipping steeply towards the surrounding Bushveld Complex granite. The Crocodile River dome showed a succession of sedimentary and volcanic rocks, which are uncomfortably overlain by the Black Reef Formation (Hartzer, 1995). The sedimentary rocks from this Formation range from pure carbonates, carbonates with distinct detrital contribution (Al2O3:3.53 wt-%) to mudstone samples with Total Organic Carbon (TOC) values up to 1.73% and showed no silicification of mudstones or carbonates (Eroglu *et al*., 2015).

2.1.2.1 Structural Geology

Hartzer (1995) documents that the Crocodile River Fragment is located on the intersection of two major anticlines with an ENE and a NW striking fold axis with the Crocodile River fault separating the dome from the synformal Rooiberg fragmentation (see figure 2.6). Hartzer (2000), mentioned that the deformation preceded metamorphism caused by the intrusion of the Bushveld Complex in the Crocodile River Fragment.

According to Hartzer (2000) the Crocodile River Fragment of the Malmani Subgroup can be described as an anticline that has been refolded around another anticline, the deformation is as follows:

- A NW-SE striking fault was formed from NE-SW compression;
- Refolding occurred along the ENE strike due to NE and SE compression;
- Previous structures were refolded, buckling and tightening along the NW strike. The deformation on this stage was less than the first two phases, secondary faulting occurred to release the compression stress;
- Normal faulting occurred along two major faults in the last stage of deformation.

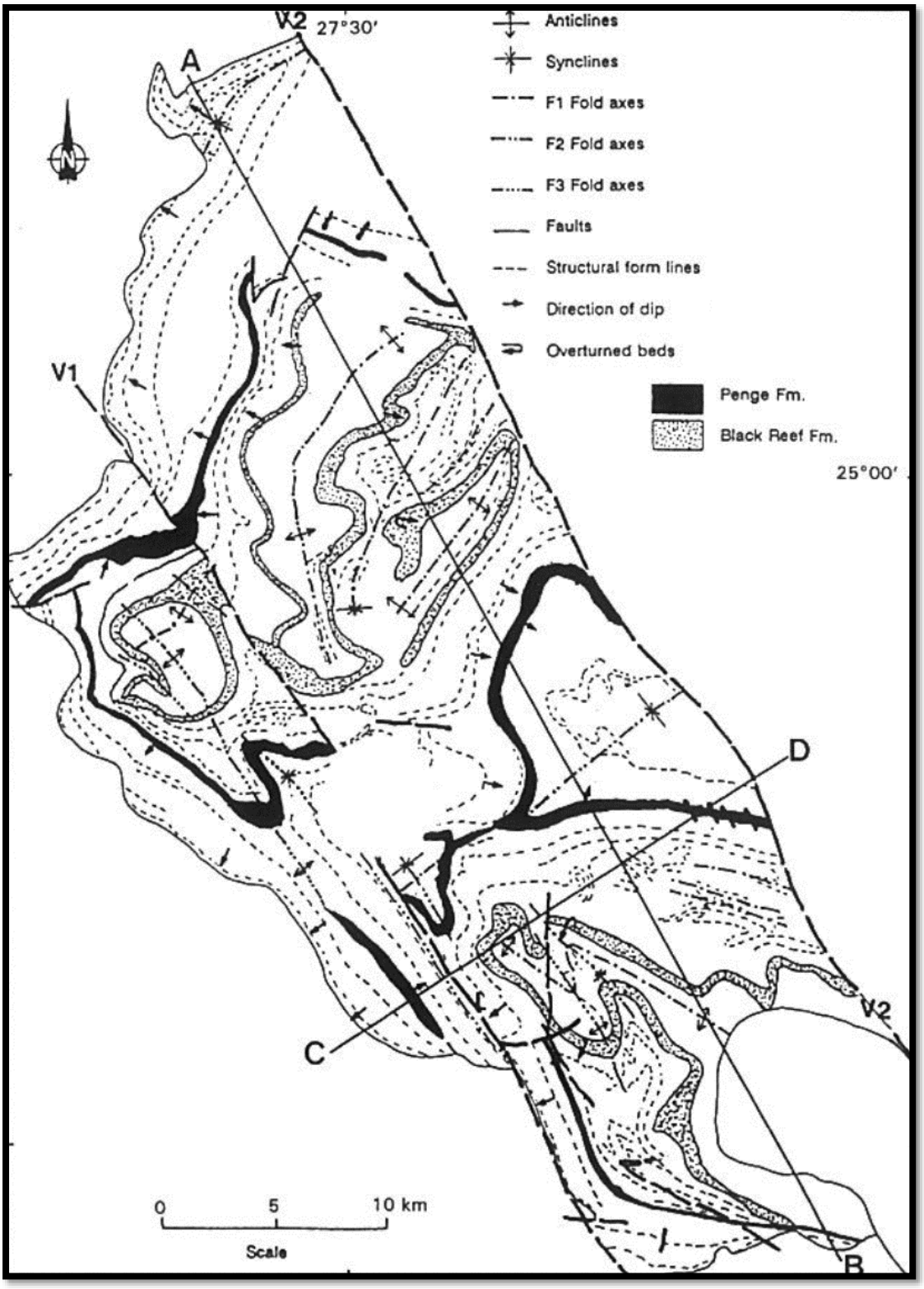


Figure 2.6 Simplified geological structure of the Crocodile River Fragment (Hartzer, 2000).

2.2 Analytical techniques in the study of carbonates

The 30 samples selected for ore microscopy were taken to the geoscience laboratory for thin section petrography preparation. According to the website for the laboratory the standard method for preparing these thin sections is as follows:

- STEP 1: The sample is cut to size to make a thin section block;
- STEP 2: The thin section block is coarsely ground using an automated grinder. Grit powder (silicon carbide) and water are used in the grinding process;
- STEP 3: The block is further smoothed by hand on a glass plate using fine grit powder;
- STEP 4: The block is impregnated with araldite to fill pores spaces. The block is then mounted on glass and placed under pressure until the glass is firmly glued to the block;
- STEP 5: Once set, the block is cut away from the glass leaving a thin slab of rock glued to the glass. The residue block is retained for reference purposes. The section is roughly smoothed by hand;
- STEP 6: The unfinished slide is mounted in a LOGITECH machine to automate the reduction of the thin slab of rock to approximately 0.3 mm thickness. However, the final reduction in thickness to 0.3 mm requires considerable skill and is best achieved by hand using fine grit powder.;
- STEP 7: The precision required to achieve a 0.3 mm thickness also demands repeated checking of the thickness of the section under the microscope.

In order to examine the micro textural and mineralogical features in the thin section of a rock with higher resolution than that of the naked eye, a microscope was used. This microscope has two systems of lenses where the first lens system (objective) produces a magnified image of the object and the second lens system (ocular or eyepiece) produce the real image through further magnification (Raith *et al.,* 2012).

2.3 Electron probe micro-analyzer (EPMA)

Goodge (2017) describes EMPA as a microbeam instrument used primarily for the in-situ non-destructive chemical analysis of minute solid samples. The EPMA is fundamentally the same as an SEM, with the added capability of chemical analysis but the primary importance of an EPMA is the ability to acquire precise, quantitative elemental analyses at very small "spot" sizes (as little as 1-2 microns), primarily by wavelength-dispersive spectroscopy (Goodge, 2017). Geological EMPA is often carried out by means of O stoichiometry, this Stoichiometry is described as the quantitative relationship among reactants and products (UWaterloo, 2018). Lane *et al.* (1994) mentioned that the valences of most geological cations are well known, and O is commonly the only anion present and described the EMPA method is:

- Oxide and carbonate standards were used.
- Calculations are to be carried out by means of O stoichiometry using the true valencies for O and the metals analyzed for.

According to Goodge (2017) the EPMA consists of four major components which are:

- An electron source, commonly a W-filament cathode referred to as a "gun";
- A series of electromagnetic lenses located in the column of the instrument, used to condense and focus the electron beam emanating from the source; this comprises the electron optics and operates in an analogous way to light optics;

- A sample chamber, with movable sample stage (X-Y-Z), that is under a vacuum to prevent gas and vapour molecules from interfering with the electron beam on its way to the sample; a light microscope allows for direct optical observation of the sample;
- A variety of detectors arranged around the sample chamber that are used to collect x-rays and electrons emitted from the sample.

2.4 Major and trace element geochemistry using X-ray fluorescence (XRF)

The 70 samples which were collected from the Beestekraal and Lime Acres deposits were prepared for major and trace element analysis following the process as summarised in figure 2.7.

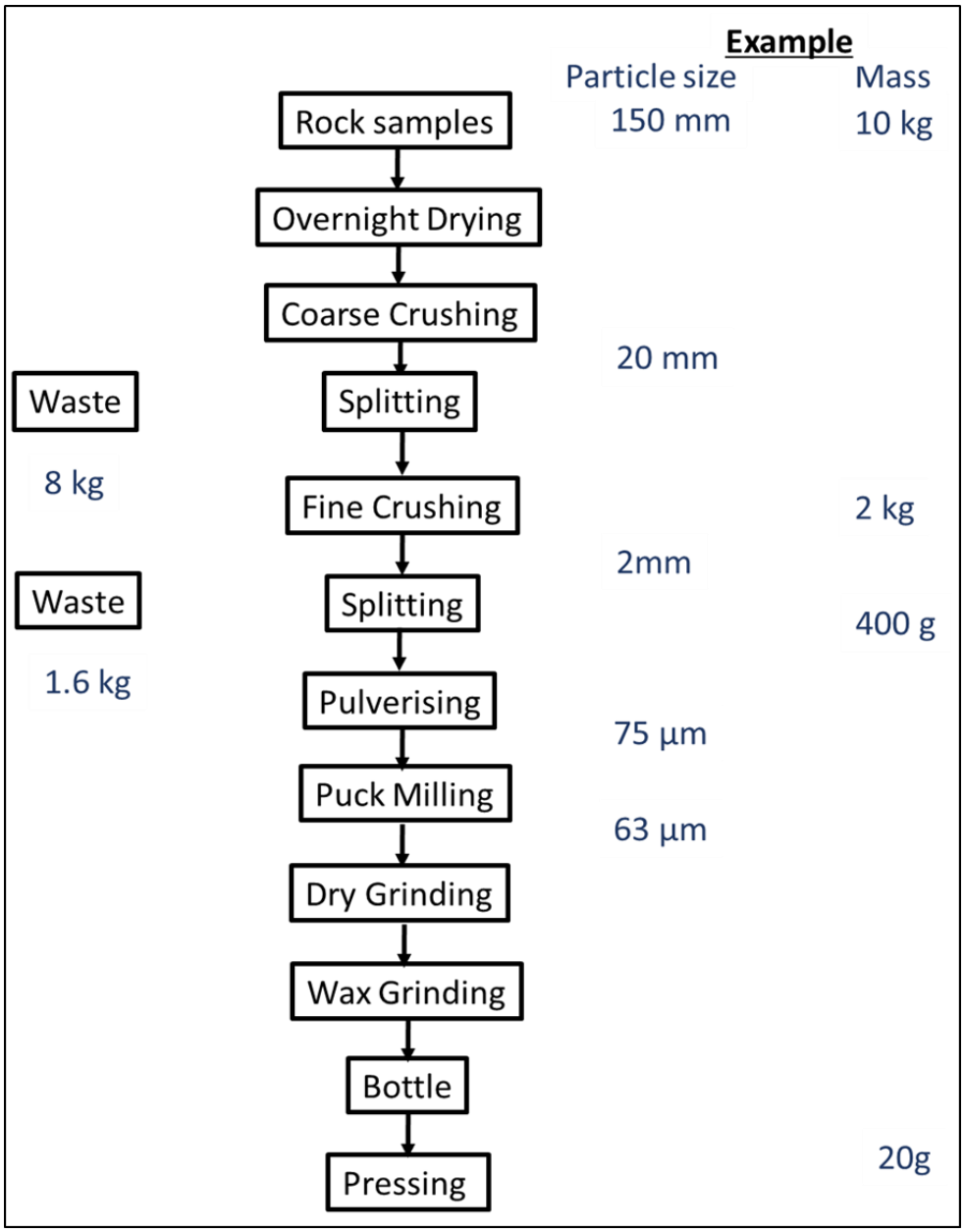


Figure 2.7 Steps in preparation of a sample for XRF analysis. The particle size and mass are given as examples (Modified from Willis *et al.,* 2014).

Mg/Ca measurements were performed on the XRF in a laboratory where “reference material accompanied by a certificate, one or more of whose property values are certified by a procedure which establishes traceability to an accurate realization to the unit in which the property values are expressed, and for which each certified value is accompanied by an uncertainty at a stated level of confidence” were used (Phophi, 2017).

2.5 Mineral identification (XRD)

Nottingham Myriad Solutions (2017) has described X-ray diffraction (XRD) as a versatile, non-destructive analytical technique that reveal detailed information about the chemical composition, crystallographic structure and physical properties of materials. In the case of powder diffraction, this technique is used to characterize the crystallographic structure, crystallite size and preferred orientation in polycrystalline or powdered solid samples (Nottingham myriad solutions, 2017).

Kisch (1991) recommended that sample preparation for XRD analysis should:

- Use a jaw crusher or hammer for initial reduction;
- Use a hammer mill with built-in sieve, or possibly a porcelain or agate mortar and pestle for limited periods (=30 s) with sieving between use;
- Avoid use of disc or swing mills and ball mills, except for short grinding times that can be shown not to affect the IC of the <2-pm size fraction.

Chapter 3
Methods

3.1 Field data

Two active limestone mining areas were chosen for the petrology, XRD, XRF, EMP and structural geology analysis. Both study areas occurs in rocks of the Transvaal Supergroup of South Africa ,with the Beestekraal Mine located outside of Brits in the North West Province, where the Limestone of the Oaktree Formation in the Malmani Subgroup, while the Lime Acres site occurs on the Campbellrand Subgroup which is in the Northern Cape Province. The Campbellrand limestone was chosen as it contains high content of calcium and has preserved a lot of the sedimentary structures. The Malmani limestone has been extensively studied and has little sedimentary structures. A decision was taken to compare the two Subgroups which have already been correlated by age.

Geological field mapping was carried out, with data collected including photographs, descriptions of sedimentary textures, strike measurements; dip measurements; depth measurements and the collection of physical samples. Using a clinometer data was collected by taking measurements on various locations of the exposed mining faces.

The Beestekraal mine in the Oaktree Formation limestone extends over a seven hectors (Ha) area, and is mined to about 123 m in depth with 1 km width. The mine has limestone that is mined for the purpose of producing cement, surrounded by a highly dolomitized zone. 40 representative samples were collected on the eastern hanging wall and the western foot wall of each working bench. This was conducted to represent the different sections of the vertical section as per figure 3.1.



Figure 3.1: Beestekraal's Mining face.

The 30 samples collected from the Lime Acres mine were representative of the vertical interval of a stratigraphy as figure 3.2. The carbonate deposit is estimated at 3000 m thick and the limestone is being mined for the production of lime to a maximum depth of 85 m. The samples collected were large (~100 g), this was done to ensure that the sample would be sufficient for all the required analysis. Some drilled core was available at Lime Acres during this study and logging was performed to verify the sedimentary structures that Lime Acres has preserved.

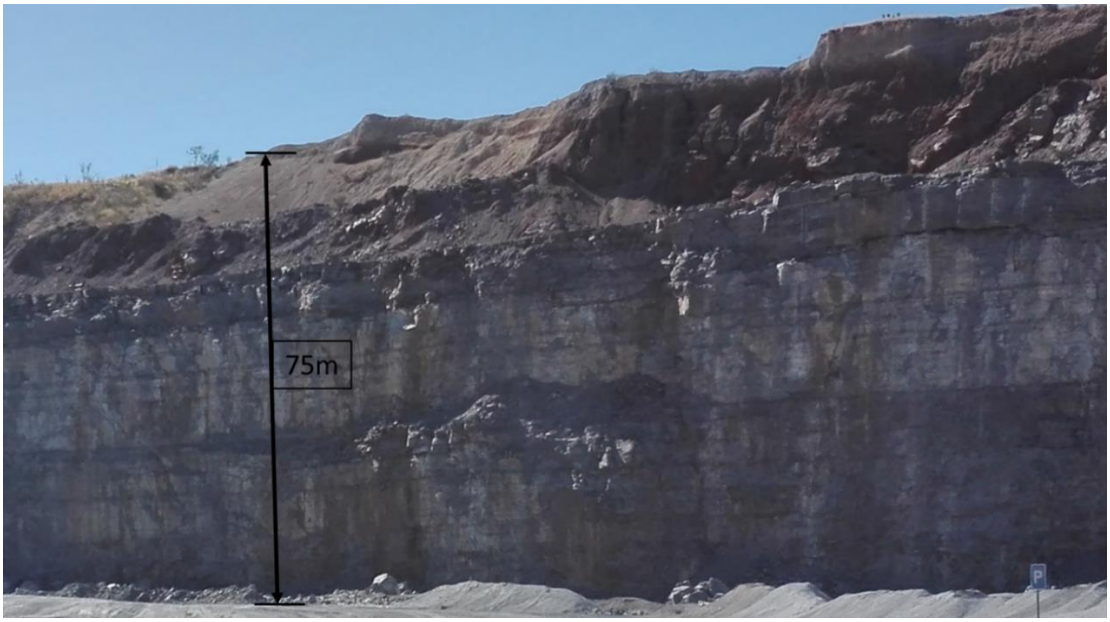


Figure 3.2: Cross sectional indication of Lime Acres' Mining face.

3.2 Thin Section Petrography and Electron Microprobe (EMP)

EPMA standards were applied in the preparation of the 50 µm polished thin sections. These were prepared by first using a saw to cut the sample along the predetermined and marked lines to a size that is <40 mm across the representative stratigraphic column. These were then cut smaller using a trim saw. The samples were cleaned then allowed to dry. The side of a thin section which will be analysed was polished to remove marks from the saw blade using an automated grinder to coarsely ground the sample then grit powder (silicon carbide) and water were used in the grinding process. The sample was smoothed further by hand on a glass plate using fine grit powder then it was impregnated with araldite to fill pores spaces. The sample was then placed on a glass and mounted together under pressure using epoxy and hardeners. Once the two were glued together the edged of the sample were cut away from the glass leaving a thin slab of rock glued to the glass. The cover slip was not added as the 50 µm sample were analysed under a microscope.

The sedimentary structures and textures were analysed under a microscope under reflected and transmitted light. Properties analysed included morphological aspects such as grain shape, cleavage, fracture, deformation-recrystallization, twinning and optical characteristics such as colour and light refraction. Some of the samples that were polished and analysed under a microscope were polished further for EMPA. The points of EMP analysis were marked on the polished samples. These samples were then analysed using an EMPA for point analysis of sedimentary composition. The Mg/Ca ratios of the EMP analysis were plotted and compared to XRD and XRF data analysis.

Electron probe microanalysis (EMPA) was performed using a Cameca SX-5FE electron microprobe equipped with 5 WDS spectrometers housed at the MMU (Microscopy and Microanalysis Unit) of the University of the Witwatersrand. Analytical conditions were 15 kV acceleration voltage and 20 nA beam current. Natural and synthetic standards were used for calibration. A 10 µm diameter electron beam was used during quantitative analysis. Counting times were 10 seconds on the peak, and 5 seconds total on the background, for all elements.

Carbonate analyses were standardized for Ca on calcite, Mg on dolomite, Mn on rhodonite and Fe on almandine.

The data was collected with CAMECA software. An automated X-PHI matrix algorithm was applied to correct for differential matrix effects. Oxygen was calculated by stoichiometry.

3.3 Major and Trace element geochemistry

A wavelength dispersion XRF analysed was used for the analysis of major and minor elements. The analyser was calibrated in line with ISO 17025 using primary and secondary reference standards where the primary standards were certified material of known concentrations. The reference material were in a form of melted glass beads and powdered pallets. This is done to ensure accuracy of both major and minor element analysis. The beads were prepared by fusing the samples at high heat to eliminate mineralogical effects therefore some of the volatile minor elements were lost due to the heat. The minor elements were therefore calibrated using the powdered pallets of known concentrations. Multiple reference material of known variable concentrations (low to high) were used to create a calibration curve, which was then used to measure the concentrations of each sample. Counting statistics of the XRF then produces qualitative mass based results.

The 70 bulk samples that were collected form the mine were initially cut to a size which ranges from about 150 mm to 100 mm. To ensure that all excess moisture was removed; all the collected samples were dried at 45° overnight. These samples were then coarse crushed to reduce the size to about 20 mm, the crushed samples were further crushed using a smaller crusher to further reduce the size to about 2 mm. A riffling splitter was then used to get a representative sample of about 400 g. The representative sample was then pulverised through further grinding to produce a 75 µm particle size which was then puck milled to form a particle size of 63 µm. The sample was again split in half and pulverised further to get to a <44µm of a 20g sample. At this stage the sample may be fine and stick on ring mill therefore should be cleaned using only a clean and dry paper towel. Where the sample was composed of high silica then binders (i.e. Sasol wax) was added to the milled sample and mixed with the sample properly.

An aluminium cup was labelled and used to press the powdered pill using the Herzog Press. The cup was first filled with the sample and compacted on the surface. The base of the cup was cleaned then placed into the press bore of the Herzog Press. The start button was pressed then the aluminium was automatically pressed to create a pressed powder pill for Major and Trace element geochemistry.

The Mg/Ca ratios of the limestone samples collected in Beestekraal and in Lime Acres were quantified using the X-ray fluorescence (XRF) technique.

3.4 Mineral identification

Powder specimens were prepared for quantitative XRD analysis. These specimen were prepared as follows;

Crushing:

- Before each sample was prepared the crusher was decontaminated as follows;
  - Front jaw and small holder was removed;
  - Jaws and surfaces within the vicinity of the crushing area were brushed with mire brush;
  - Using Acetone and paper towel, surfaces were wiped off excess dirt and dust;
  - All excess paper towels were vacuumed from the surface;
  - The sample collection tray was cleaned using water then wiped with acetone and drying with a paper towel;
- Place removable jaws and sample collection tray back into the jaw crusher;
- The <250 g sample was then dropped into the wedge between the jaws of the operating jaw crusher;
- Once the jaws stopped moving the crushed sample which fell into the tray was removed and placed into a clearly sample bag.

Milling of the crushed sampled was performed as follows:

- At the start of each sample the mill bowl was decontaminated as follows;
  - A scoop of quartz was placed between the rings inside the bowl;
  - The bowl was placed inside the mixing machine;
  - The quartz was then milled for 30 seconds;
  - After milling the bowl was removed, brushed then wiped using a paper towel;
  - The rings and mill surface were cleaned using a paper towel and acetone;

- The cleaned items were reassembled and allowed the next sample was prepared for milling;

- 40-60g of the jaw crushed sample was placed in a carbon steel bowl equipped with several carbon steel rings and mechanically shaken the bow in the milling machine;
- The sample was milled for 2 minutes until it was fine.

The pulverised sample was then placed into the glass mount and pressed using a glass slide.

Chapter 4

Results

4.1 Beestekraal

4.1.1 Lithostratigraphy

Beestekraal Mine is located outside of Brits in the North West Province, where limestone of the Oaktree Formation of the Malmani Subgroup occurs. Geological field mapping was carried to look for sedimentary textures and collect physical samples.

The mineralogical variations on the exposed material at Beestekraal were noted through mapping of the footwall which lies east of the quarry. Beestekraal has reddish-pink dolomite which is characterized by minor iron staining and is medium grained. The evidence of leaching was noted from about 50 m in depth where the limestone was stained.

The brittle chert band which is over 1 m thick occurs at 28 m below surface where deformation of sedimentary structures was prevalent. This band is followed by light grey limestone and dolomitised areas which have carbon parting/chert where the chert occurs in a form of laminae within the limestone. In this area +10 m of micritic dolomite with interbedding of light grey and medium grey dolomite dominates the exposed mining face of the stratigraphy. From about 40 m Beestekraal presents light grey limestone with a thickness of about 6 m where the dominance of calcite rich veinlets and dolomite blobs was noted. This is underlain by medium dolomite with evidence of leaching in parts and fine grained. The dolomite is dominated by veinlets of calcite. The underlying limestone has chert blobs, which are coarse grained and dark grey to black in colour. Below 90 m of depth there is a dominance of medium grained limestone. The coarser grained limestone lies below 114 m and has well defined crystals of calcite with no evidence of calcite veinlets. Figure 4.1.1 shows the details of the mineralogical variations mapped at Beestrekraal. The calcite veinlets which were noted range from 1 mm to 5 mm in thickness. The veinlets cross-cut the lithology at a dip of 70-90 degrees.

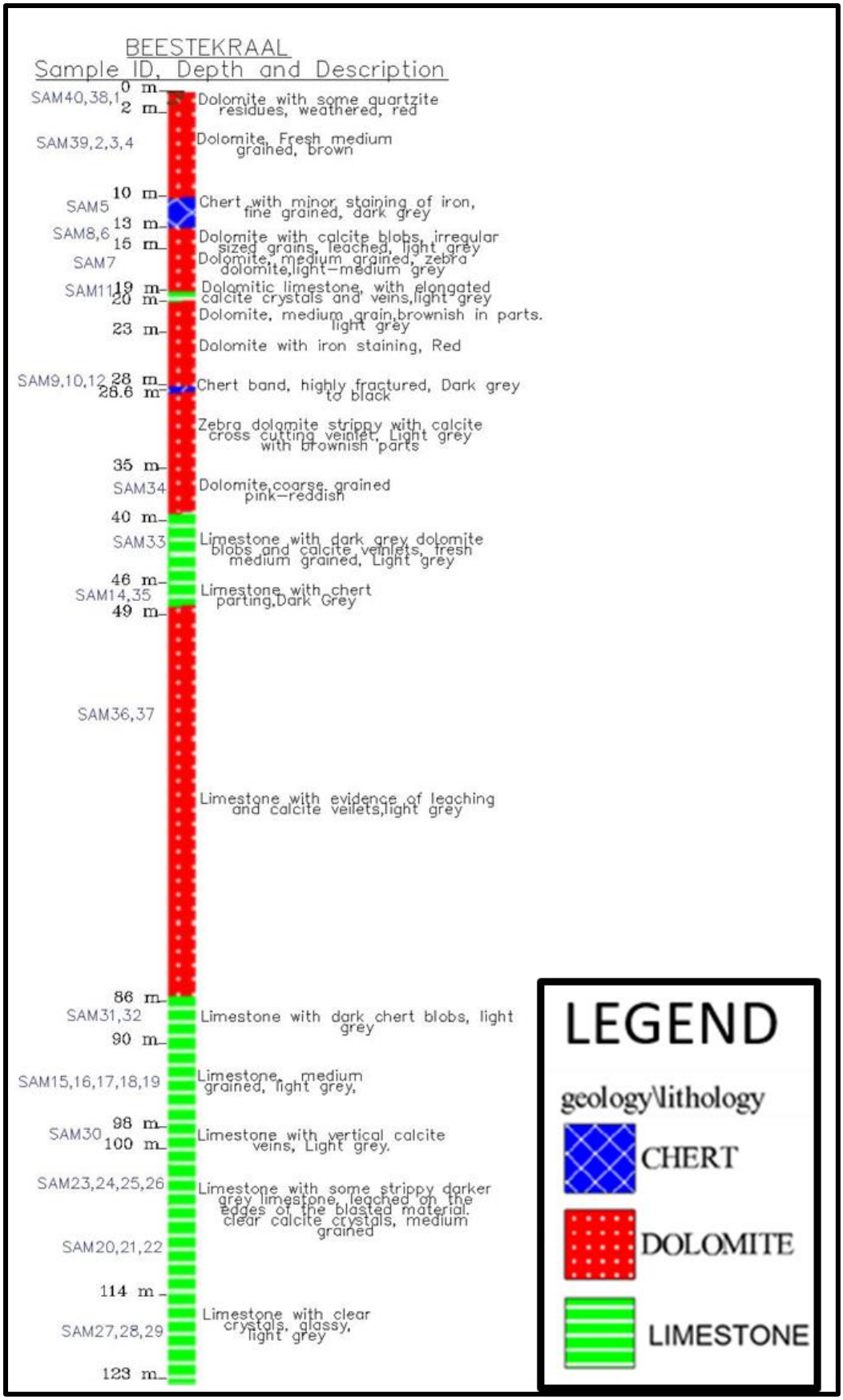


Figure 4.1.1: Lithostratigraphical log of Beestekraal's exposed face.

4.1.2 Structural Geology

Geological field mapping was carried out where data that was collected included photographs, measurements of strike; dip; dip direction and depth measurements.

There are four minor near surface faults that were noted at Beestekraal; these are shown in figure 4.1.2 and Appendix 1. These faults are all near vertical dipping and present with shifting of 0.4 m - 1.6 m. Fault 1 was noted at the area where there is no economic mining activities. The area shows movement of about 1.6 m movement at a southerly 56^{o} of dip. There was dense brittle carbonaceous material around the fault. The faults which have been labelled as fault 2 (F2) and fault 3 (F3) on Appendix 1, has a 82^{o} and 87^{o} dip towards the south with no notable shift of the vertical calcite veinlets, which dominate the faulted area. These faults are near vertical and parallel to each other with a spacing of less than 2 m between the faults. Fault 4 is a southerly dipping fault with a 70^{o} dip. Both fault 1 and 2 represent normal faulting. As can be noted in figure 4.1.2, Beestekraal has dipping angle differences between the ore and the hanging wall material where the ore ranges from 20^{o} to 35^{o} towards the north. The foot wall material ranges from 31^{o} to 33^{o} towards the north of the pit. Calcite filled near vertical joints were noted with three major joints being labelled as J1-J3 in Appendix 1. The W-E Joints have a dip which ranges between 76 m to 86 m and are filled with calcite veins of 2-5 mm in thickness.

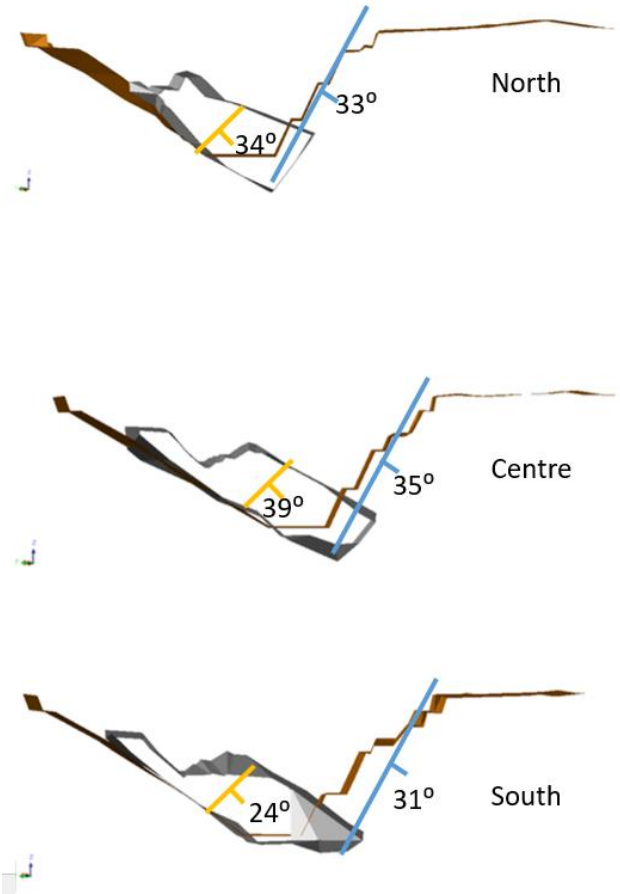


Figure 4.1.2: West-East cross sectional view of the Beestekraal quarry with indications of dip and strike.

4.1.3 Thin Section Petrography

The mineral content and textural features of the samples were examined at under a microscope where the crystal shapes were used to identify mineralogy, textural relationships and determine crystallisation history. The sedimentary textures and structures discussed in this report can be seen have been described in Appendix 3.

At the top 10m there is crystal structure with a dominance of re-entrance angles on the edges of the limestone and dolomite crystals (see figure 4.1.3). These re-entrance angles show an event where some new crystals were introduced while the crystal was still forming. The sample further showed the dominant calcite veinlets which were noted throughout the deposit. These veinlets are shown in figure 4.1.4, where twining is evident on the coarse grained crystals along the veinlets of calcite, while silt sized quartz which have also been cut across have no notable sedimentary textures. As indicated in figure 4.1.5, there is some rounded chert nodules along the high magnesium calcites at depths of 15 m -19 m showing evidence of a diagenetic event where these nodules are introduced to the dolomite/limestone deposit. Fenestrae were noted at depths of 15 m -19 m in fine grained clay carbonates where infills of crystalline quartz have filled the vugs. The carbonates have elongated grain structure showing evidence of a second diagenetic event which occurred to have filled the cavities. Calcite crystals are well defined at depths of 19 m to 20 m and seem to have been deposited post deposition of the carbonate platform. There is preserved rhombic structures in parts which show elongation at depth, these could be due to the pressure exerted by the overlying deposit. At depths of 23 m -28m there is inter bedding of crystal structures forming laminae with varying colour and crystal size and crystal shape. There is prevalence of twining and quartz crystal infills on the contacts (see figures 4.1.6 and 4.1.7). There are faults which cut across the deposit where calcite veins and chert filled fenestrae were observed. At lower depths of about 90 m -96 m the hanging wall on the west of the quarry shows evidence of high pressure as a result of the faulting. This section of the deposit contains quartz as seen in figure 4.1.5. At depths of 100 m - 114 m there calcite crystals have re-entrance angles and twinning. This zone is being mined for cement manufacturing. The chert, which was described as brittle, has microcrystalline grains under a microscope.

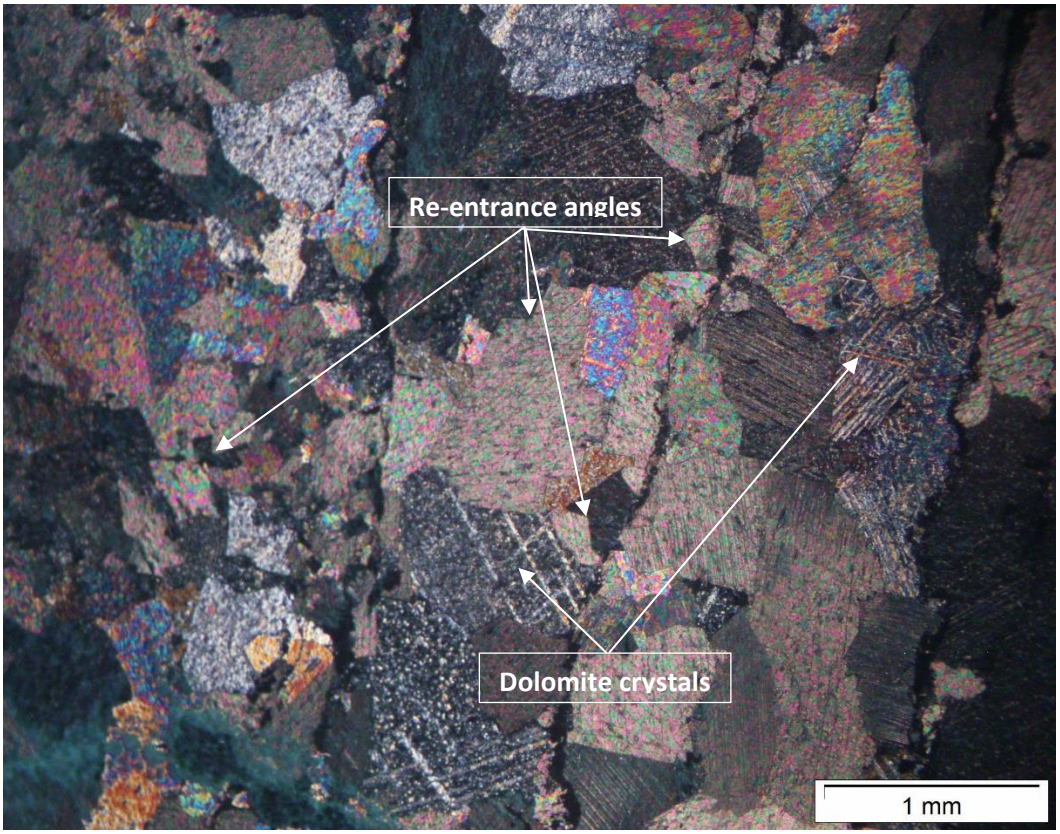


Figure 4.1.3. An indication of the crystal structure with re-entrance angles and twinning patterns.

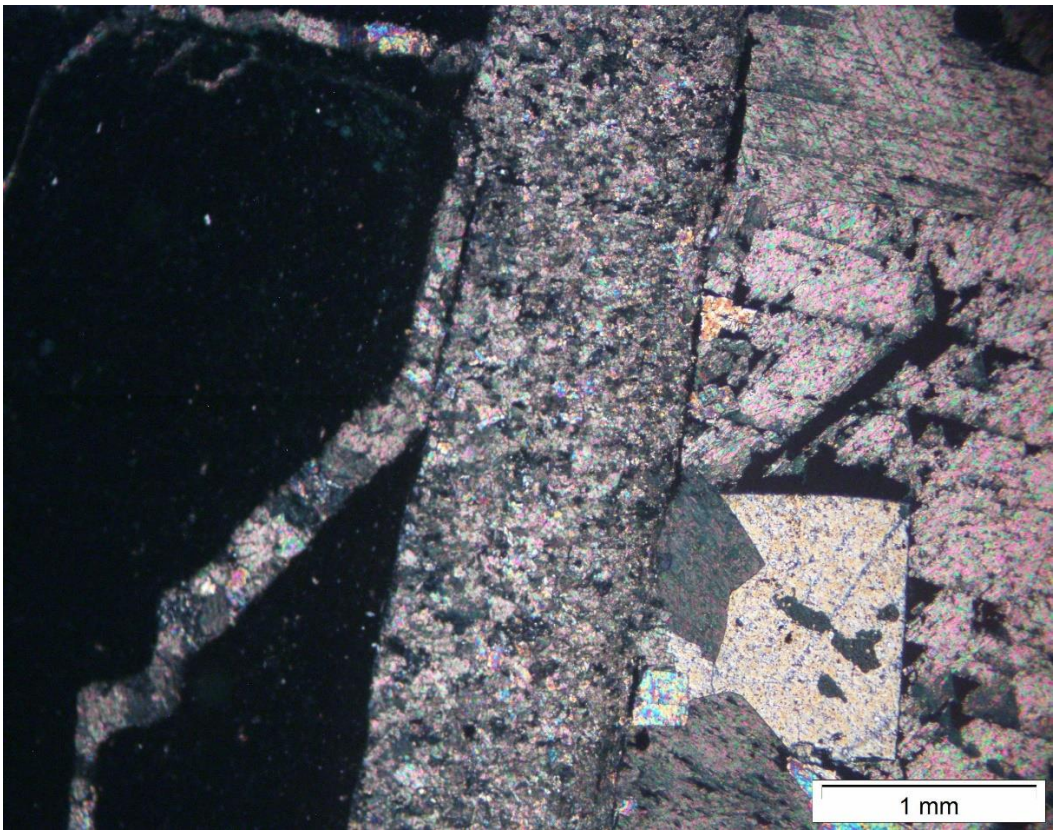


Figure 4.1.4 Calcite veinlets which cuts between the coarse grained crystals with twining and quartz in cementation.

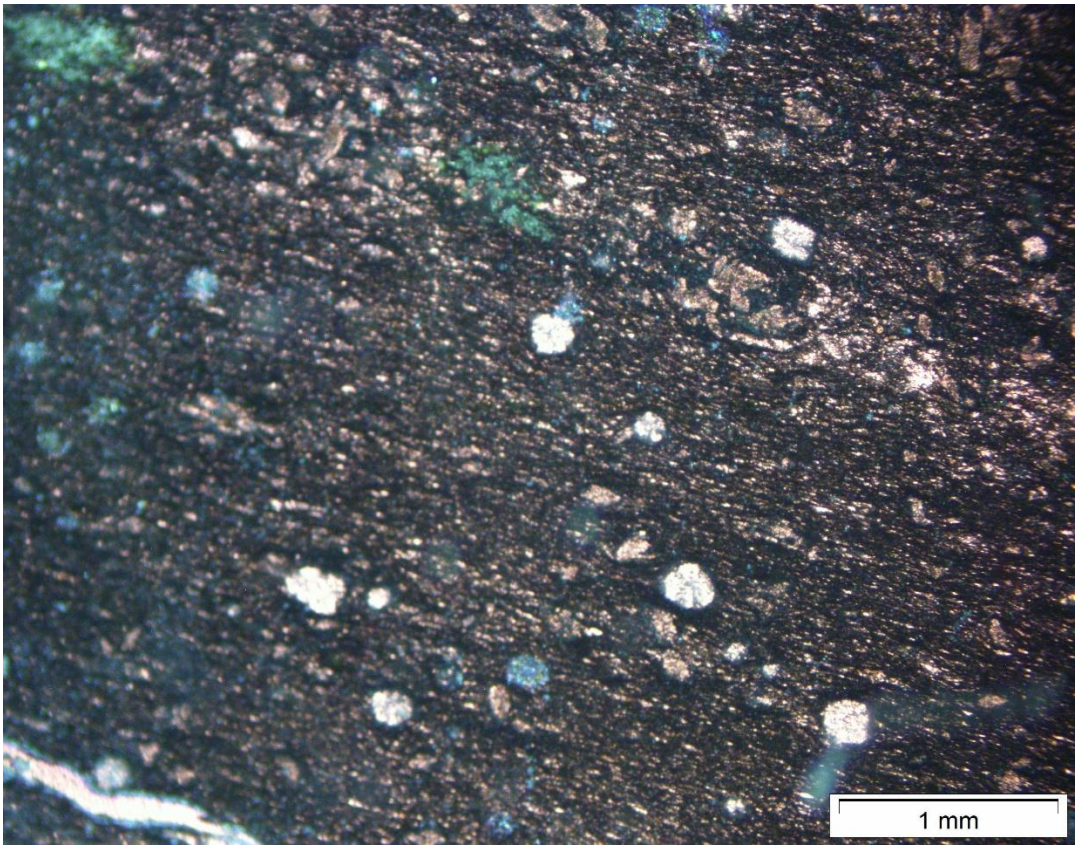


Figure 4.1.5 Fenestrae filled with chert nodules in high magnesium calcites.

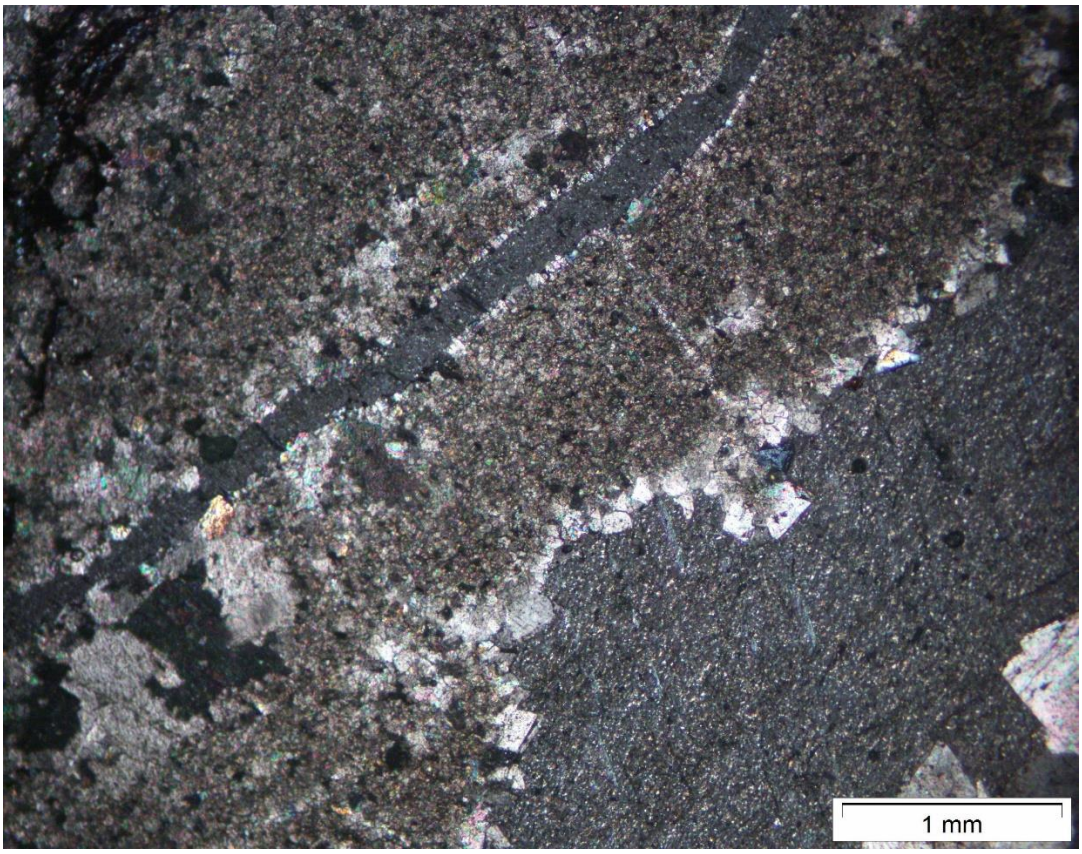


Figure 4.1.6 bedding plane showing the quartz crystals on the contacts.

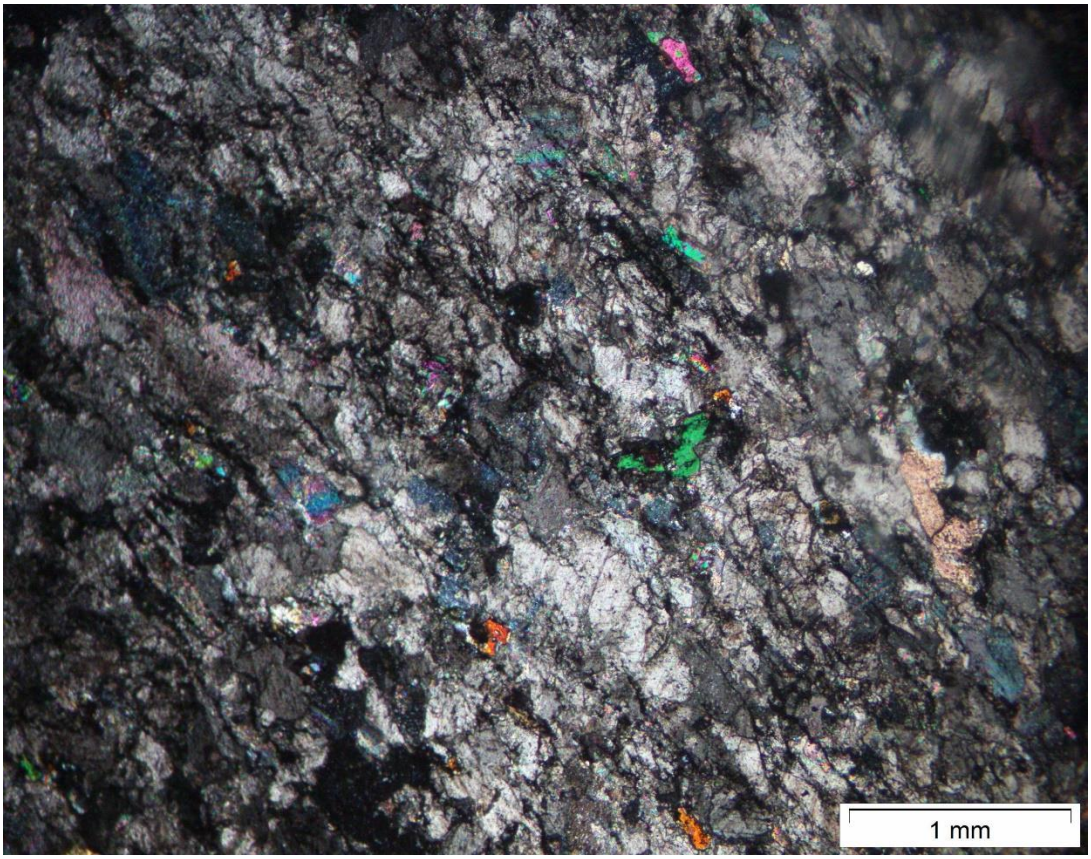


Figure 4.1.7 Deformed crystals of dolomite with some quartz inclussions.

4.1.4 Major and Trace element geochemistry

The Mg/Ca ratios of the samples collected in Beestekraal were quantified using the XRF technique. Complete geochemical data for all samples is provided in Appendix 5.

Dolomites found at the top part of the Beestrekraal quarry have high calcium and relatively lower magnesium content, which results in Mg/Ca ratios of less than 0.2. Figure 4.1.8 shows that the Mg analysis is lower than 10 molar percentage, Ca that is lower than 40 molar mass percentage. Mg/Ca ratios which are provided in figure 4.8 are not relational to depth, but relate to the variation in dolomite, calcite and quartz content. There seems to be no regular path for the Mg/Ca ratios and all Mg/Ca ratios are lower than 1.5 throughout the pit except for three of the samples. Two samples have Mg/Ca ratios of 1.5 - 2. There is only one sample which has been treated as an anomaly and excluded from the scatter graph in figure 4.1.8. The anomaly sample has Mg/Ca ratio of 5.7 and was taken from the brittle chert at about 28 m below surface.

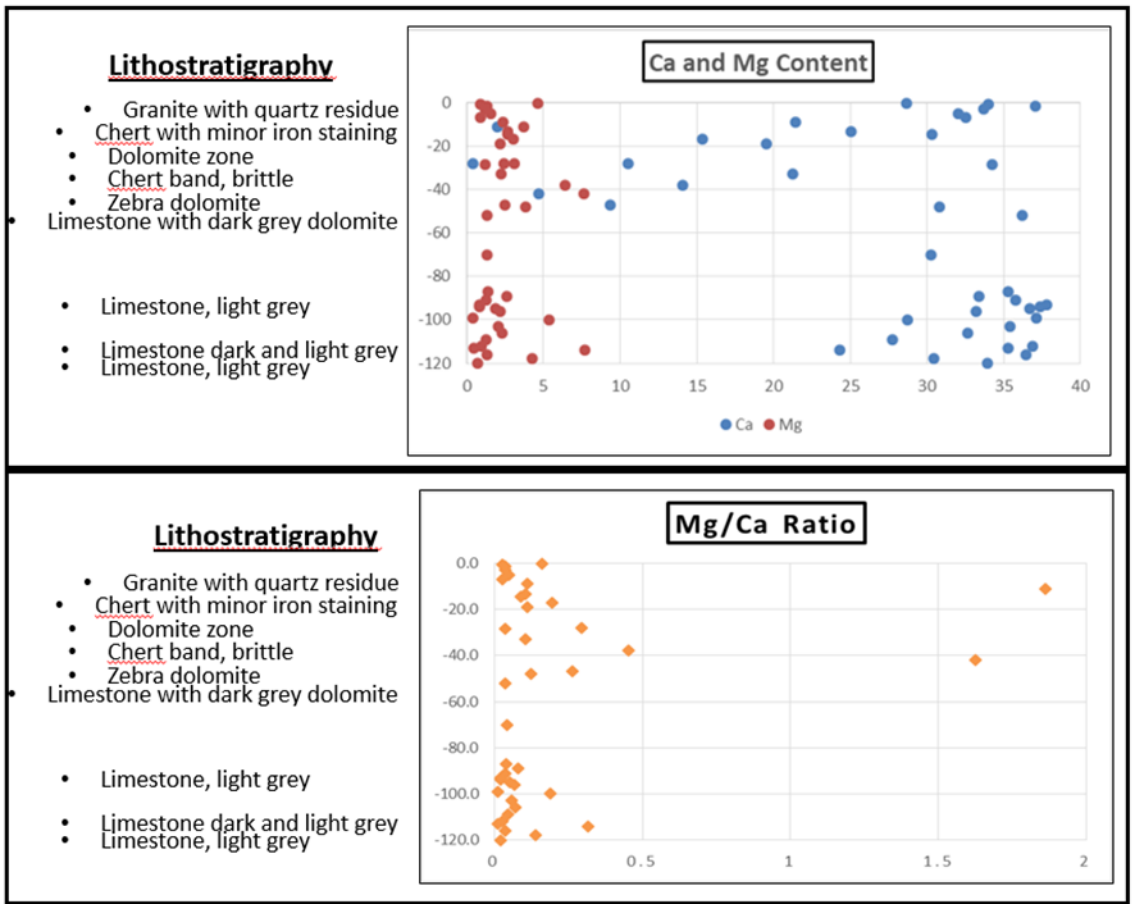


Figure 4.1.8 Calcite Magnesium representation at Beestekraal and Mg/Ca ratios with corresponding depths and brief field descriptions of the samples.

The economic zone of limestone has calcium content in excess of 28 molar percent and magnesium content of less than 5 molar percent. This data has shown that an increased calcite content is inversely proportional to magnesium content. The dolomites and limestones have low Mg/Ca ratio.

4.1.5 Electron Microprobe

The three samples that were analysed through EMP work are indicated on Table 4.1, where depth of sampling and field description are provided. The data on the EMPA analysis as presented in Appendix 6 was collected using point analysis of the different structure present on the samples. This data can be used to verify the bulk analysis conducted through XRD and XRF analysis.

Table 4.1 Samples analysed through microprobe showing the sample ID, depth at which sampling occurred and related field description.

Site	Sample ID	Depth	Field description.
Beestekraal	SAM 12	28 m -28.6 m	Dark grey to black highly fractures chert
Beestekraal	SAM 26	100 m -114 m	Light – dark grey limestone with leaching and clear calcite crystals
Beestekraal	SAM 21	100 m -114 m	Fault material, stylolite rich limestone

The dark grey to black chert, is which was noted as highly fractures has a notable mixture of high magnesium cementation and dark grey stylolite as respectively indicated in annotation 1 and 2 of figure 4.1.9. These stylolite were not visible under the naked eye and therefore not spotted during the field mapping. In SAM 12 these stylolite are found around the high calcium crystals, which are coarser grained. These have proven to have contents of 1.57 FeO, 20.2 MgO and 28.22 CaO.

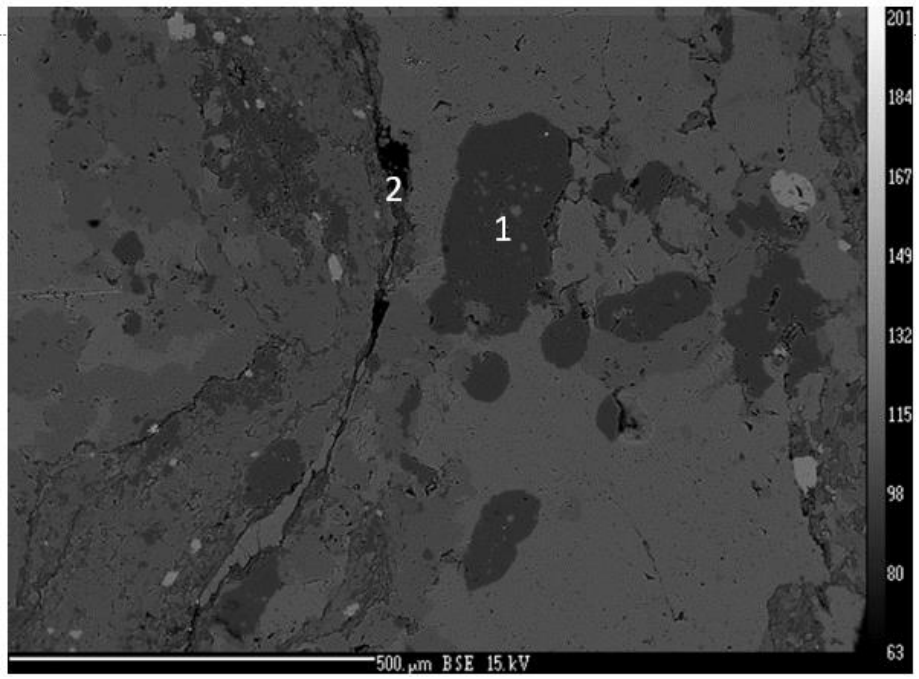


Fig 4.1.9 Microprobe image of the stylolite on Beestekraal sample SAM 12.

SAM 26 showed the contact between the limestone area and the fault hence the deformed point samples were noted where the light – dark grey Limestone with leaching had clear calcite crystals with cleavage lines that cut across each other. The sample has varying grain sizes ranging from fine grained to coarse grained. There is no relationship between the grainsize and the chemical composition. SAM 21 shows fault material with stylolite. The sample was consistent high in CaO content. There is no CaO content variation between the darker limestone and the lighter limestone and there was no notable difference in chemical composition between the infill material and the host rock.

4.1.6 XRD Analysis

SAM 1, SAM 33 and SAM26 were analysed via XRD.

The sample represented in figure 4.1.10 was taken in Beestekraal at a depth of about 0-2 m and described as a dolomite with quartzite residue. The sample was highly weathered and red in colour. This sample has proven to have the characteristics described in the field with a mixture of dolomite, magnesium calcite and quartz.

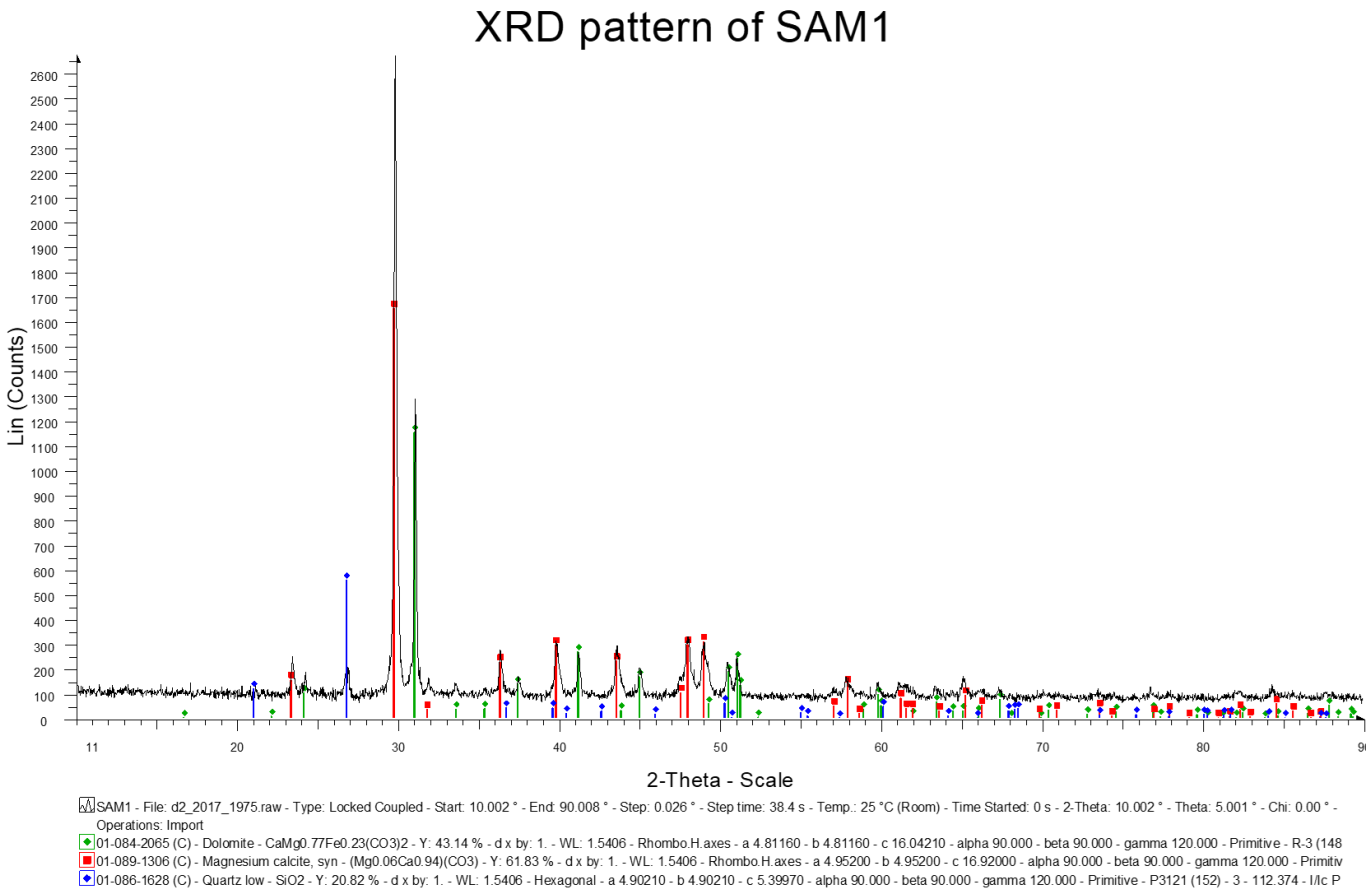


Figure 4.1.10 Whole rock XRD data for SAM1 showing dolomite (green) magnesium calcite (red) and quartz (blue) of SAM 1 collected in Beestekraal.

Sam 33 was sampled at depths of 40-46 m below surface at Beestekraal and described as a limestone sample with dark grey dolomite blobs and calcite veinlets. The fresh medium grained sample is represented in figure 4.1.11 as a highly magnesium calcite rock with some traces of quartz.

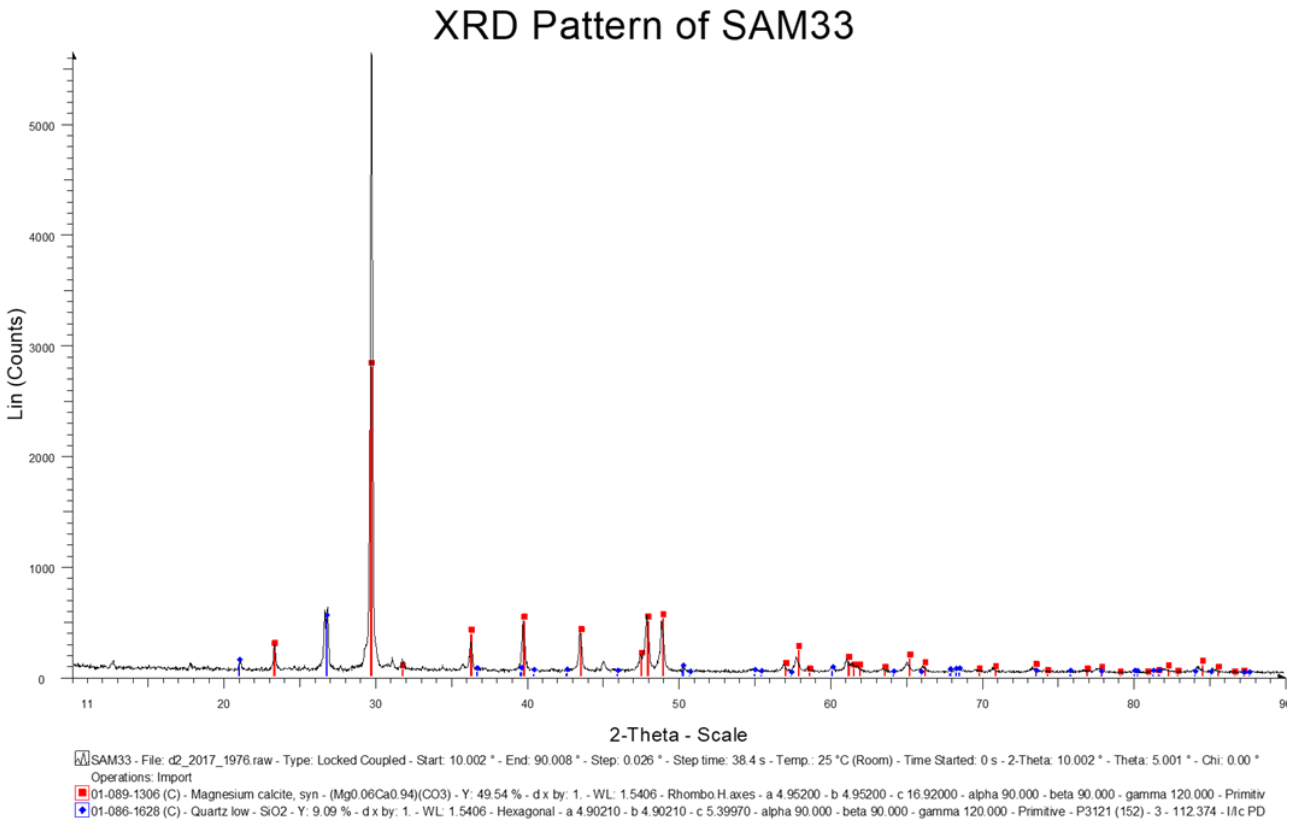


Figure 4.1.11 Whole rock XRD data showing magnesium calcite (red) and quartz (blue) of SAM 33 collected at Beestekraal.

Sam 26, a medium grained limestone with some darker grey limestone and evidence of leaching, was collected on one of the production faces, and showed that the magnesium calcite had some dolomite traces. Between the two parallel faults in the pit (F2 and F3) there was some material which is represented in figure 4.1.13 that shows magnesium content with quartz impurities.

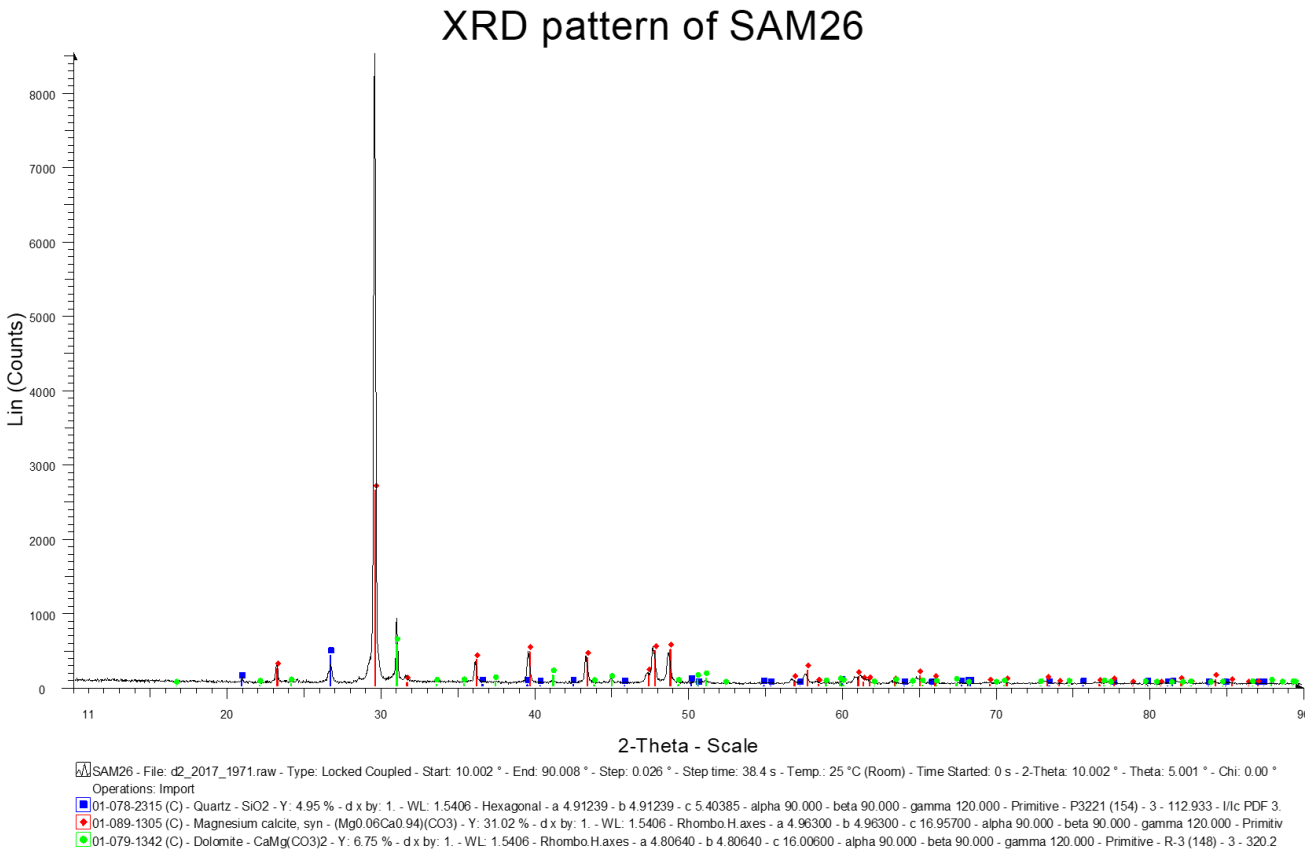


Figure 4.1.12 Whole rock XRD data showing dolomite (green) magnesium calcite (red) and quartz (blue) of SAM 26 collected at Beestekraal.

4.2 Lime Acres

4.2.1 Lithostratigraphy

Lime Acres is located north of Postmasburg in the Northern Cape Province, where limestone of the Lime Acres Member of the Campbellrand Subgroup occurs. Geological field mapping was carried out where data was collected included notes on sedimentary textures and physical samples being collected. Lime Acres was mapped to characterise the mineralogical variations on the exposed material. Lime Acres was mapped on a South-East direction of the pit as per exposed mining faces.

There was very little evidence of topsoil in Lime Acres as the top face and surrounding surface was dominated by fine grained and highly weathered Banded Iron Formations (BIF). The BIF pebbles are irregular shaped with no evidence of rounding therefore no suggestion of transportation. The BIF at depths of 2 m to 15 m below surface is more preserved and has chert bands, which are leached. This BIF forms as irregular shaped boulders in reddish clay matrix. From 15 m below surface some fine grained limestone with dominance of well preserves low pressure stylolite and leaching occurs. This limestone is underlain by well-preserved stromatolite which is hosted by dark grey dolomite with chert.

The brittle chert band which is over 1 m thick occurs at 27.5 m. Lime Acres has well preserved chert rich stylolite, within this zonation of dolomitised limestone. From about 40 m there is light grey limestone with a

thickness of about 1 m. Limestone with brittle chert partings underlies the chart band. The limestone has lenticles and calcite crystals which are well preserved. The limestone is underlain by dolomite blobs and chert within a limestone that is fine grained and light grey. The light grey limestone which lies between 39.5 m and 47 m has stylolites at the bottom. Another layer of dolomite blobs and chert underlies the stylolites. These blobs of dolomites overlie another bed of stylolites which is underlain by dark grey dolomite extending to a depth of 52 m.

From 52 m of depth there is light grey limestone with irregular dolomite blobs which is underlain by a well-defined and preserved 0.6 m thick stromatolite which is dark grey in colour. The next prominent stromatolite is 1 m thick and lies within the most economic limestone bed between 77 m and 78 m below depth. The stromatolite has features that are distinctly similar the stromatolic bed found at about 100 .5 m below surface. All the stromatolites are occurring within light grey limestone with stylolites.

It has been noted that material that lies at 52 m in Lime Acres presents chert blobs which were sampled. The blobs are particles of rocks that are irregular shaped. Figure 4.2.1 shows the details of the mineralogical variations mapped at the two sites. The calcite veinlets in Beestrekraal range from 1 mm to 5 mm in thickness with a dominance of veinlets that are about 2 mm. The veinlets cross cut the lithology at a dip of 70-90 degrees. Lime Acres has interbedded layers of dolomite and limestone which overlay each other. The sedimentary structures which have been noted in Lime Acres are a dominance of chert blobs, vugs on high magnesium limestone, stromatolite features, stylolite and stromatolites which are all well preserved.

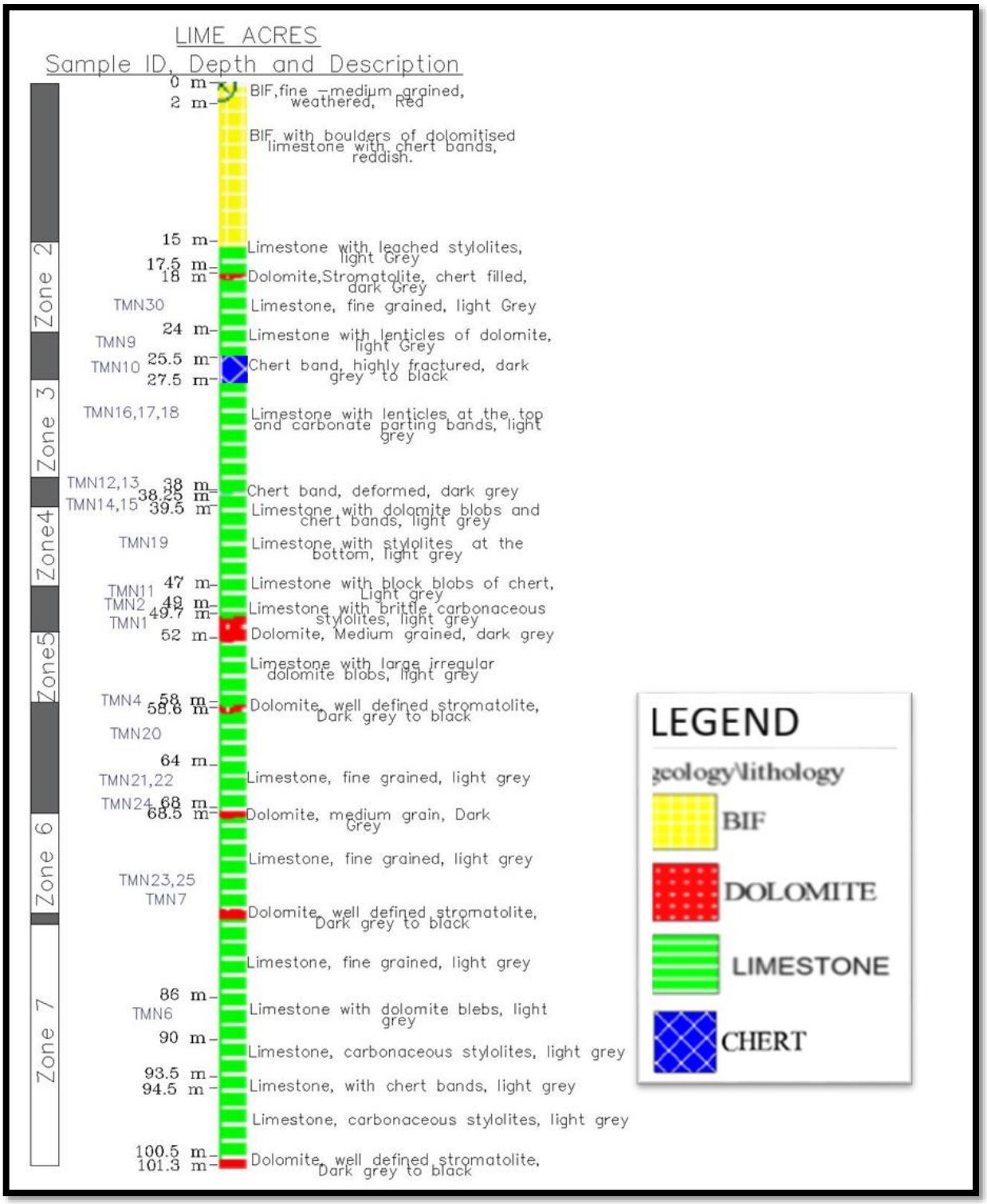


Figure 4.2.1 Cross sectional indication of the lithostratigraphic mapping at Lime Acres' mining face.

4.2.2 Structural Geology

There are two major near vertical N-S faults in Lime Acres and these are shown in figure 4.2.2 and 4.2.3 and Appendix 2. Fault 1 (F1) has boreholes around it therefore making it easier to map, the area that lies east of fault 2 (F2) had dolomitised therefore there is no borehole data on the eastern part of F2. Location of both fault 1 and 2 can be noted in figure 4.2.2 west-east cross sectional views of fault 1 has been displayed in figure 4.2.3.

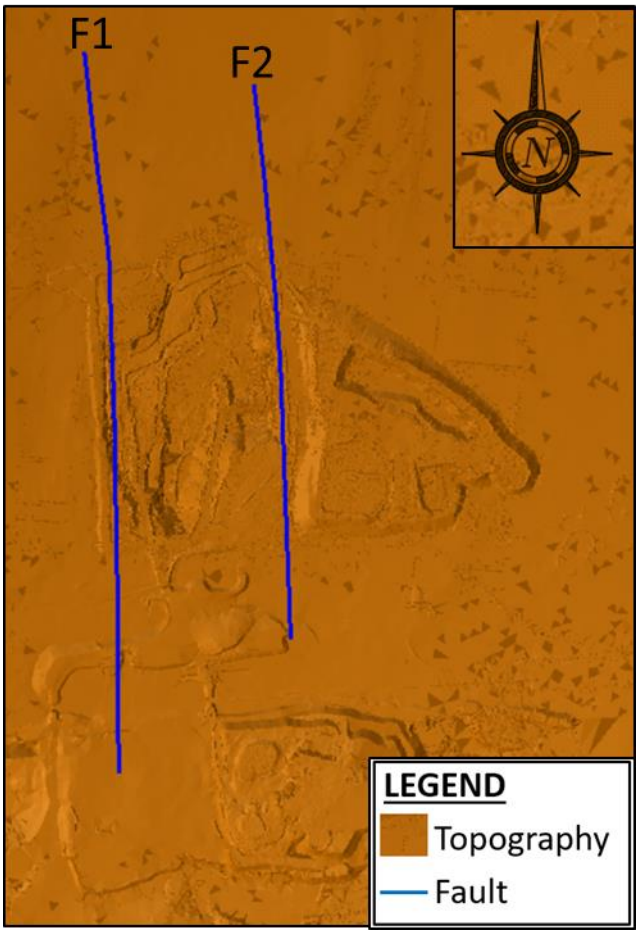


Figure 4.2.2 Fault 1 and Fault 2 as noted in Lime Acres. Fault 1 (F1) lies west of the existing quarry while Fault 2 (F2) lies on the Eastern edge of the quarry.

The Lime Acres ore lies at a westerly dip of 1.3^{o} - 2^{o} with well jointed limestone-dolomite successive layers. Fault 1 dips at 70^{o} and strikes N-S and can be classified as a normal fault with the existing stratigraphic layers on the east of Fault 1 being about 20 m deeper than similar features/ layers west of the fault. The area where fault 1 occurs is west of the current pit and is indicated as mud fissures on the exposure eastern wall.

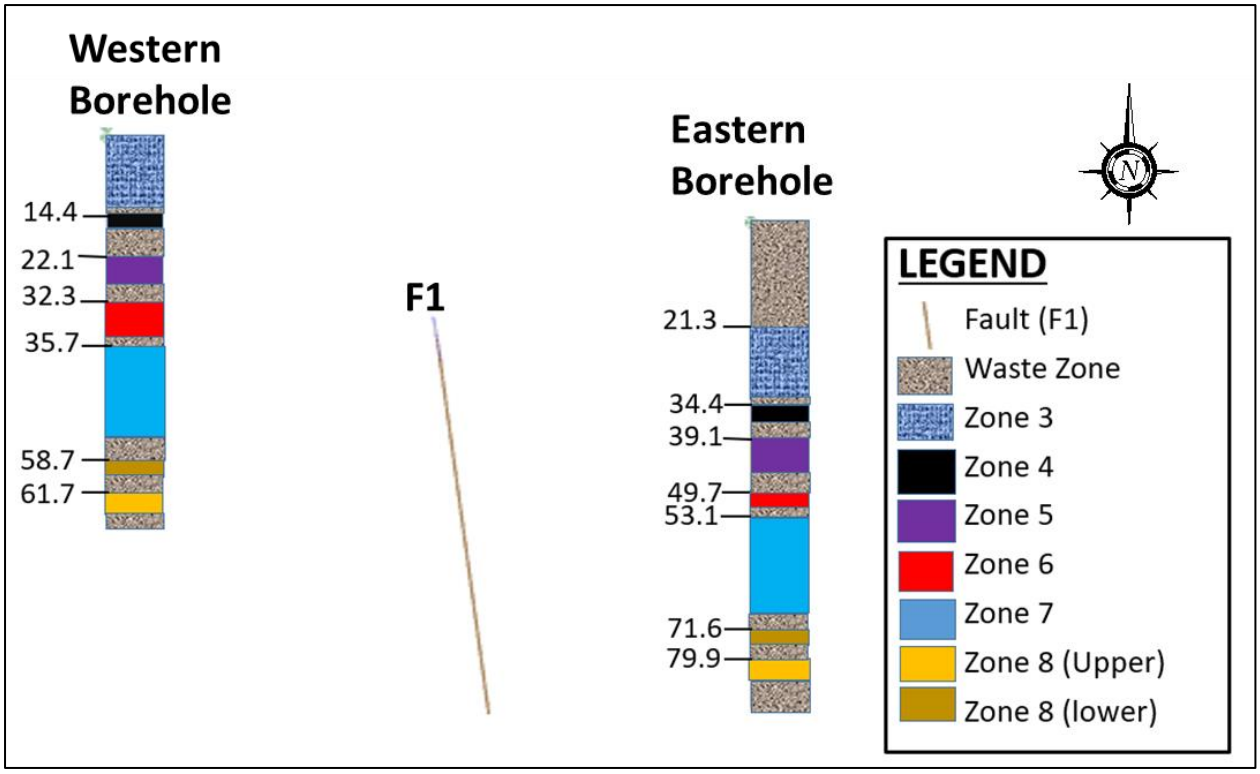


Figure 4.2.3 West-East cross sectional view Fault 1 with depth indications of how each limestone zone is shifted.

It has been noted that a dolomite quarry exists west of Fault 2. The dolomite has $MgCO_3$ content of about 40% and lies at depths of between 10 m – 27 m below surface. The dolomite which is being mined east of Fault 2 has coarse grained crystals and calcite sheets. The dolomite quarry is highly deformed with mud-fissures and clear evidence of weathering. Fault 2 is a normal fault however there is insufficient data to calculate the extent of the fault and the offset depth.

4.2.3 Thin Section Petrography,

The mineral content and textural features of the samples were examined at under a microscope where the crystal shapes were used to identify mineralogy, textural relationships and determine crystallisation history. The sedimentary textures and structures discussed in this report can be seen have been described in Appendix 3.

East of the fault 2 lies a dolomite quarry where it was noted that the crystal structures are deformed with no twining. The waste above the dolomite, which is being mined at depths of about 10- 25 m show low pressure stylolite which is well preserved and wavy, with opaque minerals forming along stylolite. The dolomite with quartz crystals and some hematite traces has been noted along the stylolite (blue line) as depicted in figure 4.2.4.

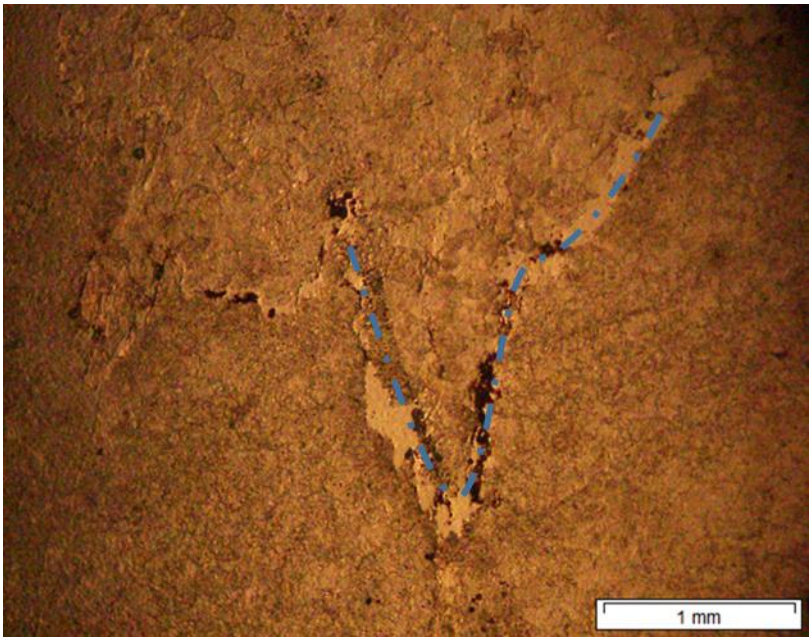


Figure 4.2.4: wavy stylolite on the fine grained dolomite with some quartz crystals.

At depths below 26 m where dolomite mining occurs a sample was collected. The sample is shown in figure 4.2.5 where fenestrae filled with coarse grains can be noted. The cleavage planes are prevalent with no twinning. The dolomite coarse grained crystals are irregular shaped with re-entrance angles.

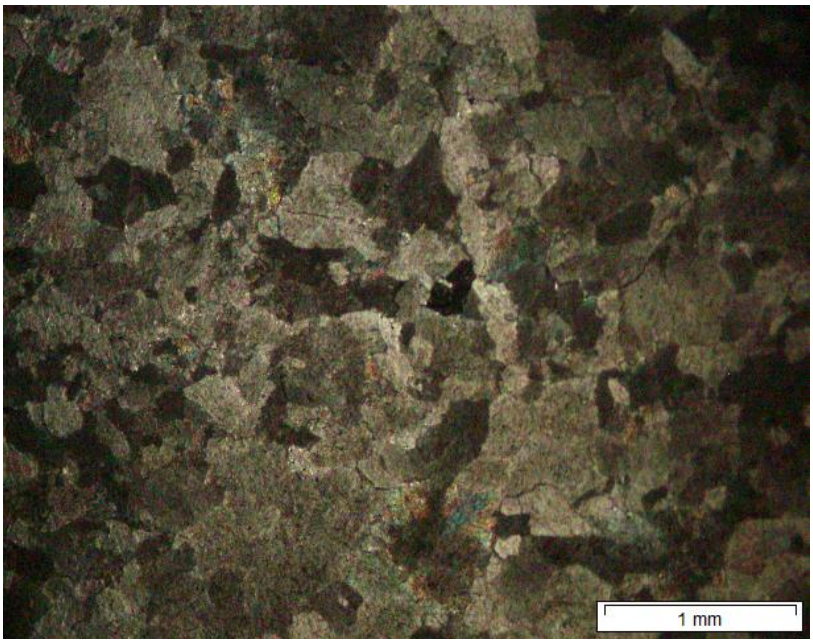


Figure 4.2.5 coarse to medium grained dolomite with fenestrae and re-entrance angles.

The limestone deposit, which lies west of fault 2 and east of fault 1, shows that there is evidence of fine grained particles that are in the upper dolomite samples where hematite has formed. On the shallow depths of up to 25 m there is a dominance of BIF and silty grained crystal sizes. The grains are graded from silt size to medium grain sizes of dolomite with poorly defined sedimentary structures. At depths of 38 m -38.25 m there is prominent re-entrance angles on the edges of the crystals as shown in figure 4.2.6. There seems to be some evidence of a second event where quartz crystals occur as inclusions introduced.

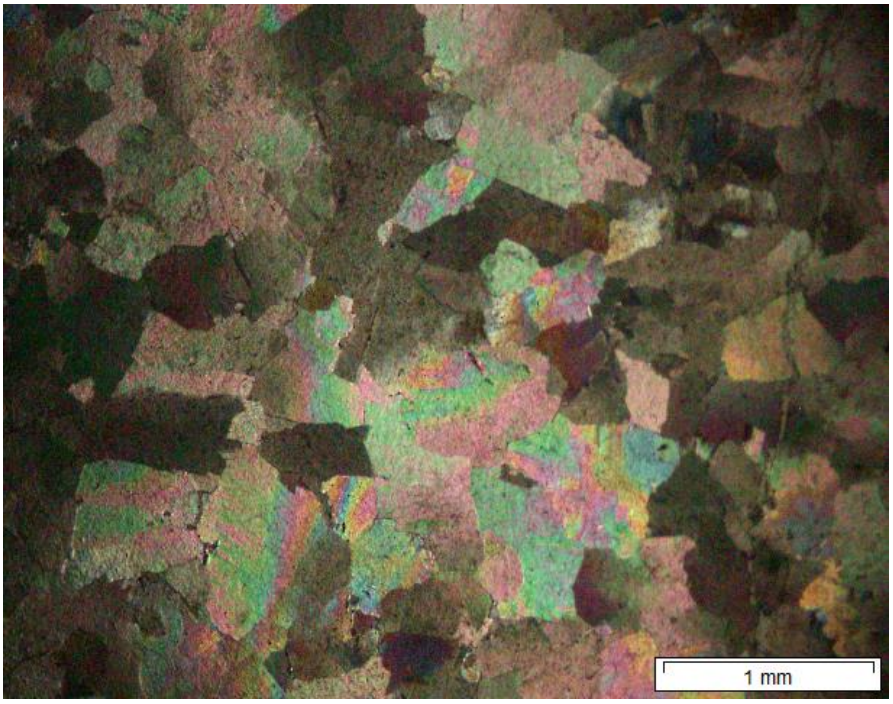


Figure 4.2.6 dolomite sample with re-entrance angles and no twinning.

At depths of 49 m - 49.7 m there is well defined coarse crystals that have twinning and some quartz crystals with evidence of two diagenetic events where the quartz crystals are silty in texture. Re-entrance angles are prominent on the coarse crystals as indicated in figure 4.2.7.

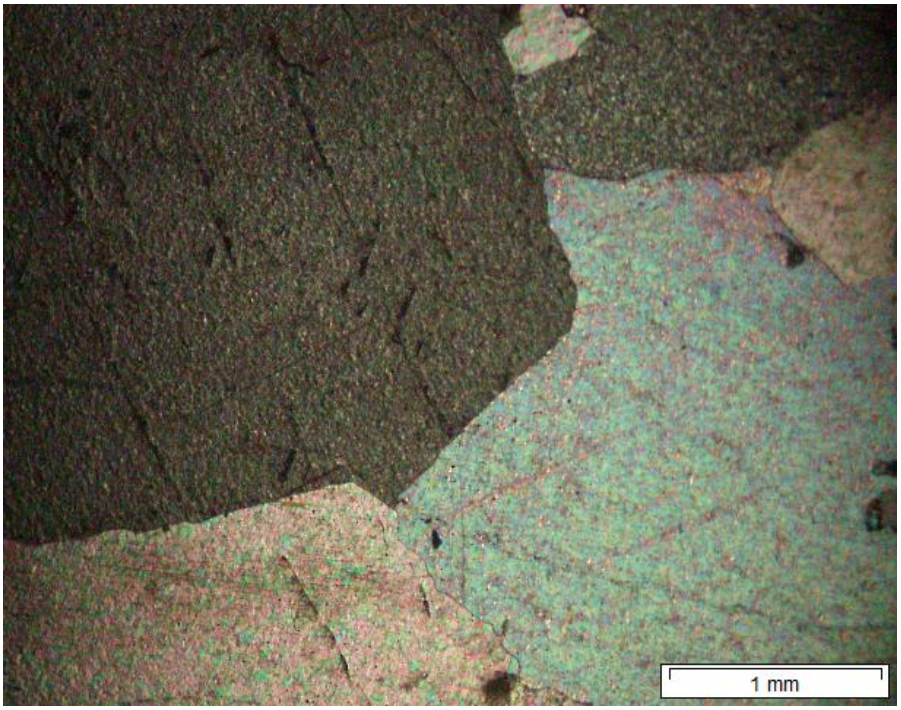


Figure 4.2.7 Coarse grained crystals with re-entrance angles.

Interbedding occurs where fine grained, deformed or rounded chert nodules along the high magnesium calcites showing evidence of a diagenetic event. There is a dominance of re-entrance angles on the edges of

the limestone and dolomite crystals therefore showing an event where some new crystals were introduced while the crystal was still forming. At depths of 58 m -58.6 m limestone with rounded cavities filled with finer grained clay was noted. There was also minor traces of finer grained hematite and quartz on the interlocked crystals of calcite. Fenestrae dominated samples that were collected at depths of 64 m -68 m. Figure 4.2.8 shows these samples which are also composed of varying grain sizes of calcites with elongated rhombic structures and coarse grained matrix where there cleavage and twining is well defined.

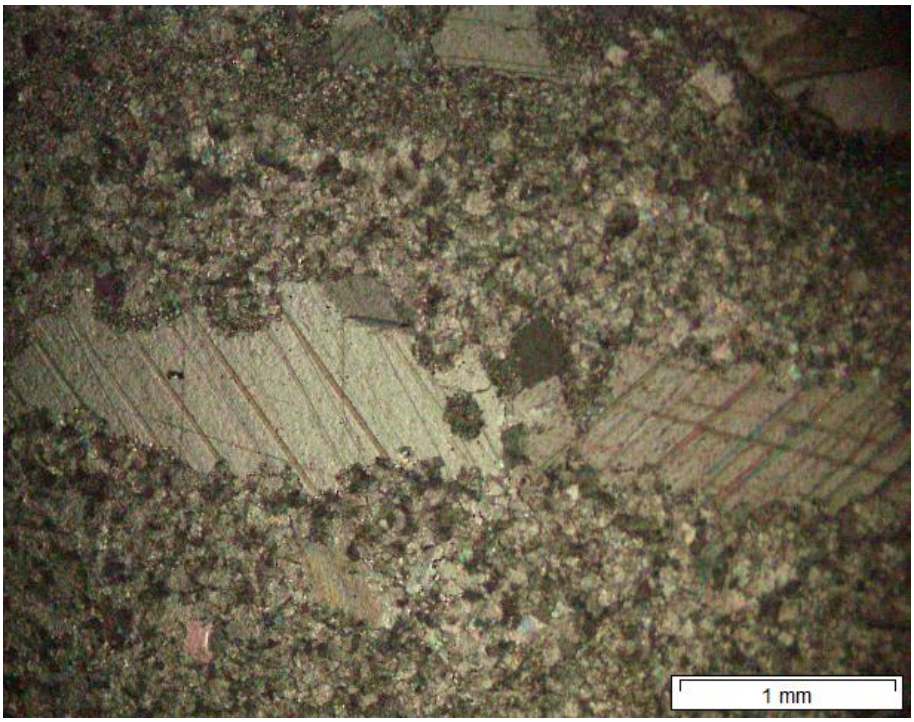


Figure 4.2.8 fenestrae in varying grain sizes filled with well-defined twinning structures.

There is transition of crystal sizes from medium grained to fine grained at depths of 68 m -68.5 m where there is the crystals are interlocked. The stylolite contact is of medium grained and silt sized crystals, and it is of high pressure. The styolites are the contacts found between the interbedded materials. In Figure 4.2.9 the samples collected at depths of 68 m -86 m shows irregular shaped silicate crystals are surrounded by fine grained crystals. These are hosted by medium grained dolomite with diminished sedimentary textures or structures. Below these some cavities have been noted. These cavities are filled with fine grained material and compressed to form stylolites. Well-developed crystals of calcite are dominant at 86 90 m depth.

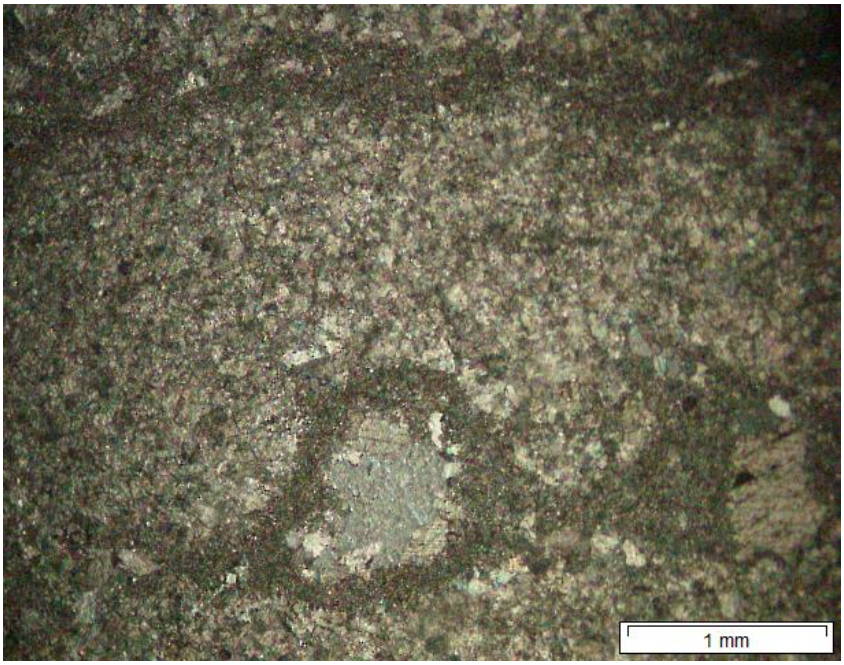


Figure 4.2.9 Irregular shaped silicate crystals are surrounded by fine grained crystals.

There is an abundance of well-defined stylolite found in the deposits where the limestone and dolomite bedding forms a contact. The beds were squashed together therefore forming sedimentary structures of wavy stylolite under pressure.

4.2.4 Major and Trace element geochemistry

The Mg/Ca ratios of the samples collected at Lime Acres were quantified using the XRF technique. Complete geochemical data for all samples is provided in Appendix 4.

The dolomitised area, which lies east of Fault 2 (F2) is mined for dolomite, with an economically viable zone extending from about 15 m to 26 m in depth. This zone has Mg/Ca ratios below 1. The calcium values are on molar percentage and Mg/Ca ratios are shown with correlating depths in figure 4.2.10. The Mg/Ca values that are less than 0.2 are dominated by waste material in the dolomite quarry where Si content is relatively higher as shown in Appendix 4.

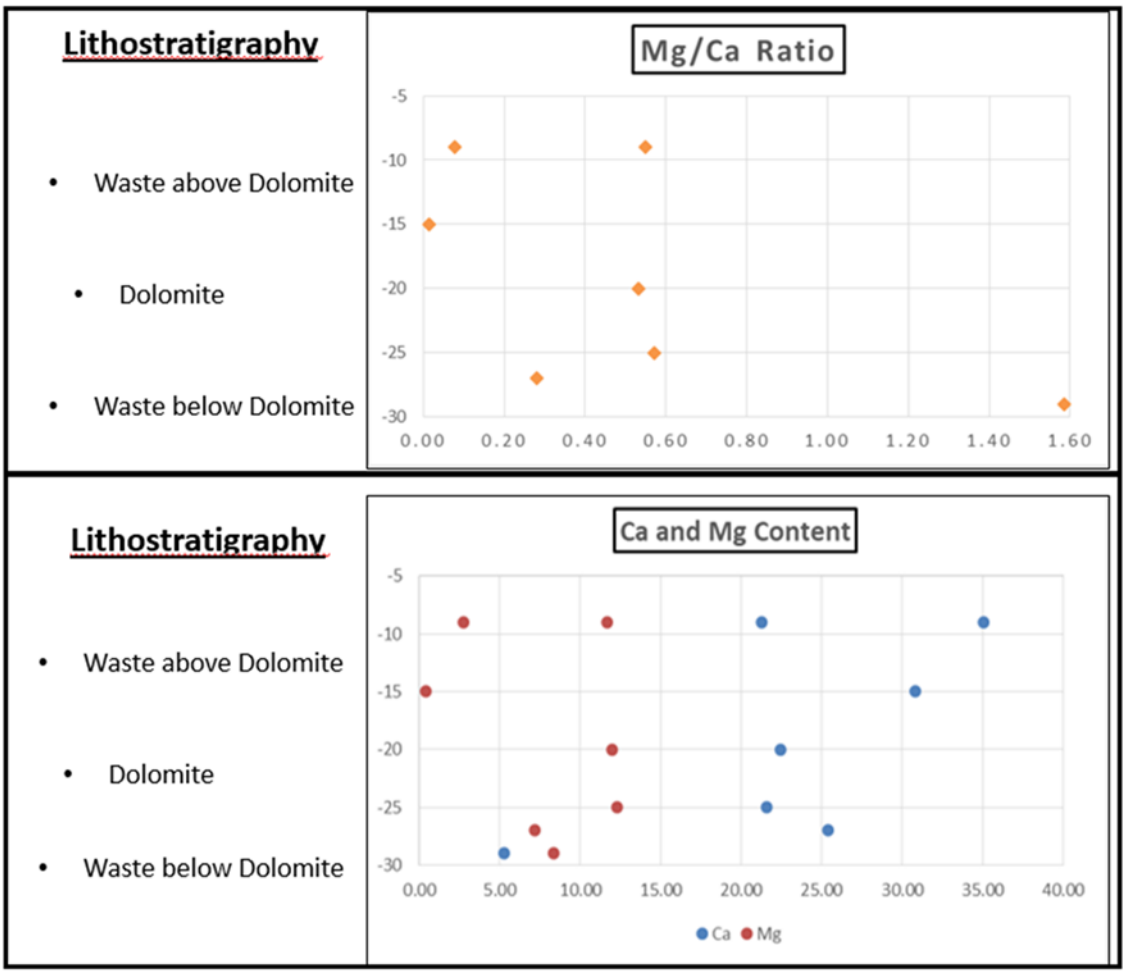


Figure 4.2.10 Whole rock XRF data showing Mg/Ca (orange) ratios and Calcite (blue), Magnesium (red) representation at the Lime Acres dolomite quarry with corresponding depths.

Limestone quarry lies between two faults (F1 and F2) as shown in Appendix 2. The quarry has near horizontal interbedded limestone and dolomite/chert zonation which can explain the variation in Mg/Ca ratios with depth in figure 4.2.11. There is no relationship between the depth and Mg/Ca. The Ca content that exceeds 40 molar mass are relational to the limestone zones which are mined for lime production. All dolomite and limestone samples have Mg/Ca ratios which are less than 0.6 while the chert bands can be identified by the Mg/Ca ratios above 1 in figure 4.2.11. The brittle chert band thus has the highest Mg/Ca ratio in Lime Acres.

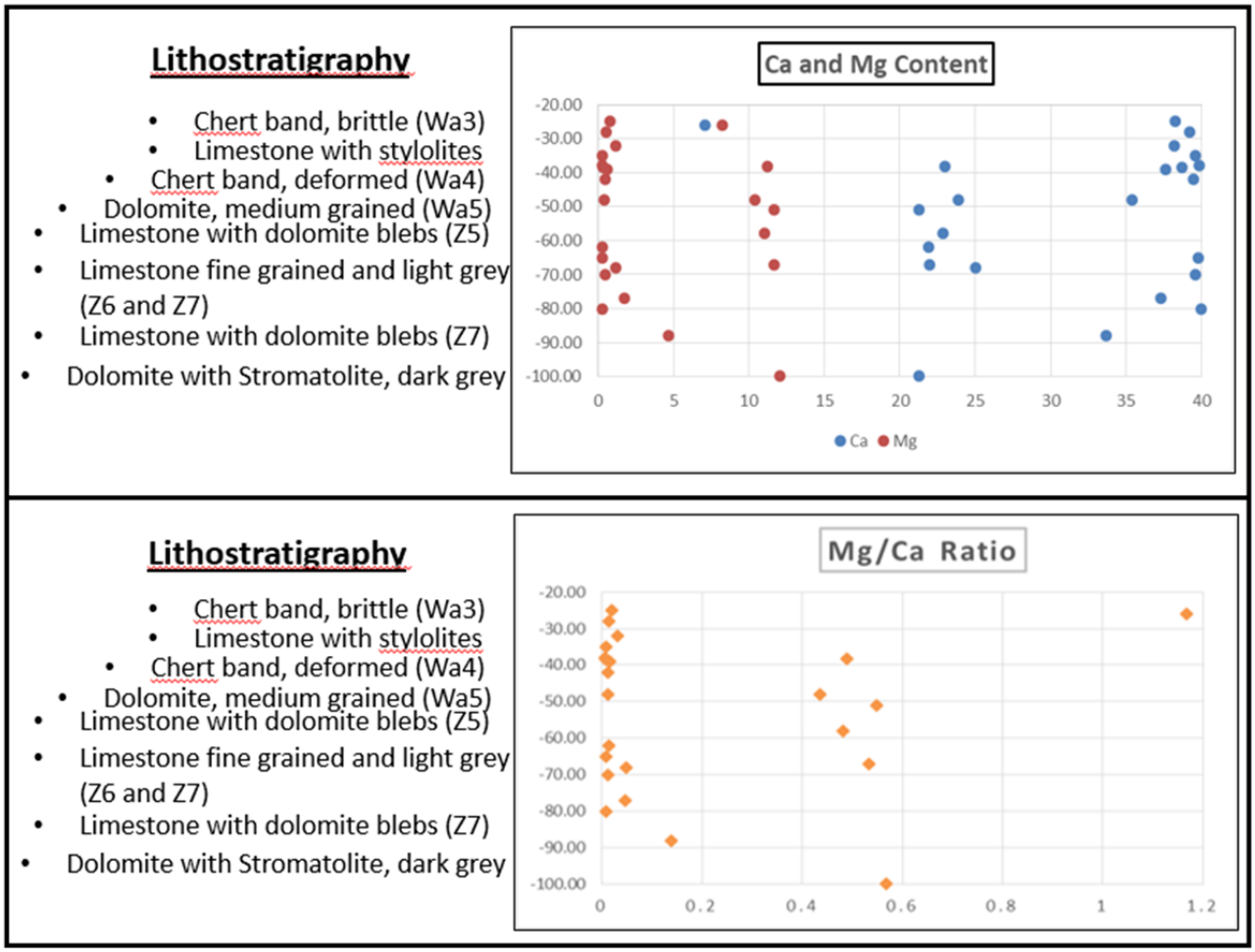


Figure 4.2.11 Whole rock XRF data showing Calcite (blue) Magnesium (red) representation at the Lime Acres limestone quarry and Mg/Ca (yellow) ratios with corresponding depths.

The economic zones of limestone have MgO of less than 2 with Mg/Ca ratio of less than 0.1. The uneconomic zones have higher Mg/Ca content due to increased MgO content due to increased mg content and love Ca content. Figure 4.2.11 shows that the Mg analysis is lower than 5 molar percentage and Ca that is lower than 40 molar mass percentage. The molar mass percentage for zones currently being mined for lime production is higher than 35. Mg/Ca ratios, which are shown in figure 4.8, are not related to depth, but rather to the interbedded variation in dolomite, calcite and quartz content. There is no regular path for the Mg/Ca ratios and all ratios are lower than 1.2 throughout the pit. The dolomite and limestone samples all have Mg/Ca ratios lower than 0.6 with the brittle chert band having a ratio of 1.2.

4.2.5 Electron Microprobe

The 9 samples that were analysed through microprobe are indicated on Table 4.2 where depth of sampling and field description is indicated. The data on the EMPA analysis as presented in Appendix 6 was collected using point analysis of the different structure present on the samples, this data can be used to verify the bulk analysis conducted through XRD and XRF analysis.

Table 4.2 Samples analysed through microprobe showing sample ID, depth at which sampling occurred and related description.

Site	Sample ID	Depth	Field description.
Lime Acres-Dolomite	TMN 28	26 m	Dolomite with fenestrae filled with quartz crystals
Lime Acres	TMN 13	38 m -38.25 m	Chert band
Lime Acres	TMN 19	39.5 m -47 m	Light Grey Limestone with stylolite
Lime Acres	TMN 2	49 m -49.7 m	Light Grey Limestone with brittle carbonaceous stylolite
Lime Acres	TMN 4	52 m -58 m	Light Grey Limestone with large crystals of dolomite
Lime Acres	TMN 21	64 m -68 m	Light Grey Limestone
Lime Acres	TMN 24	68 m -68.5 m	Dark Grey Dolomite
Lime Acres	TMN 23	68.5 m -86 m	Light Grey Limestone
Lime Acres	TMN 6	86 m -90 m	Grey limestone with Dolomite blebs

A dolomite sample was analysed as TMN 28 and proved to be a pure dolomite sample with Mg and Ca contents of 17-21 and 26-28 respectively. The sample was coarse grained with preserved cleavage structures. There was cleavage directions, which criss-crossed each other, and the finer matrix is reflective in light.

TMN 13 in Lime Acres is a mixture of uniform and very coarse grains that have twining and is highly reflective with some magnesium content that is elevated. The CaO content averages 29 % and MgO content is 21 % throughout the sample. The samples TMN 19, TMN 21 and TMN 2 also showed highly homogenous carbonate shapes with coarse grained fluorescent crystals which have a high content of calcium. All these samples have caO content of +54 % with less than 0.2 % mgO content. The TMN 2, TMN 24 and TMN 21 sample has stylolite with re-entrance angles and show grading between coarse, medium and finer grained matrix. The sample image with the different sedimentary textures is indicated in figure 4.2.12.

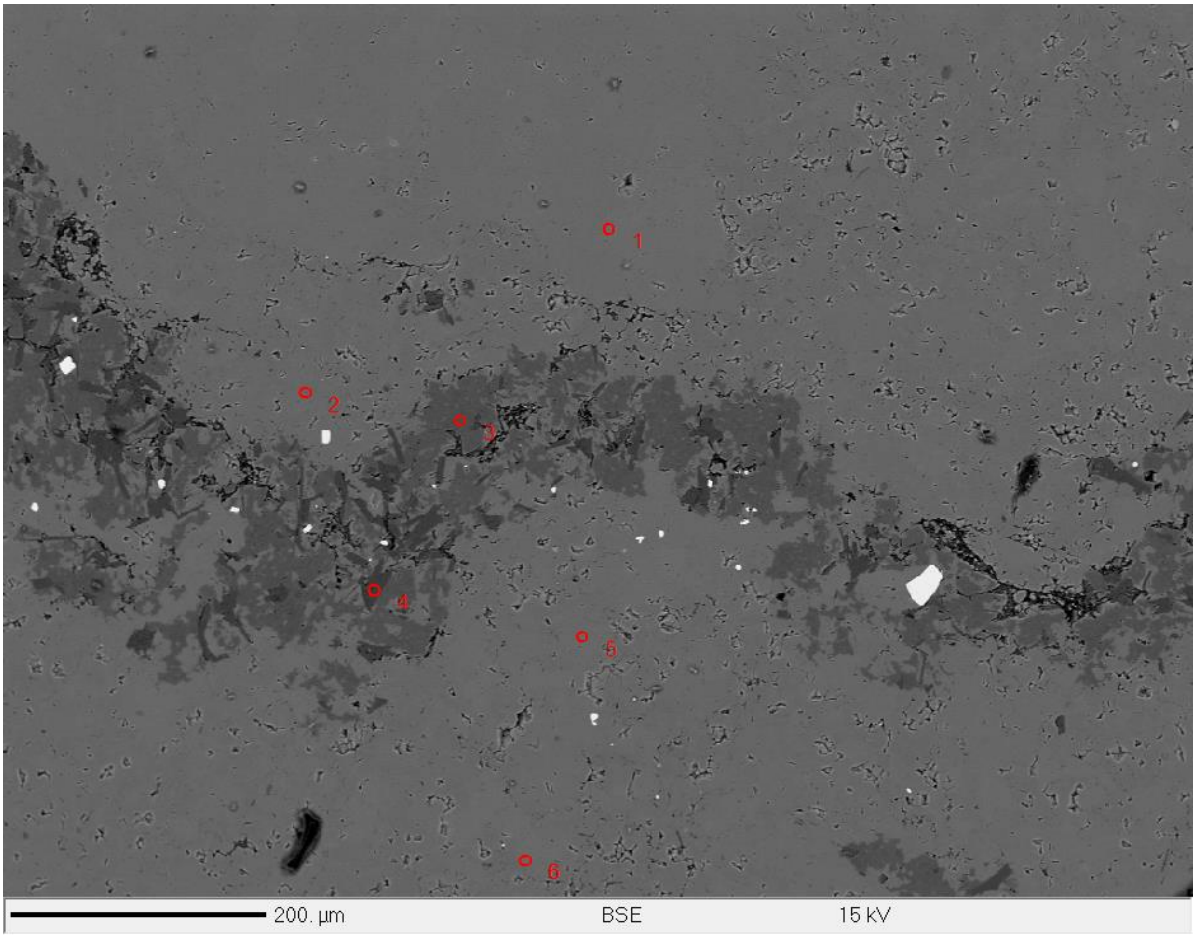


Fig 4.2.12 Point analysis analysed on the stylolite of Lime Acres sample TMN 24.

The grain sizes have no influence no chemical content as all points have content of CaO that is +53% and <0.5% MgO. The analysis from point 3 of TMN 4 showed that stylolite material and dolomite have elevated MgO content of 18 %. TMN 4 is a prominent stromatolite which has been well preserved and dolomitised. The sample showed poor sedimentary structures with deformation in parts where dark blobs and good cleavage are present around the well preserved coarse grained. All points analysed inside and outside the stylolite had consistent chemical composition, therefore the stylolite did not affect the composition except for TMN 24, which showed an increased MgO content within the stylolite.

Light grey limestone which is on the lower levels of the Lime Acres quarry has properties similar to TMN 2, TMN 21, TMN 19 where the material is of an interbedded structure with larger grained that are well preserved. The twining is preserved and the sample has high magnesium content. TMN 6 is indicated in figure 4.2.13 and has high calcium content on the lighter limestone and increased magnesium content of the lighter blocks. Where the content is at 53 % for the lighter limestone and 28 % for the darker dolomitised zones. The dolomitised zones have increased MnO content of +1.2 %.

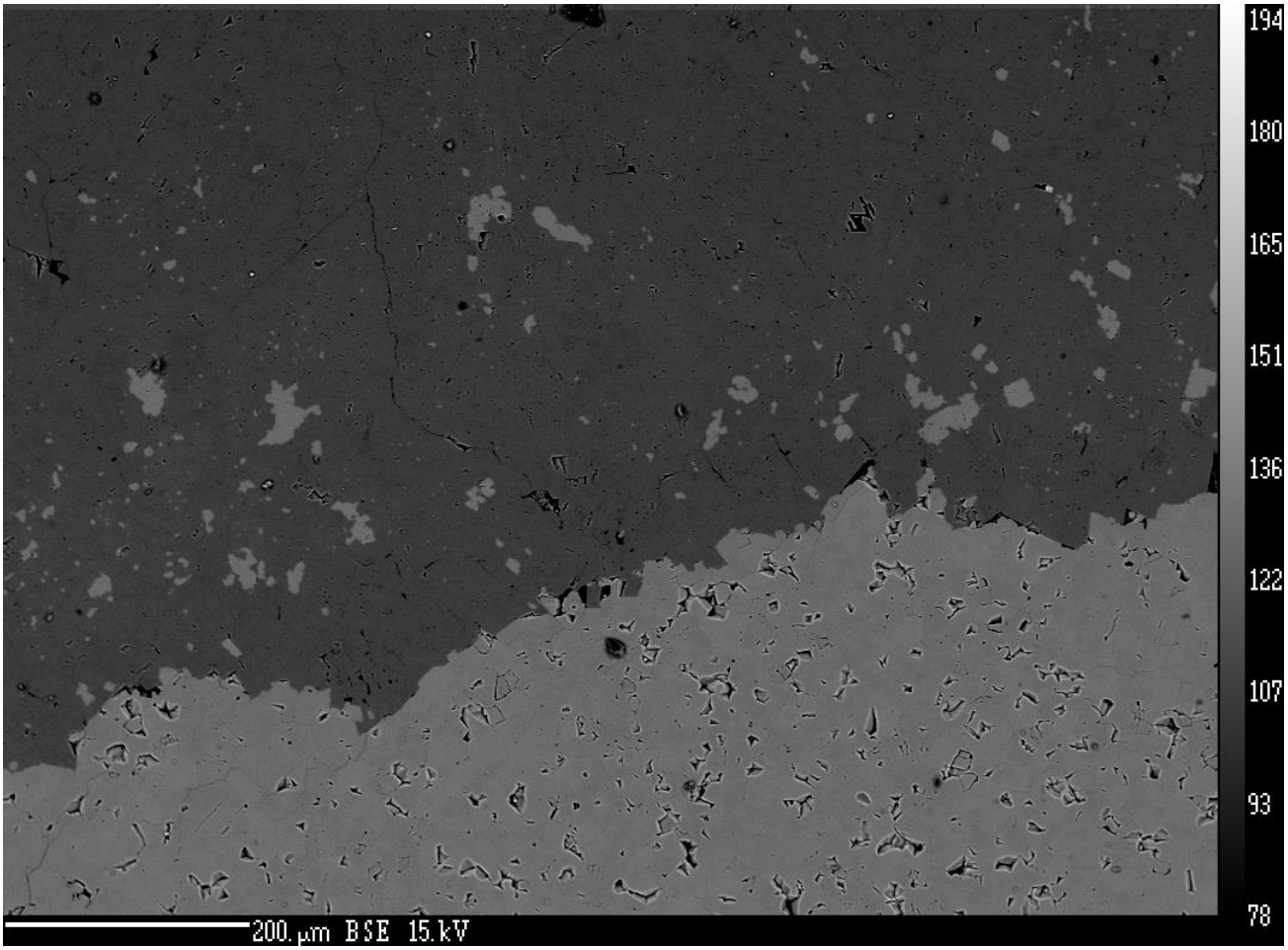


Fig 4.2.13 Microprobe image of Lime Acres sample TMN 6.

4.2.6 XRD Analysis

The samples analysed through XRD are TMN 12, TMN 1, TMN 4, TMN 21 and TMN 28. The samples described on this section are a representation of the limestone from Lime Acres. The XRD results are represented in figure 4.2.14 – figure 4.2.18. TMN 28 is a sample that lies at the bottom of the dolomite that is being mined at Lime Acres. This sample shows that the sample is a pure dolomite as shown in figure 4.2.14. The sample was taken east of the fault (F2) and is a pure dolomite sample. The material is a coarse grained dolomite with calcite with fenestrae where pure white to milky calcite crystals forms.

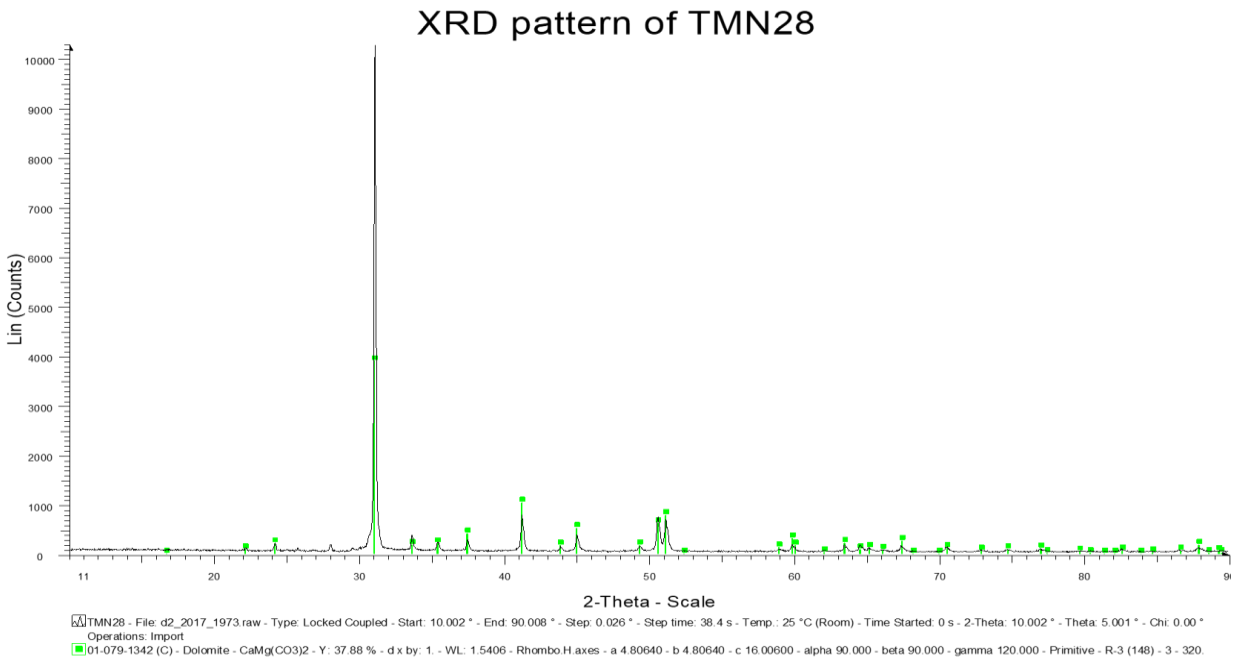


Figure 4.2.14 Whole rock XRD data showing dolomite (green) of TMN 28 collected at Lime Acres.

TMN 12 is a representation of a 0.2 m chert band which lies at about 38 m below surface, the sample is the waste that lies below the zone 3 bedding. The data in figure 4.2.15 shows that this is a magnesium calcite material with quartz inclusions.

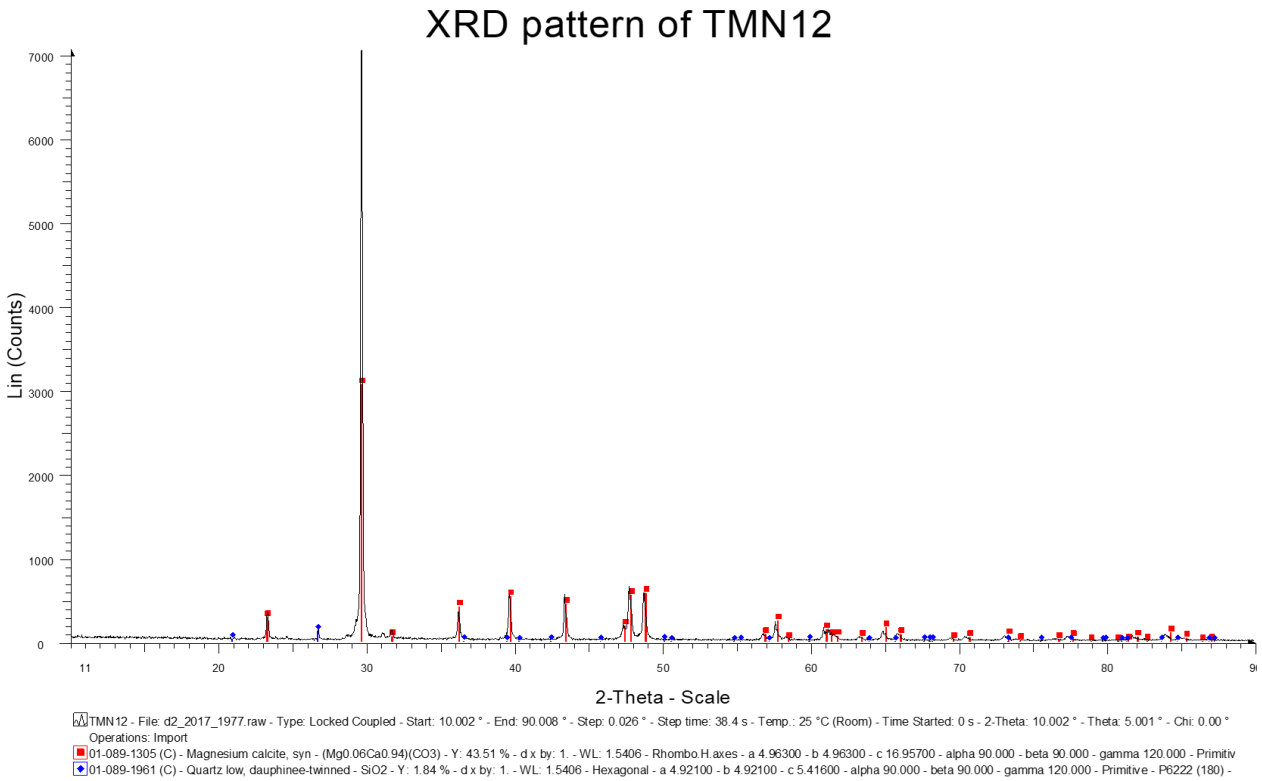


Figure 4.2.15 Whole rock XRD data showing magnesium calcite (red) and quartz (blue) of TMN 12 collected at Lime Acres.

At 49.7 m to 52 m there is a prominent dark grey dolomite which is quartz rich and its shown in figure 4.2.16.

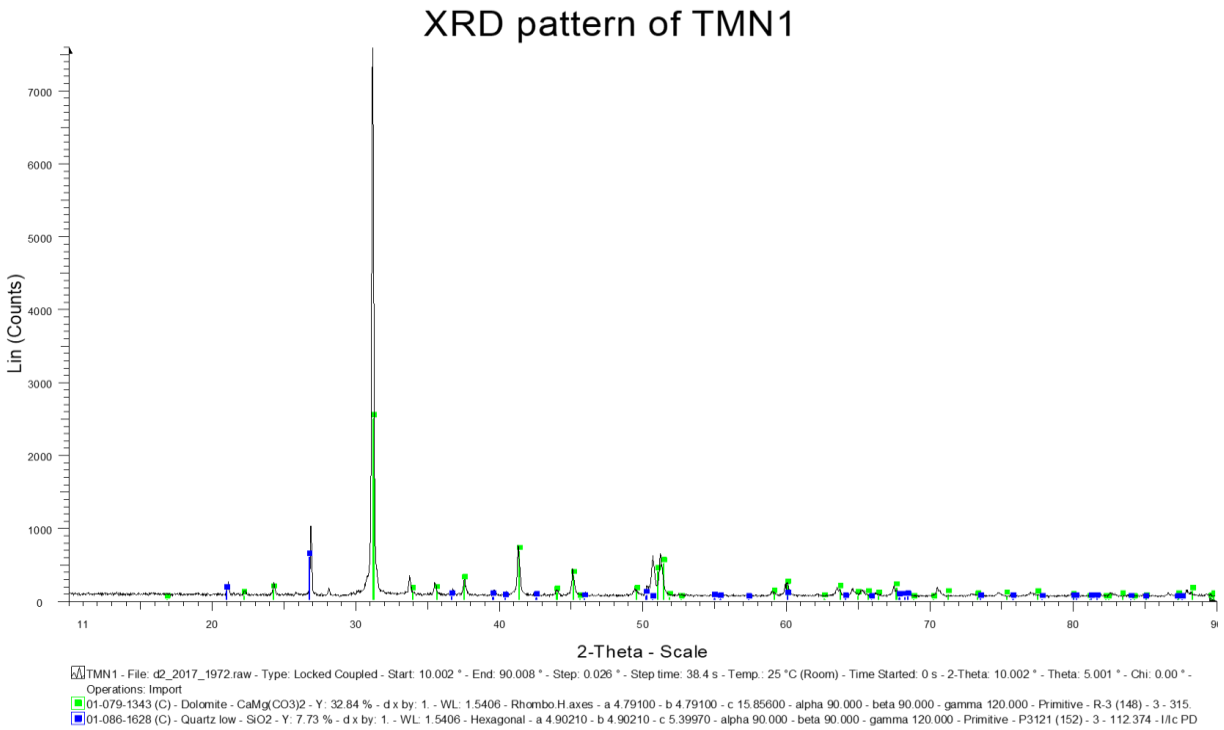


Figure 4.2.16 Whole rock XRD data showing dolomite (green) and quartz (blue) of TMN 1 collected at Lime Acres.

The dark well preserved stromatolites at 58 m is represented in figure 4.2.17. This sample is dolomite rich with no trace of quartz impurities.

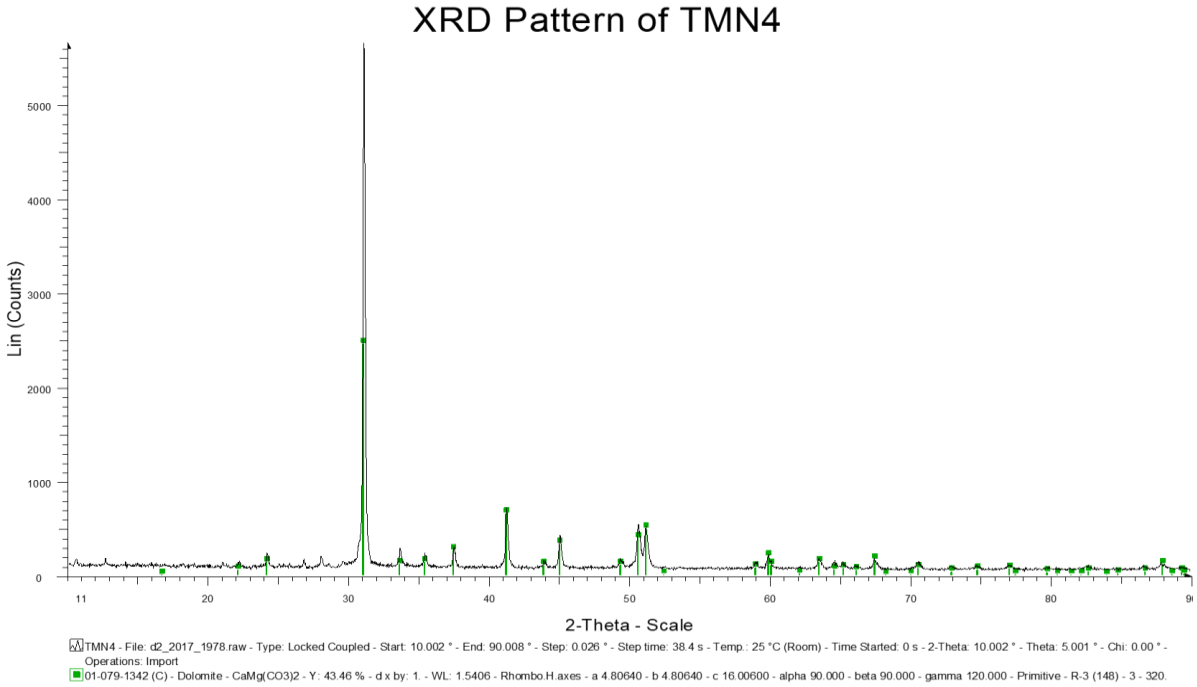


Figure 4.1.17 Whole rock XRD data showing dolomite (green) of TMN 4 collected at Lime Acres.

The light grey limestone at depths below 64 m is rich in magnesium calcite with some traces of quartz. The sample lies within the waste above zone 6 material and is represented in figure 4.1.18.

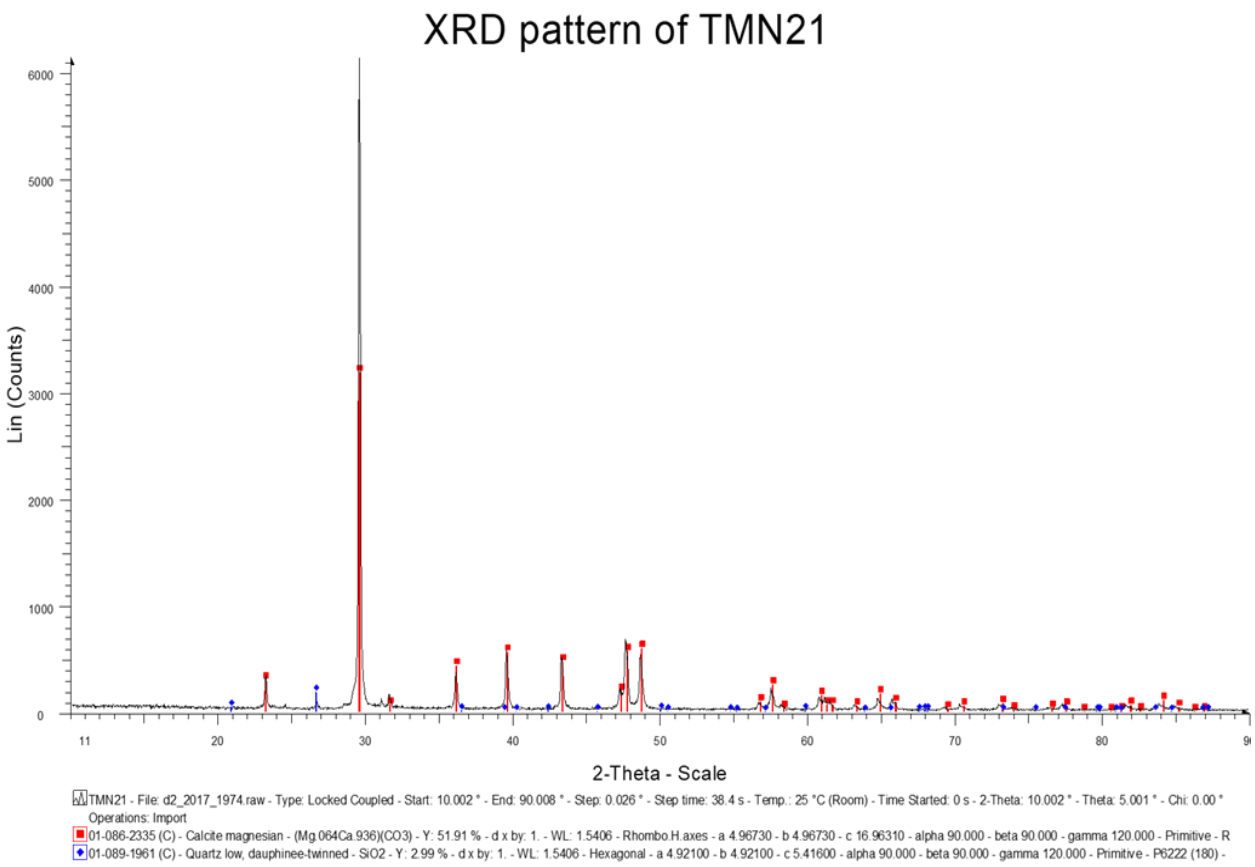


Figure 4.2.18 Whole rock XRD data showing magnesium calcite (red) and quartz (blue) of TMN 21 collected in Lime Acres.

Chapter 5

Discussion and Conclusion

5.1 Discussion

This project integrated geological mapping, petrology, microprobe analysis, mineral identification and bulk geochemistry with the aim of understanding and comparing the calcite rich limestone zonations which lie in both the Malmani and Campbellrand subgroups. The calcite-rich limestone either pre-existed the deformation of the Transvaal Supergroup or it is a result of dedolomitisation of the deformed material. Some of the specific objectives that were addressed are discussed in this chapter.

5.1.1 Structural controls that host calcite rich deposits

There are two major faults noted in Lime Acres, and four major faults faults noted at Beestekraal, striking NS and WE respectively. Both sites only have normal fault systems. The two faults found at Lime Acres are near vertical and serve as mining boundaries on the east and western edges of the quarry. The fault on the western edge has been labelled as Fault 1 (F1) and the eastern fault as Fault two (F2). The limestone structures and textures which are found on the in Lime Acres were well preserved. Eroglu *et al.,* (2015) described the Campbellrand Subgroup of the Griqualand West Basin in the western Kaapvaal Craton as being dominated by shallow shelf carbonates, which were deposited under shallow subtidal conditions. The material lying east of the Fault 2 is coarse grained dolomite, which dips shallowly towards the west and that is overlain by weathered material. Martini and Wilson (1998) had also mentioned that the strata dips gentle to the west and the limestone is present in large lenses up to 10 km long. This shallow dip is notably consistent throughout the Lime Acres deposit.

The Beestekraal deposit is located in the Oaktree Formation of the Malmani Subgroup. The deposit was best described in Buttrick *et al*., (1993), as dark coloured, chert-poor dolomite with some carbonaceous shale towards the base. These sedimentary rocks are of fine grained limestone, chert zonations and medium grained dolomitic matrix. The deposit is uniform and dips towards the west at an angle of about 33^{o} with a NS strike direction. Hartzer (1995) said that the Crocodile River dome is located on the intersection of two major anticlines with an ENE and a NW striking fold. The data collected within the mining area could not ascertain this information however the folding was noted on the hanging wall. Four normal faults that are WE striking were observed. The faults cut across the deposit and the folding which is prominent on the western hanging wall. These faults have varying dip of 56^{o} -87^{o} towards the north.

Hartzer (2000) mentioned that the deformation preceded metamorphism, which was caused by the intrusion of the Bushveld Complex in the Crocodile River Fragment. The study has found that the mining areas have somehow not been deformed during the said dolomitization phase which affected the Transvaal Supergroup. The pockets of high calcium deposits can be classified as primary limestone which was preserved during the dolomitisation phase. Post depositional alterations had two different effects on the sites. Early, fabric-retentive dolomite replaced most of the Malmani carbonates, however, significant amounts of the Campbellrand Subgroup still consist of limestone (Sumner *et al.,* 2006). At Lime Acres the chert, which filled the contacts between the different bedding, was compressed due to high pressure from the overlying material

and faulting. The traces of chert have been noted as stylolite and small traceable carbon partings/bands within the limestone and dolomites. At Beestekraal there is infill of iron rich and chert material, which is within the cleavage planes and contacts. Further events show the ingress of the calcite rich veinlets in Beestekraal, which upgraded the deposit to high Ca content dolomite.

There is evidence of three (3) geological events that have occurred on both sites where:

- Deposition of the magnesium-calcite occurred;
- Some silica and calcite veinlets were introduced by fluids, the fluid introduction put pressure on the deposit which resulted in compaction. Re-entrance angles formed during compaction and left the prominent calcite veinlets. The calcite veins only appear in Beestekraal;
- Faulting occurred post the formation earlier compaction events. The faulting caused compression of the existing structures and resulted in wavy stylolites at Lime Acres, deformation along the faults and mud fissures being introduced to the joints.

It was noted that there are some mineral descriptions which were similar for the two quarries. The orientation of the limestone was however different with Lime Acres having a shallow dipping layered succession of limestone and dolomitised-chert zonations.
Truswell (1990) mentioned that the dip in Lime Acres is usually very low and to the west while Hatzer (2000) described the Crocodile River dome as a large domal structure with the beds of the Pretoria Group dipping steeply towards the surrounding Bushveld Complex granite. The dip variations as described by Hatzer (2000) and Truswell (1990), has been confirmed for both Beestekraal and Lime Acres respectively. Beestekraal has a uniform ore body which dips steeper than Lime Acres. The limestone at both sites is dark grey to blue and fine-grained.

5.1.2 Mineralogical variations between the two deposits

Point analysis through the EMPA may in general vary significantly from bulk analysis, which was conducted through XRF and XRD. In the case of the samples collected in Lime Acres and Beestekraal it has however been noted that there is a great deal of uniformity between the XRF, XRD and EMPA results. The three data sets have therefore been used to complement each other. It can be noted through the data analysed that both sites have similar mineral compositions, which are rich in calcium with little deformation.

The dolomite which is mined lies near surface on the eastern side of the fault 2 (F2) at Lime Acres. The dolomite has prominent limestone structures and textures in fenestrae which have been filled by chert. Weathering in some parts of the geological contacts has caused the contacts to be filled by clay fissures. The cherty dolomite, which is leached and highly weathered, overlies the dolomite deposit that is mined economically. This layer of cherty-dolomite has undergone sedimentary processes to become secondary limestone. The dolomite samples are coarsely crystalline when studied at under a microscope or EMP analyser. Zenger *et al*. (1994), mentioned that the coarsely crystalline dolomites are classified as secondary rocks due to the presence of limestone textures and structures, these dolomites have formed by diagenetic replacement of the older limestones, however, the fine-crystalline dolomites cannot be linked to the process of diagenetic alteration of limestone. The crystal structure therefore shows that Lime Acres has primary deposits of the west of Fault 2 (F2) and secondary deposits on the east of the fault.

All samples collected at Lime Acres where mining occurs for lime production were found to be light grey limestone with varying degrees of stylolite and stromatolite textures. Altermann *et al.* (1995) described the Lime Acres Member of the Ghaap Plateau Dolomite as composed chiefly of stromatolitic limestones and dolostones with its top consisting of platy dolostones and shales. The limestone at Lime Acres has well preserved stylolite at depth showing that there was diagenetic events which were near surface. The sections that are deformed show coarser grained limestone and now therefore classified as secondary chain sedimentary rocks. This section is classed as secondary sediment as it is medium grained and deformed. These textures show the impact that the pressure that resulted from faulting had on the bedding planes of the Lime Acres carbonates.

There was some reddish, iron staining with iron content at the topsoil and subsoil of the Lime Acres Formation, these characteristics can be linked to the presence of the highly weathered BIF. The BIF was noted by Schröder et al., (2006), where the Campbellrand was said to be conformably overlain by the Kuruman Member of the Asbestos Hills BIF. The BIF, interbedded chert and dolomite which overlie the limestone was deposited at a stage where the sedimentary features were not well defined therefore the faults easily deformed these structures. The interbedding and faulting did not affect the sedimentary structures and textures of primary limestone. The preservation of structures is consistent with the finding that there was unique preservation of the Postmasburg Group in the western Griqualand West portion, which was not affected by the strongly erosive forces in pre- and early Pretoria Group times (Moore *et al.,* 2012).

The samples which were collected in Beestekraal had less preserved sedimentary structures within the economically viable ore body. Boggs (2006), described early-formed dolomites as those that formed at or near the surface in an unconsolidated state. The limestone has less sedimentary structures through the naked eye yet have proven to be well preserved under a microscope therefore classified as primary limestone which formed near surface. Bridge and Demico (2008), mentioned that these dolomites may faithfully preserve sedimentary structures and calcite grain types or can occur as an interlocking mosaic of dolomite crystals with no preserved sedimentary features. It can be concluded that both the Campbellrand and the Malmani Formation can be classified as near surface early-forming dolomites where the sedimentary structures were mostly preserved on the Lime Acres Member.

Eriksson and Warren (1983) tested the mixing-zone model in the Malmani dolomite and concluded that near-surface diagenetic features existed in the shallow subtidal, intertidal and lower supratidal facies and produced coarse-grained dolomite and chert nodules. There was a grain size grading from fine to coarse grain material at both sites where cementation occurred between medium to fine grained crystals. These different sizes were noted through the EMPA and petrolographic analysis therefore supporting Eriksson and Warren's conclusion that the mixing zone did not occur in the Malmani dolomite. Seawater (shallow-subtidal) Model described by Boggs (2006), where new Mg^{2+} is constantly being supplied while replaced Ca^{2+} ions and other ions that might "poison" the dolomite crystal structure are removed has been noted and is not applicable for either site. This cannot be applied as the dolomites are high in Ca content and have impurities such as Si, Mn and Fe.

There are some similar characteristics in the chert that overlie the limestone ore, the chert has been correlated between Lime Acres and Beestekraal by this report. The overlying chert zonation on both sites which is highly fractured is a can be used to correlating the geology of the two ore deposits as its features are distinctly similar on both sites. Eroglu *et al.,* (2015) said that the chert-free Oaktree Formations are dominantly composed of very dark gray fine micritic dolomite structure while Buttrick *et al.,* (1993) described the Oaktree Formation as

a chert-poor dolomite with some carbonaceous shale towards the base. It has been evident during this study that Eroglu *et al*., (2015) described the ore deposit while Buttrick *et al.,* (1993) gave a description that is aligned to the characteristics noted within the material that is considered as waste in the mining of limestone for lime and cement production. The XRD data for both sites shows that the economic limestone zones are calcite rich with some quartz or magnesium impurities, this material is the grey limestone with fine-medium sized grains. The material which is not exploited for lime or cement production is of similar minerals which the key difference being that it is more dolomitic than the magnesium calcite rich. The content of quartz varies for all sites but the common source of the silica content is the prevailing dark chert on both sites.

The dominance of re-entrance angles on the edges of the calcite rich crystals indicate that the limestone is primary limestone which was introduced to cementation at early stages of crystal formation. The concept of primary limestone based on re-entrance angle can be applied on the limestone for both in Lime Acres and Beestekraal as this is a consistent sedimentary structure on both sites. The overlying dolomite and the dolomite being mined at Lime Acres is of secondary sedimentary nature, the dolomites can be classified as coarse crystalline sedimentary deposits while the economic limestone is classified as fine crystalline sedimentary deposits of primary nature.

There is no relation that has been established between depth and mineral content or sedimentary structures therefore deposition occurred at or near surface.

5.1.3 Geochemical data

Both sites have significantly increased calcium content with low magnesium content on production zones therefore having little impurities from the chert and dolomites that overlie the limestone. Theoretical considerations suggest that dolomite formation is favoured kinetically by high Mg/Ca ratios, low Ca/CO_3 ratios, and low salinity (Machel and Mountjoy 1986). The Mg/Ca showed that for all zones used for cement and lime production the Mg/Ca ratio are below 0.6 and 0.1 respectively. Mg/Ca closer to 1 and above are not economic viable for lime and cement production. The salinity was near negligible for all samples analysed therefore the samples only met one of the three theoretical considerations for dolomite formation. These low Mg/Ca ratios indicate that the dolomites are more of magnesium calcite content and of primary depositional environment than secondary.

The samples collected in the dolomite quarry which lies east of the faults in Lime Acres can been classified as secondary dolomites due to the sedimentary structures it possesses. The dolomite has proven to be perfectly dolomite crystals with the Mg/Ca value of 0.8-0.9.

5.2 Conclusion

The dolomite sample which was taken east of the fault 2 (F2) at Lime Acres has been proven to have elements of a modern sedimentary dolomite with some presence of clay material in the form of mud fissures. These mud fissures filled the fenestrae in dolomite. The matrix material between the very coarse grained dolomites has some preserved sedimentary structures and textures, where smaller fenestrae are filled with crystal of quartz. In this section the dolomite crystals show twinning and cross-cutting of the cleavage planes. The Mg/Ca ratio is almost 1 and there is a perfectly dolomite curve on XRD analysis showing almost no impurities

therefore rendering the part which lies east of the fault 2 (F2) as a well-defined secondary rock. This part of the fault can therefore not be used to explain the dolomite problem as it is very coarse grained and secondary in nature.

West of the dolomite lies a limestone deposit with well-preserved sedimentary structures and textures. This limestone is medium-fine grained light and darker grey and extends to the east towards fault 1 (F1). No evidence was found that the faults could have eroded or downgrade the limestone zones that lie east of the fault. All the faults are filled with reddish-clay fissures which are similar to those noted west of the fault 2 (F2) on the dolomite quarry, therefore the fault (F2) may have downgraded the material lying west of the fault.

The presence of the calcite rich veinlets at Beestekraal indicates that the high calcite dolomite was further upgraded by the introduction of these near vertical veinlets, which re-introduced calcite that was essential in deeming the deposit an economic cement production deposit. The Lime Acres deposit, with less than 0.6 Mg/ca ratios is a +96 % calcium carbonate rich rock which has been downgraded to +92 % calcium carbonate deposit, the said downgrade came from the inclusion of the chert filled stylolite during formation. The stylolite formed as inter bedding during deposition and are almost invisible during bulk sampling analysis therefore rendering the limestone deposit as high economic. The chert is not inherent on both sites and has been significantly pinched out at depths at both the Lime Acres and Beestekraal sites. This pinch out could be attributed to the pressure resulting from faulting and increased specific gravity of the overlying limestone and dolomites compare to the chert. The preserved chert on the upper layers of the quarries is significantly fractured and highly affected by weathering, therefore showing that the other zones of dolomites and BIF, which have also undergone sedimentary processes, are more resistant than the chert zone.

Both limestone deposits at the two sites are primary limestone which formed at surface and could not be accurately applied to any of the dolomite models as the structures that host these deposits differ significantly. At both sites the present of faults seem to have occurred post the formation of the deposits therefore have little bearing on the depositional history. The main contribution of the fault is that it avoided the dolomitisation on the deposit which lies west of F2. The mineralogy and sedimentary structures or both sites have distinct similarities therefore could be suggested that these formed under the same or similar processes. The limestone and dolomites which lie about the 25 m depth are not consistent with each other therefore cannot be fully correlated. It has been noted that material that lies at 52 m in Lime Acres represents the same characteristics as material found at about 86 m in Beestekraal, these chert blobs were sampled.

The characteristics that affect each site are different as Lime Acres has preserved sedimentary structures such as stylolite and stromatolites. These structures are lacking in Beestekraal where there is a dominance of calcite rich veinlets. The calcites have upgraded the dolomites in Beestekraal while the chert downgrade the deposits. Calcite veinlets and quartz inclusions were post depositional of the limestone and dolomite deposit.

6. REFERENCES

Altermann, W. and Schopf, J.W., 1995. Microfossils from the Neoarchean Campbell Group, Griqualand West Sequence of the Transvaal Supergroup, and their paleoenvironmental and evolutionary implications. Precambrian Research, 75, 65-90.

Altermann, W. and Siegfried, H.P., 1997. Sedimentology and facies development of an Archaean shelf: carbonate platform transition in the Kaapvaal Craton, as deduced from a deep borehole at Kathu, South Africa. Journal of African Earth Sciences, 24, 391-410.

Altermann, W. and Wotherspoon, J.M., 1995. The carbonates of the Transvaal and Griqualand West sequences of the Kaapvaal craton, with special reference to the Lime Acres limestone deposit. Mineralium Deposita, 30, Issue 2, 124–134.

Badiozamani, K., 1973. The dorag dolomitization model — application to the middle Ordovician of Wisconsin. Journal of Sedimentary Petrology, 43 (4), 965-984.

Bau, M., Romer, R.L., Lüders, V., Beukes, N.J., 1999. Pb, O, and C isotopes in silicified Mooidraai dolomite (Transvaal Supergroup, South Africa): implications for the composition of Paleoproterozoic seawater and `dating' the increase of oxygen in the Precambrian atmosphere. Earth and Planetary Science Letters, 174, 43-57.

Bekker, A., Holland, H.D., Wang, P.L., Rumble D., Stein, H.J., Hannah, J.L., Coetzee, L.L., Beukes, N.J., 2004. Dating the rise of atmospheric oxygen. *Nature* 427, 117-120. Doi: 10.1038/nature02260

Beukes, N.J., 1977. Transition from siliciclastic to carbonate sedimentation near the base of the Transvaal Supergroup, northern Cape Province, South Africa. Sedimentary Geology, 18 (1-3), 201-221.

Beukes, N.J., 1984. Sedimentology of the Kuruman and Griquatown iron formations, Transvaal Supergroup, Griqualand West, South Africa. Precambrian Research, 24 (1), 47-84.

Beukes, N.J. and Smit, C.A., 1987. New evidence for thrusting in Griqualand West, South Africa: Implications for stratigraphy and the age of red beds. South African Journal of Geology, 378-394.

Bouazza N., Mrihi A.E., and Maate A., 2015. Geochemical assessment of limestone for cement manufacturing. In: 9th International Conference Interdisciplinarity in Engineering, INTER-ENG 2015, 8-9 October 2015, Tirgu-Mures, Romania, Morocco: Elsevier, Procedia Technology, 22, 211 – 218.

Boggs, S., 2006. Principles of sedimentology and stratigraphy. 4th ed, University of Oregon: New Jersey, 182-187.

Bridge, J. and Demico, R., 2008. Earth Surface Processes, Landforms and Sediment Deposits. Cambridge University Press: Cambridge, 697-700.

Button, A., 1999. The stratigraphic history of the Malmani dolomite in the eastern and north-eastern Transvaal. Economic Geology Research Unit, University of the Witwatersrand, Johannesburg, Society on 6.8.73.

Buttrick, D.B., Rooy J.L., and Ligthelm, R., 1993. Environmental geological aspects of the dolomites of South Africa. Journal of African Earth Sciences (and the Middle East), 16, Issues 1–2, 53-61.

Carballo, J.B., Land L.S., and Miser D.E., 1987. Holocene dolomitization of supratidal sediments by active tidal pumping, Sugar-loaf Key, Florida. Sedimentary Petrology, 57 (1), 153–165.

Clendenin, C.W., 1989. Tectonic Influence on the Evolution of the Early Proterozoic Transvaal Sea, Southern Africa. PhD Thesis, Johannesburg, University of the Witwatersrand, 21-27.

De Kock, M.O., Evans, D.A.D., Kirschvink, J.L., Beukes, N.J., Rosea, E., Hilburn, I., 2009. Paleomagnetism of a Neoarchean-Paleoproterozoic carbonate ramp and carbonate platform succession (Transvaal Supergroup) from surface outcrop and drill core, Griqualand West region, South Africa. Precambrian Research, 169, 80–99.

Eriksson P.G., Altermann W., and Hartzer F.J., 2006. The Transvaal Supergroup and its precursors. In: M.R. Johnson, C.R. Anhaeusser, and R.J. Thomas, Geology of South Africa. Johannesburg, Geological Society of South Africa, 237-260.

Eriksson K.A., McCarthy T.S., and Truswell J.F., 1975. Limestone formation and dolomitization in a lower proterozoic succession from South Africa. Journal of Sedimentary Petrology, 45 (3), 604-614.

Eriksson, K.A. and Truswell, J.F., 1974. Stratotypes from the Malmani Subgroup northwest of Johannesburg, South Africa. Transactions of the Geological Society of South Africa, 77 (3), 211-222.

Eriksson K.A., Truswell J.F., and Button A., 1976. Palaeoenvironmental and geochemical models from an early Proterozoic carbonate succession in South Africa. In: M.R. Walter (Editor), Stromatolites. Elsevier, New York, United States of America, 635-643.

Eriksson, K.A., 1977. Tidal flat and subtidal sedimentation in the 2250M.Y. Malmani Dolomite, Transvaal, South Africa. Sediment, Geology, 18, 223- 244.

Eriksson, K.A., and Warren, J.K., 1983. A paleohydrologic model for Early Proterozoic dolomitization and silicification. Precambrian Research, 21, 299–321.

Eroglua, S., Schoenberga, R., Willea, M., Beukes, N.J., and Taubalda, H., 2015. Geochemical stratigraphy, sedimentology, and Mo isotope systematics of the ca. 2.58–2.50 Ga-old Transvaal Supergroup carbonate platform, South Africa. Precambrian Research, 266, 27–46.

Fairchild, I.J., 1983. Chemical controls of cathodoluminescence of natural dolomites and calcites: new data and review. Sedimentology, 30 (4), 579– 583.

Frauenstein, F., Veizera, J., Beukes, N., Van Niekerk, H.S., Coetzee, L.L., 2009. Transvaal Supergroup carbonates: Implications for Paleoproterozoic $\delta^{18}O$and $\delta^{13}C$ records. Precambrian Research, 175, issue 1-4, 149-160.

Fairey, B., Tsikos, H., Corfu, F., Polteau, S., 2013. U–Pb systematics in carbonates of the Postmasburg Group, Transvaal Supergroup, South Africa: Primary versus metasomatic controls Brenton. Precambrian Research, 231, 194–205.

Goodge, J., 2017. Electron probe micro-analyzer (EPMA). University of Minnesota-Duluth; https://serc.carleton.edu/research_education/geochemsheets/techniques/EPMA.html

Hardie, L.A., 1987. Dolomitization: A critical view of some current views. Sedimentary Petrology, 57, 166-183.

Hartzer, F.J., 1995. Transvaal Supergroup inliers: geology, tectonic development and relationship with the Bushveld complex, South Africa. Journal of earth Science, 24, (4) 521-547.

Hartzer, F.J., 2000. Lithostratigraphic subdivision and geological structure of inliers. Geological Survey, 22, Johannesburg, Council of Geoscience, 7-16.

Kisch, H.J., 1991. Mite crystallinity: recommendations on sample preparation, X-ray diffraction settings, and interlaboratory samples. Metamorphic Geology, 9, 665-670.

Knoll, A.H. and Beukes, N.J., 2008. Introduction: Initial investigations of a Neoarchean shelf margin-basin transition (Transvaal Supergroup, South Africa). Precambrian Research, 169, 1-14.

Land, L.S., 1991. Dolomitization of the Hope Gate Formation North Jamaica by seawater: reassessment of mixing zone dolomite. In: H.P. Taylor, J.R. O'Neil, and I.R. Kaplan, Stable Isotope Geochemistry: A Tribute to Samuel Epstein, Geochem Society Special Publication, 3, 121–133.

Lane, S.J. and Dalton, J.A., 1994. Electron microprobe analysis of geological carbonates. American Mineralogist, 79, 745-749.

Lenhardt, N., Eriksson, P.G., Catuneanu, O., Bumby, A.J., 2012. Nature of and controls on volcanism in the ca. 2.32–2.06 Ga Pretoria Group, Transvaal Supergroup, Kaapvaal Craton, South Africa. Precambrian Research, 214–215, 106–123.

Machel, H.G. and Mountjoy, E.W., 1986. Chemistry and environments of dolomitization — a reappraisal. Earth Science, 23, 175–222.

Miller, J., 1988. Cathodoluminescence microscopy. In: M. Tucker, Techniques in sedimentology. Oxford: Blackwell Scientific, 174–190.

Martini, J.E.J. and Wilson, M.G.C., 1998. Limestone and Dolomite. In: M.G.C. Wilson, and C.R. Anhaeusser, The Mineral Resources of South Africa. 6th Ed, Johannesburg: Council of Geoscience, 433-440.

Molengraaf, G.A.F., 1901. Geology of the Transvaal. Société géologique de France, 13-92.

Moore J.M., Tsikos H., and Polteau S., 2001. Deconstructing the Transvaal Supergroup, South Africa: Implications for Paleoproterozoic paleoclimate models. Journal of African Earth Sciences, 33, 437–444.

Moore, J.M., Polteau, S., Armstrong, R., Corfu, F., Tsikos, H., 2012. The age and correlation of the Postmasburg Group, southern Africa: Constraints from detrital zircon grains. Journal of African Earth Sciences, 64, 9–19.

Nottingham MyRIAD Solutions SDN BHD., 2017. X-Ray Diffraction (XRD) Analysis.

Phophi, S., 2017. ISO 17025 and SANAS guidelines for use of reference materials and PT scheme participation. In: The Innovation Hub, Pretoria

PPC Cement Ltd., 2015. Mandatory cop to combat rock fall and slope instability related accidents in surface mines: Beestekraal. South Africa, Pretoria: PPC Cement Ltd, Ref No. 7/4/118-AB4, 7-12

PPC Lime Ltd., 2015. Mandatory cop to combat rock fall and slope instability related accidents in surface mines: Lime Acres. South Africa, Kimberly: PPC Lime Ltd, Ref No. 7/4/118 AB4, 19-29.

Raith M.M, Raase P., Reinhardt J., 2012. Guide to thin section microscopy. 2nd ed, e-Book ISBN 978-3-00-037671-9, 1-127.

School of Geosciences Facilities., 2017. Thin Section Preparation Labs. https://www.wits.ac.za/geosciences/about-us/facilities/thin-section-preparation-labs/

Schröder S., Lacassie J.P., and Beukes N.J., 2006. Stratigraphic and geochemical framework of the Agouron drill cores, Transvaal Supergroup (Neoarchean-Paleoproterozoic), South Africa. South African Journal of Geology, 109, 23-54.

Shinn, E.A., 1986. Modern Carbonate tidal flats, their diagnostic features. Journal of Sedimentary Petrology, 81, 7-35.

Sumner, D.Y., 1995. Facies, Paleogeography, and Carbonate Precipitation on the Archean (2520 Ma) Campbellrand-Malmani Carbonate Platform, Transvaal Supergroup, South Africa. Thesis, Massachusetts Institute of Technology, United States of America, 514.

Sumner, D.Y. and Beukes, N.J., 2000. Sequence Stratigraphic Development of the Neoarchean Transvaal carbonate platform, Kaapvaal Craton, South Africa. South African Journal of Geology, 109, 11-22.

Sumner D.Y., Nicolas J., and Beukes N.J., 2006. Sequence stratigraphic development of the Neoarchean Transvaal carbonate platform, South Africa. South African Journal of Geology, 109, 11-22.

Truswell, J.F., 1990. The Transvaal and Griqualand West sequence: some Current issues. Johannesburg: Economic Geology Research Unit, University of the Witswatersrand, Information Circular No. 232, 1-39.

UWaterloo., 2018. Chemical Stoichiometry. http://www.science.uwaterloo.ca/~cchieh/cact/c120/stoichio.html

Warren, J., 2000. Dolomite: occurrence, evolution and economically important associations. Earth-Science Reviews, 52, 1–81.

Willis J., Feather C., and Turner K., 2014. Guidelines for XRF analysis: setting up programmes for WDXRF and EDXRF. Cape Town, South Africa, 2-28.

Zenger, D.H., Bourrouilh-Le Jan, F.G. and Carozzi, A.V., 1994. Dolomieu and the first description of dolomite. In: B. Purser, M. Tucker and D. Zenger, Dolomites: A Volume in Honour of Dolomieu, International Association of Sedimentologists Special Publication, 21, 21–28.

Appendix 1

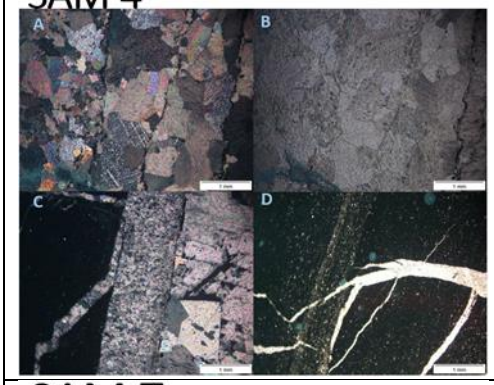
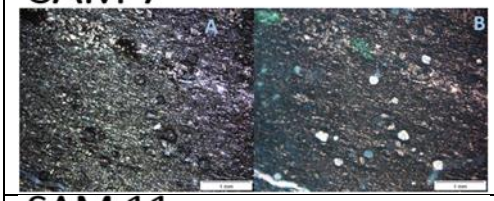
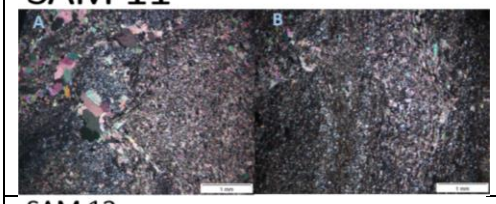
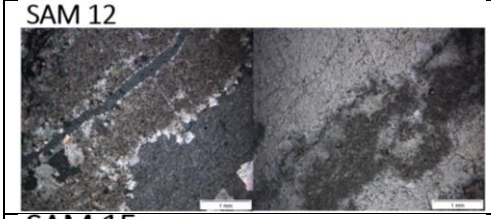
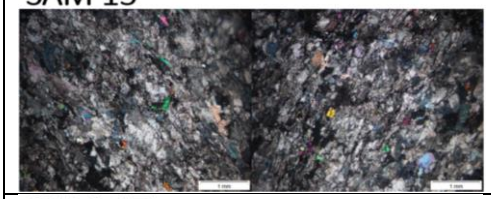
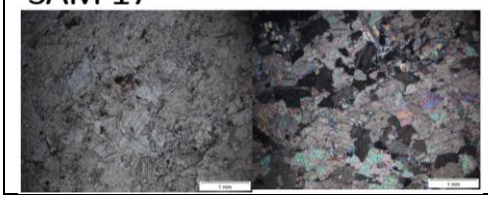
Map of Lime Acres

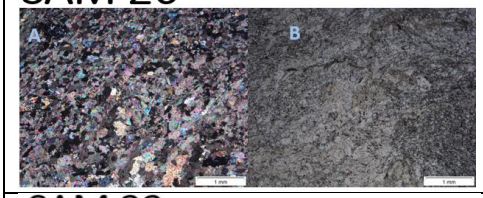
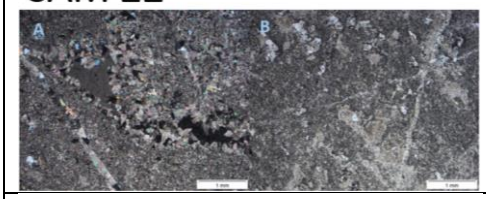
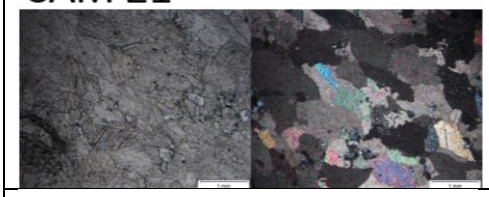
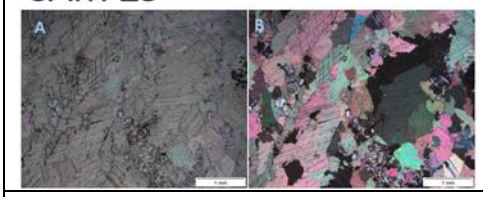
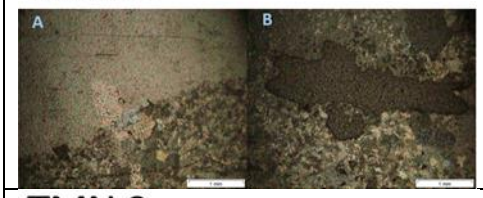
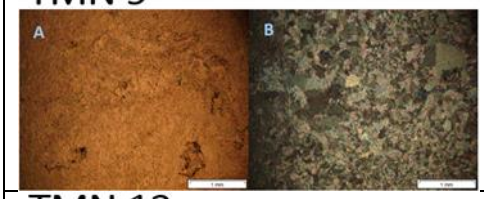
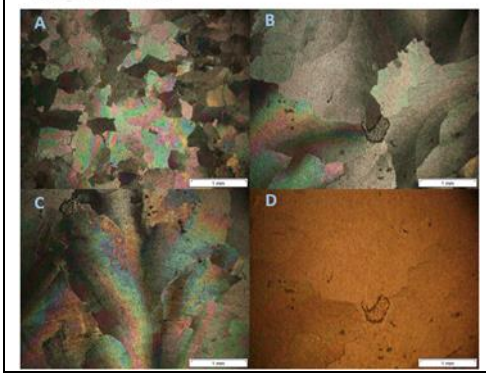
Appendix 2

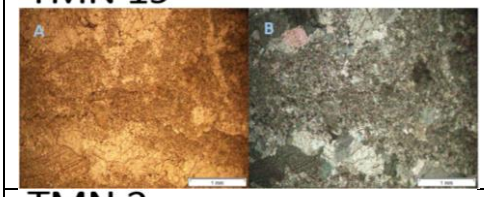
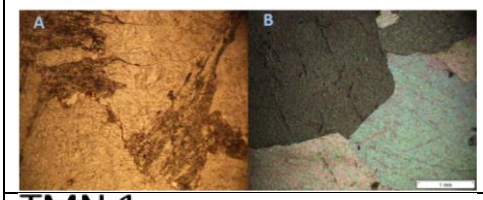
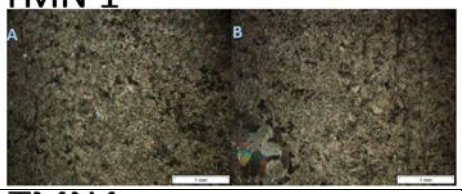
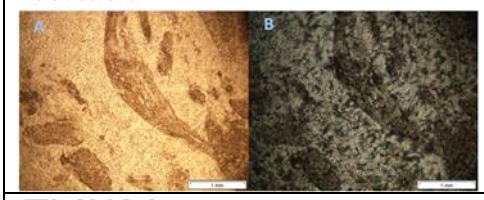
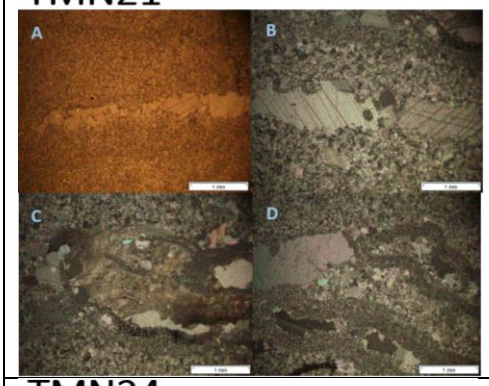
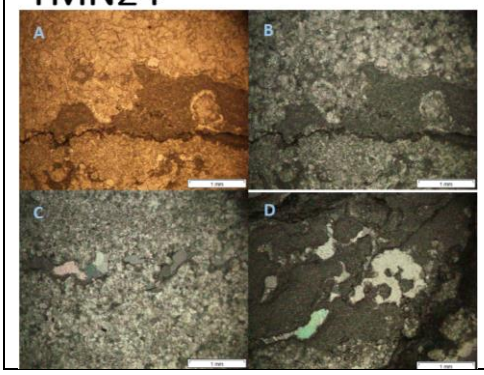
Map of Beestekraal

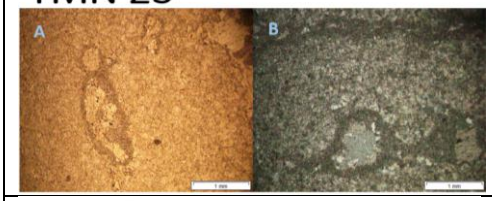
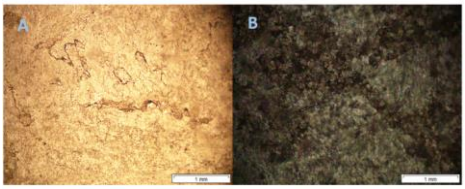
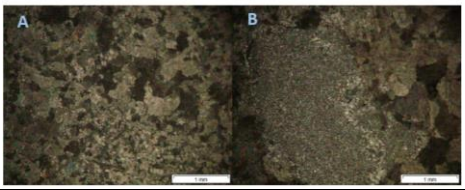
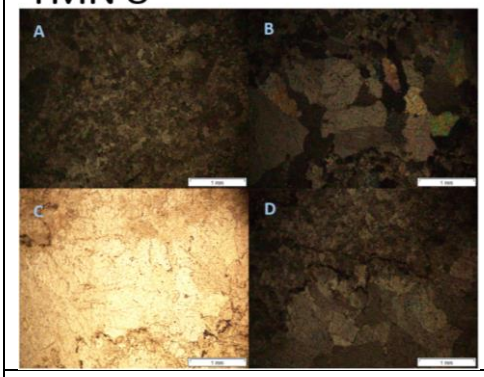
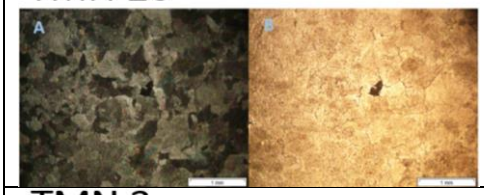
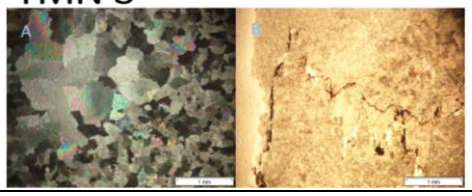
Appendix 3

Petrology Data of Lime Acres and Beestekraal

Images	Description
SAM 4 	Collected at depths of 2 m -10 m Well-developed crystal structure with evidence of re-entrance angles. The twining is evident and veinlets of calcite. Silt sized quartz which have also been cut across by the prevalent calcite veins.
SAM 7 	Collected at depths of 15 m -19 m Fenestrae in silt in fine grained clay carbonates. Infills of quartz have filled the cavities on the carbonates. Elongated grains of the calcite. 2 events occurred to have filled the cavities
SAM 11 	Collected at depths of 19 m -20 m Small crystals with varying mineral composition. Mostly quartz grains cemented by high magnesium calcite which are elongated towards the quartz crystals. Quartz crystals are well defined and seem to have been deposited post deposition of the carbonate platform.
SAM 12 	Collected at depths of 23 m -28m There is inter bedding of crystal structures forming laminae with varying colour and crystal size and crystal shape. There is prevalence of twining and quartz infills.
SAM 15 	Collected at depths of 90 m -96 m Evidence of high pressure showing that the material was affected by faulting and contains quartz blobs which affected the dolomite. Schist infill
SAM 17 	Collected at depths of 90 m -96 m Well defined calcite crystals with re-entrance angles and twinning.

SAM 26 	Collected at depths of 100 m -114 m Quartz grains in schist showing evidence of high pressure. Calcite crystals have some twining.
SAM 22 	Collected at depths of 100 m -114 m Calcite with quartz cross cuttings and veinlets of calcites, grading of crystal sizes and infills of quartz crystals
SAM 21 	Collected at depths of 100 m -114 m Well defined calcite crystals with re-entrance angles and twinning and quartz inclusions.
SAM 29 	Collected at depths of 114 m -120 m Well defined calcite crystals with re-entrance angles and twinning. Infills of quartz crystal in parts
TMN30 	Collected at depths of 18 m -24 m Elongated cavities of silty grain sized quartz. There are siliclastic and poorly defined medium grained structures showing evidence of low pressure deformation.
TMN 9 	Collected at depths of 24 m -25.6 m Siliclastic structures of poorly defined and size graded bedding with little to no sedimentary structures
TMN 13 	Collected at depths of 38 m -38.25 m Dolomite crystals with no twining. Prominent re-entrance angles on the edges of the crystals. No twinning or sedimentary structures on the dolomite Quartz crystals occur as inclusions i.e. the quartz was introduced through a second event

TMN 19  	Collected at depths of 39.5 m -47 m Large calcite crystals with twinning and undefined cleavage planes. Stylolite shows evidence of increased magnesium spots.
TMN 2  	Collected at depths of 49 m -49.7 m Well defined coarse crystals that have twinning and some quartz crystals with evidence of 2 diagenetic events where the quartz crystals are silty in texture. Re-entrance angles are prominent on the coarse crystals. stylolites can be noted in A.
TMN 1  	Collected at depths of 49.7 m -52 m Fine grained, deformed micro-veins of calcite with quartz infilling into that cavities. The cavities are almost round. Inclusions of orange rich hematite which is weathered.
TMN4  	Collected at depths of 58 m -58.6 m Limestone with rounded cavities filled with finer grained clay. Minor traces of finer grained hematite and quartz on the interlocked crystals of calcite.
TMN21  	Collected at depths of 64 m -68 m Dominance of filled fenestrae. Algae which lives in the carbonates form on the crystals. Dominated by different grain sizes of calcites with elongated rhombic structures and coarse grained matrix with well-defined cleavage and twining.
TMN24  	Collected at depths of 68 m -68.5 m Transition of crystal sizes from medium grained to fine grained. There is the crystals are interlocked. There is a stylolite contact of medium grained and silt sized crystals.

TMN 23  	Collected at depths of 68 m -76 m Irregular shaped Silicate crystals are surrounded by fine grained crystals. These are hosted by medium grained dolomite with diminished sedimentary textures or structures.
TMN 7  	Collected at depths of 77 m -78 m Cavity filled with hexagon shaped crystals. These crystals form around the compressed cavity which has become a stylolite that is well preserves.
TMN6  	Collected at depths of 86 m -90 m Poorly defined twining with calcite crystals being well developed. There is fine grained and medium grained crystals. The two size of crystals are joined by fine grained a calcite vein which cuts.
TMN 8  	Occurs at depths of 100 m -101.3 m Irregular shaped infill of coarse grained crystals. Stylolite with infilled with fine grained mud therefore does not allow light to pass through. No twining with evidence of deformation in high pressure.
TMN 28  	Collected at depths of ~26 m Fenestrae filled with coarse grains of quartz. The cleavage planes are prevalent with no twinning. The dolomite coarse grained crystals are irregular shaped with re-entrance angles.
TMN 3  	Collected at depths of ~25 m Stylolite is well preserved and wavy, with opaque minerals forming along stylolite. Dolomite with quartz crystals and some hematite traces. Twinning on coarse grained crystals. Rhombic shaped, high pressure dolomite.

Appendix 4

Geochemical Data of Lime Acres

Appendix 5

Geochemical Data of Beestekraal

Appendix 6

EMPA Data of Lime Acres and Beestekraal